MODELING OF NEWTONIAN FLUIDS AND CUTTINGS TRANSPORT ANALYSIS IN HIGH INCLINATION WELLBORES WITH PIPE ROTATION

A THESIS SUBMITTED TO
THE GRADUATE SCHOOL OF NATURAL AND APPLIED SCIENCES
OF
MIDDLE EAST TECHNICAL UNIVERSITY

BY

MEHMET SORGUN

IN PARTIAL FULFILLMENT OF THE REQUIREMENTS
FOR
THE DEGREE OF DOCTOR OF PHILOSOPHY
IN
PETROLEUM AND NATURAL GAS ENGINEERING

AUGUST 2010

Approval of the thesis:

MODELING OF NEWTONIAN FLUIDS AND CUTTINGS TRANSPORT ANALYSIS IN HIGH INCLINATION WELLBORES WITH PIPE ROTATION

Submitted by **MEHMET SORGUN** in partial fulfillment of the requirements for the degree of **Doctor of Philosophy in Petroleum and Natural Gas Engineering Department, Middle East Technical University** by,

Prof. Dr. Canan Özgen _________________
Dean, Graduate School of **Natural and Applied Sciences**

Prof.Dr. Mahmut Parlaktuna _________________
Head of Department, **Petroleum and Natural Gas Engineering**

Prof.Dr. Mahmut Parlaktuna _________________
Supervisor, **Petroleum and Natural Gas Engineering Dept., METU**

Assoc.Prof.Dr. İsmail Aydın _________________
Co- Supervisor, **Civil Engineering Dept., METU**

Examining Committee Members:

Prof.Dr. Tanju Mehmetoğlu _________________
Petroleum and Natural Gas Engineering Dept., METU

Prof.Dr. Mahmut Parlaktuna _________________
Petroleum and Natural Gas Engineering Dept., METU

Prof.Dr. Mustafa Göğüş _________________
Civil Engineering Dept., METU

Assoc.Prof.Dr. İ. Hakkı Gücüyener _________________
Petroleum and Natural Gas Engineering Dept., METU

Assoc.Prof.Dr. M. Evren Özbayoğlu _________________
Petroleum Engineering Dept., University of Tulsa

DATE _________________

I hereby declare that all information in this document has been obtained and presented in accordance with academic rules and ethical conduct. I also declare that, as required by these rules and conduct, I have fully cited and referenced all material and results that are not original to this work.

Name, Last name : MEHMET SORGUN

Signature:

ABSTRACT

MODELING OF NEWTONIAN FLUIDS AND CUTTINGS TRANSPORT ANALYSIS IN HIGH INCLINATION WELLBORES WITH PIPE ROTATION

Sorgun, Mehmet

Ph.D., Department of Petroleum and Natural Gas Engineering

Supervisor: Prof. Dr. Mahmut Parlaktuna

Co- Supervisor: Assoc.Prof.Dr. Ismail Aydın

August 2010, 152 pages

This study aims to investigate hydraulics and the flow characteristics of drilling fluids inside annulus and to understand the mechanism of cuttings transport in horizontal and deviated wellbores. For this purpose, initially, extensive experimental studies have been conducted at Middle East Technical University, Petroleum & Natural Gas Engineering Flow Loop using water and numerous drilling fluids for hole inclinations from horizontal to 60 degrees, flow velocities from 0.64 m/s to 3.05 m/s, rate of penetrations from 0.00127 to 0.0038 m/s, and pipe rotations from 0 to 120 rpm. Pressure loss within the test section and stationary and/or moving bed thickness are recorded. New friction factor charts and correlations as a function of Reynolds number and cuttings bed thickness with

the presence of pipe rotation for water and drilling fluids in horizontal and deviated wellbores are developed by using experimental data. Meanwhile empirical correlations that can be used easily at the field are proposed for predicting stationary bed thickness and frictional pressure loss using dimensional analysis and the effect of the drilling parameters on hole cleaning is discussed. It has been observed that, the major variable influencing cuttings transport is fluid velocity. Moreover, pipe rotation drastically decreases the critical fluid velocity that is required to prevent the stationary cuttings bed development, especially if the pipe is making an orbital motion. A decrease in the pressure loss is observed due to the bed erosion while rotating the pipe. Cuttings transport in horizontal annulus is modeled using a CFD software for different fluid velocities, pipe rotation speeds and rate of penetrations. The CFD model is verified by using cuttings transport experiments.

A mathematical model is also proposed to predict the flow characteristics of Newtonian fluids in concentric horizontal annulus with drillpipe rotation. The Navier-Stokes equations of turbulent flow are numerically solved using finite differences technique. A computer code is developed in Matlab 2007b for the proposed model. The performance of the proposed model is compared with the experimental data which were available in the literature and gathered at METU-PETE Flow Loop as well as Computational Fluids Dynamics (CFD) software. The results showed that the mechanistic model accurately predicts the frictional pressure loss and the velocity profile inside the annuli. The model's frictional pressure loss estimations are within an error range of $\pm 10\%$.

Keywords: Hole cleaning, friction factor, frictional pressure loss, mechanistic model, cuttings transport, concentric annulus, CFD, finite difference approximation, horizontal and deviated wells.

ÖZ

BORU DÖNME HIZI DİKKATE ALINARAK NEWTONIAN AKIŞKANLARIN MODELLENMESİ VE YÜKSEK AÇILI KUYULARDA KESİNTİLERİN TAŞINMA ANALİZİ

Sorgun, Mehmet
Doktora, Petrol ve Doğal Gaz Mühendisliği Bölümü
Tez Yöneticisi : Prof. Dr. Mahmut Parlaktuna
Ortak Tez Yöneticisi: Doç.Dr İsmail Aydın

Ağustos 2010, 152 sayfa

Bu çalışma, sondaj akışkanlarının halkasal ortamdaki akış mekanizmasını ve hidroliğini incelemeyi ve kesintilerin yatay ve eğimli kuyulardan taşınma mekanizmasını anlamayı amaçlamaktadır. Bu amaçla, Orta Doğu Teknik Üniversitesi, Petrol ve Doğal Gaz Mühendisliği Bölümü, Sondaj Simülatörü'nde su ve çeşitli sondaj akışkanları kullanılarak deneyler gerçekleştirilmiştir. Delme hızı 0.00127 m/s to 0.0038 m/s arasında, akışkan hızı 0.64 m/s ile 3.05 m/s arasında, boru dönme hızı 0 ile 120 rpm arasında, kuyu eğimleri yataydan 60° ye kadar değiştirilmiş ve her akışkan debisi için basınç farkı ve durağan kesinti yatağı yüksekliği kaydedilmiştir. Deney sonuçları kullanılarak, su ve sondaj akışkanları

için Reynold Sayısı ve durağan kesinti yatağı yüksekliğinin fonksiyonu olarak yeni sürtünme faktörü denklemleri ve grafikleri oluşturulmuştur. Aynı zamanda, arazi şartlarında kolayca uygulanabilecek ampirik basınç kaybı ve durağan kesinti yatağı yüksekliği denklemleri boyut analizi kullanılarak elde edilmiş ve sondaj parametrelerinin kuyu temizliğine etkisi değerlendirilmiştir. Akışkan hızının, kesinti taşınmasını etkileyen en önemli parametre olduğu gözlenmiştir. Ayrıca, borunun dönmesi, özellikle orbital hareket yaptığında, durağan kesinti yatağı gelişimini önleyen kritik akışkan hızını düşürmektedir. Boru dönerken, boru içindeki kesinti yüksekliğinin azalmasından dolayı, basınç farkında da bir düşüş gözlenmiştir. Yatay kuyularda, kesinti taşınması hesaplamalı akışkanlar mekaniği yazılımı kullanılarak çeşitli boru delme hızları, akışkan hızları ve boru dönme hızları için modellenmiştir. Model sonuçları, kesinti taşıma deneyleri kullanılarak değerlendirilmiştir.

Ayrıca, bu çalışma kapsamında, Newtonian akışkanların eş merkezli yatay borular arası akışında ortaya çıkan basınç farkının hesaplanması için bir mekanistik model önerilmiştir. Turbulent akış denklemleri, sınırlı farklar yaklaşımı kullanılarak çözülmüştür. Matlab 2007b programı kullanılarak önerilen model için bir bilgisayar kodu yazılmıştır. Önerilen modelin performansı, Orta Doğu Teknik Üniversitesi Petrol Mühendisliğinden elde edilen deney sonuçlarının yanında hesaplamalı akışkanlar mekaniği (CFD) bilgisayar yazılım programı ve daha önce yapılan çalışmalarla da karşılaştırılmıştır. Sonuçlar, mekanistik modelin basınç kaybını ve akışkanın hız profilini doğru olarak tahmin edebildiğini göstermiştir. Basınç kayıpları, ± 10% hata sınırları arasındadır.

Anahtar Kelimeler: Kuyu temizliği, sürtünme faktörü, basınç kaybı, mekanistik model, kesinti taşıma, eş merkezli halkasal ortam, hesaplamalı akışkanlar mekaniği, sonlu farklar yöntemi, yatay ve eğimli kuyular.

to
my
father
mother
wife
&
sister and brother

ACKNOWLEDGEMENTS

I would like to express my deepest gratitude to my advisor Assoc.Prof.Dr M. Evren ÖZBAYOĞLU who proposed this thesis topic and I started this study under his supervision. I would like to thank him for his endless support, help and supervision until completion of the thesis. I would like to thank also to my supervisor Prof.Dr Mahmut PARLAKTUNA and co-supervisor Assoc.Prof.Dr İsmail AYDIN for their support, advice and guidance during this study.

I wish to thank my thesis committee members Prof.Dr Mahmut PARLAKTUNA, Prof.Dr Tanju MEHMETOĞLU, Prof.Dr Mustafa GÖĞÜŞ, Assos.Prof.Dr İsmail AYDIN, Assoc.Prof.Dr M.Evren ÖZBAYOĞLU and Assoc.Prof.Dr İ.Hakkı GÜCÜYENER for their comments and suggestions.

I also wish to thank Reza Ettahadi OSGOUEI and Naci DOGRU for their help and contribution during the experimental parts of the thesis.

I would like to express my gratitude to Assoc.Prof.Dr Jerome J. SCHUBERT giving me the opportunity to do research at Texas A&M.

I want to thank my friends, Gökhan BAYAR, Sevtaç BÜLBÜL, Emre ÖZGÜR for their endless supports and helps.

Finally I would like to express my deepest thanks to my wife and my family for their endless support and encourage me during this study.

This dissertation is dedicated to my father, Şakir SORGUN.

TABLE OF CONTENTS

LIST OF FIGURES

FIGURES

LIST OF TABLES

TABLES

NOMENCLATURE

A	Area [L^2]
A_r	Cuttings Bed Thickness
C_C	Cuttings Concentration
D,d	Diameter [L]
f	Friction Factor
g	Gravitational Constant [L/T^2]
H	Half of the Parallel Plate Height [L]
l_m	Mixing Length [L/T]
$\frac{\Delta P}{\Delta L}$	Pressure Gradient [$M/(L^2T^2)$]
N_{Re}	Reynolds Number
Q	Flow Rate [L^3/T]
r	Radius [L]
ROP	Rates of Penetration [L/T]
R_T	Transport ratio
V	Average fluid velocity [L/T]
v_z	Tangential Velocity[L/T]
Ω	Pipe rotation speed [1/T]
ω_a	Angular velocity[1/T]

Subscripts

c	Cuttings
e	Equivalent
hyd	Hydraulic
i	Inner
o	Outer

Greek

μ	Viscosity [M/(LT)]
μ_e	Effective Viscosity[M/(LT)]
μ_t	Turbulent Viscosity[M/(LT)]
T_{yx}	Total Shear Stress[M/(LT^2)]
τ	Shear Stress[M/(LT^2)]
ρ	Density [M/L^3]
Π	Dimensionless Group
θ	Inclination
f_μ	Damping Function

CHAPTER 1

INTRODUCTION

1.1 Description of the Problem

Directional and horizontal drilling are increasingly used in major oil and gas fields, both on land and offshore. Horizontal wells are drilled at inclination of about 90° angle from the vertical axis. Directional wells are used in order to access reserves below inaccesible regions such as forests, swamps, marshes, hills and to avoid populated areas[1,2]. A major consideration during a successful horizontal and directional drilling is proper hole cleaning. Hole cleaning influences directly cost, time and quality of drilling operation, especially for extended reach and slim hole drilling. Poor hole cleaning can lead to a variety of problems such as high drag, higher probability of pipe stuck, higher hydraulic requirements, etc[3]. If the situation is not handled properly, these problems can ultimately lead to the loss of a well. A single stuck pipe incident may cost over million dollar[4]. Generated cuttings have to be removed from the wellbore by the help of the drilling fluid in order to avoid such problems. The ability of the drilling fluid to lift such cuttings is commonly referred to as carrying capacity of the drilling fluid. The most important parameters influencing the carrying capacity of drilling fluids can be summarized as fluid annular velocity, drillpipe rotation speed, hole inclination, drilling fluid properties, penetration rate, pipe/hole eccentricity, hole geometry and cuttings properties[5,6]. In fact, the fluid flow velocity is the dominant drilling variable on hole cleaning due to its direct relation with the shear stress acting on the cuttings bed[7]. If there exist a cuttings bed inside wellbore, generally, an increase in the fluid velocity will erode the bed significantly. However, depending on the drilling conditions, very high fluid velocities are needed for bed removal, which may not be applied due to hydraulic and physical limitations. In such cases, pipe rotation may enhance the cuttings transport mechanically, and effective hole cleaning can be achieved even at fluid velocities lower than the critical annular fluid velocities required to prevent stationary bed development[8]. Pipe rotation also changes annular frictional pressure loss which is the major force controlling hole cleaning. Proper estimation of annular flow characteristics within the wellbore during drilling operations is quite important for determining hydraulic horsepower requirements, controlling hole cleaning and selecting suitable mud pump, especially when the wellbore inclination is high. However, it is a very challenging task since frictional pressure loss inside the annulus is influenced simultaneously by numerous parameters like fluid velocity, fluid density, fluid viscosity, flow regime, drillpipe eccentricity, hole inclination, cuttings concentration, etc. In brief, proper calculations of frictional pressure loss with pipe rotation while cuttings are present in annulus are the major concern during developing hydraulic programs and controlling hole cleaning. As there are cuttings in the system, an increase in the pressure drop is observed since the stationary cuttings bed decreases the free flow area of the fluid inside the wellbore. Thus, if cuttings in the wellbore are not considered, pressure losses are underestimated.

Since 1940's, the problem of cuttings transport in horizontal and deviated wells have been the subject of research in petroleum engineering. Initial studies were focused on the effects of drilling parameters on cuttings transport for water and oil based drilling fluids. Later, mathematical models are introduced in order to determine critical fluid velocity for preventing bed development for all inclination angles. Two and three layered models[24-37] based on the mass, momentum and energy balances of each layer were developed to characterize properly the cuttings transport mechanism in horizontal and deviated wells without pipe rotation.

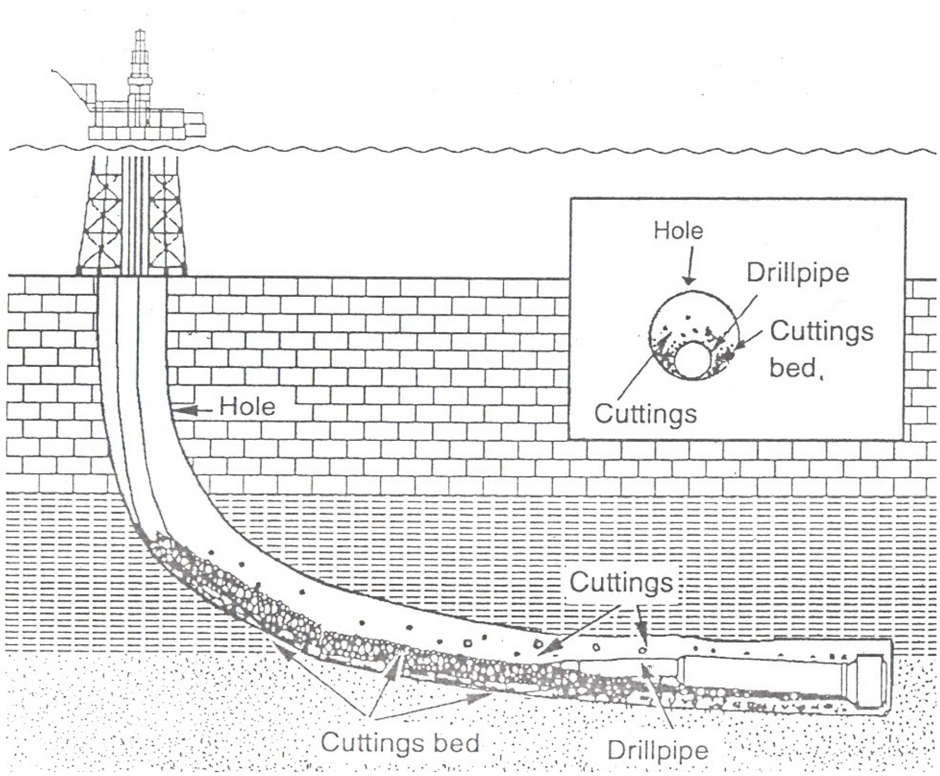

Figure 1.1- Cuttings bed buildup in directional wells[9]

As a result, although extensive studies on cuttings transport have been conducted for many years, poor hole cleaning in horizontal and deviated wells still remains one of the major problems affecting drilling operation success. Therefore, further experimental and theoretical studies are required, in order to understand the mechanism of the cuttings transport and to determine the performance of drilling fluids inside annulus.

1.2 Literature Review

1.2.1 Cuttings Transport in Horizontal and Directional Wells

A number of studies have been conducted to investigate cuttings transport in horizontal and deviated wells. These studies can be separated into two basic approaches: *i*) empirical and *ii*) theoretical.

Zeidler[10] carried out one of the pioneering experimental studies of hole cleaning. Tests were conducted with 65 ft long cuttings transport test apparatus. The annular section had 8-1/2 inch casing with 4-1/2 inch drillpipe. He reported that turbulent flow and drillpipe rotation increased cuttings transport.

Sifferman et al.[11] performed experimental investigations of cuttings transport by using a 140-ft vertical flow system and several drillpipe and casing sizes to determine the variables affecting drill cutting transport under steady state conditions. They reported that the most important factors affecting cuttings transport are annular fluid velocity and rheological properties of fluids. Moreover, cuttings size and drilling fluid density had moderate influence on hole cleaning.

Tomren et al.[12] experimentally investigated the effects of pipe rotation and hole inclination angle, eccentricity and flow regimes on hole cleaning in vertical and directional wells. Experiments were performed using 40 ft long cuttings transport flow loop having 5 in. outer pipe and 2 in. inner pipe. They pointed out that the major factors affecting carrying capacity of drilling fluids in directional wells are fluid velocity, hole inclination, and mud rheological properties. Increasing the hole inclination while keeping other parameters constant dramatically reduces the carrying capacity of drilling fluids. In this study, it was reported that, pipe rotation has only slight effects on transport performance in inclined annuli. It was also observed that high viscosity muds provided better transport than low viscosity muds.

Seeberger et al.[13] conducted an experimental study of the ability of oil base muds to clean large diameter, high angle holes. They observed that fluid viscosity at low shear rates and its initial gel strength are critical parameters in order to determine its ability to clean a well. Water based and oil based fluids having similar rheologies are equally efficient at hole cleaning.

Becker et al.[14] carried out experiments comparing the effects of fluid rheological parameters (fluid yield point (YP), plastic viscosity (PV), YP/PV ratio, power law exponent, consistency index, etc.) on annular hole cleaning using a large scale flow loop. They pointed out that turbulent flow improved cuttings transport for highly-inclined wellbores, and the effects of fluid rheology dominated at low inclinations.

Hemphill and Larsen[15] investigated hole cleaning capabilities of water and oil based drilling fluids in inclined annulus at varying fluid velocities. The results showed that water and oil based drilling fluids clean similarly for equivalent rheological and flow velocity profiles. While fluid velocity is key parameter to cuttings transport, other parameters, such as mud density and flow index ‘n’ factors, can affect cuttings transport efficiency in certain hole angle ranges.

Lou et al.[16] proposed a set of charts based on both laboratory and field measurements in order to determine hole cleaning requirements in deviated wells.

Saasen et al.[17] investigated the effects of frictional pressure loss on cuttings transport in deviated wells. They pointed out that the annular frictional pressure loss is the key parameter in obtaining optimum hole cleaning and the next important parameter is the consolidation of the cuttings bed.

Saasen and Loklinghoim[18] examined the effect of the cuttings bed properties on hole cleaning. It is reported that gel formation within the developed cuttings bed occurs due to the interaction between the drilling fluids and cuttings, which significantly increases the required shear force needed to erode the bed, and lift the cuttings particles up from the bed.

Ozbayoglu et al.[19] analyzed the effects of major drilling parameters on hole cleaning for high angle wells using incompressible non-Newtonian fluids as well as compressible non-Newtonian fluids, i.e, foams. The flow loop is approximately 100 ft long, consisting of an 8'' by 4.5'' transparent annular test section. Average annular fluid velocity is the dominating parameter on hole cleaning, which is in consistent with the observations from above studies[8,9,12] and turbulent flow is the better for preventing bed development. Cuttings size is another important parameter on cuttings transport and smaller particles are much more difficult to remove if they have built a bed. Another important observation was that, if everything else is kept constant, the developed bed also decreases as the fluid behavior index is decreased It was also noticed that rate of penetration and wellbore inclination has almost no effect on the thickness of the developed bed.

Yu et al.[20] proposed a new approach to improve the cuttings transport capacity of drilling fluid in horizontal and inclined wells by attaching gas bubbles to the surface of drilled cuttings using chemical surfactants.

Mirhaj et al.[21] performed experimental study and proposed emprical correlations in order to predict the minumum velocity that is needed to carry the cuttings out of the wellbore for deviated and horizontal wellbores.

Ozbayoglu et al.[22] conducted extensive cuttings transport experiments with water for various inclinations, flow rates and rate of penetrations and proposed easy-to-use emprical correlations for estimating the critical fluid velocity required in order to prevent formation of a stationary bed in horizontal and highly-inclined wellbores. They emphasized that the major variable influencing the cuttings bed thickness is the shear stress acting on the cuttings bed surface.

Yu et al.[23] investigated experimentally the effects of drilling fluid rheology, mud density, temparature, borehole inclination, pipe rotation, eccentricity, rate of penetration (ROP) and flow rates. Experimental results showed that drillpipe rotation, temperature and rheological parameters of drilling fluids have significant effects on cuttings transport efficiency.

Bilgesu et al.[24] examined the effects of the cutting and mud properties on the cutting transport efficiency for vertical and horizontal wellbores using a commerical CFD software. It is noticed that increase in flow rate has a more pronounced cleaning effect for smaller particles compared to larger particles for a horizontal wellbore.

Nazari et al.[25] conducted a review of cuttings transport in directional wellbores. A thorough review on previous hole cleaning studies and a approach for monitoring and controlling hole cleaning problems are presented.

Cuttings transport models introduced for describing the mechanism of bed development and cuttings transport in inclined and horizontal wells can be separated into two categories as layer models and particle models. The layer models are based on the mass, momentum and energy balances of each layer, such as a two layer and three layer model[26-37]. These models divide flow section into two or three separate layers. In a two layer model, the lower layer is stationary cuttings bed and the upper layer is heterogeneous (fluid and cuttings) layer. On the other hand, in a three layer model, the top layer consists of clear fluid, the middle layer is a heterogeneous mixture of fluid and cuttings and the bottom layer is stationary cuttings bed. These models are based on the mass, momentum and energy balances of each layer. However, the results of these studies are quite similar.

Kenny et al.[29] studied the effect of the fluid behavior index, consistency index, yield point and pipe eccentricity using Herschel Bulkley rheological model on hole cleaning. Fluid behavior index and drillpipe eccentricity have a dominant role on cuttings transport in horizontal and deviated wells and higher flow behavior index promote higher fluid velocities under the eccentric drillpipe. Also, all available rheological parameters should be used in analysing hole cleaning problems.

Kamp and Rivero[31] proposed a two layer model to perform numerical simulations, predicting cuttings bed heights, pressure drops, and transport velocities at different rates of penetrations and mudflow rates for steady state cuttings transport in highly inclined wells. The authors reported that drillpipe rotation and its effect on cuttings transport should be included in a mechanistic model, since this seems to be primordial in the correct prediction of cuttings transport in inclined wellbores.

Larsen, Pilehvari and Azar[32] presented a new cuttings-transport model which predicted critical velocity needed to keep all cuttings moving for horizontal and high-angle wells.

Cho et al.[34] developed a three-layer model similar to Nguyen and Rahman's[33] model. They developed a simulator and compared the results with existing models as well as the experimental data conducted by other researchers and proposed charts to determine the lowest possible pressure gradient to serve as an operational guide for drilling operations.

Masuda et al.[35] conducted both experimental investigation and numerical simulation for different flow conditions to determine the critical fluid velocity in inclined annulus. They proposed a transient, 1-D two-fluid numerical model which includes two-layer formulation, interactions between the fluid phase (mud) and the solid phase (drill cuttings) in the suspension layer, and interactions between the two layers to simulate the transport of drill cuttings in under balanced drilling.

Ozbayoglu[36] developed a three-layer model for cuttings transport using foam in horizontal and deviated wells. He also provided empirical correlations and artificial neural networks (ANN) in order to predict bed thickness. Model is compared with experimental results and cuttings bed thickness and total pressure drop with an error less than 20% in most cases.

Second modeling approach[38,39] focuses on the analysis of forces acting on a single particle and their balance to estimate cuttings bed thickness and cuttings concentration. Both of them assume that there is no pipe rotation. Some of these model performances were tested using experimental data collected in different cuttings flow loops. Also, there were attempts for determining the critical fluid velocity for preventing bed development, either theoretically or experimentally.

1.2.2 Pipe Rotation Effects on Cuttings Transport

Numerous experimental studies have been conducted to investigate the effects of drill pipe rotation on hole cleaning for conventional drilling fluids in horizontal and deviated wells[40-50]. The common conclusion is that pipe rotation has a significant improvement on cuttings transport, especially if the pipe is making an orbital motion. Also, pipe rotation drastically decreases the critical fluid velocity required to remove the stationary bed from the wellbore for a proper hole cleaning. However, after a certain rotation speed, pipe rotation has not additional contribution on hole cleaning. When there are no cuttings present, the frictional pressure losses are increasing as the pipe rotation speed is increased. Nevertheless, as the cuttings are introduced, due to the reduction in the stationary cuttings bed area inside annulus, frictional pressure losses decrease. Additionally, as the fluid viscosity is increased, contribution of pipe rotation on hole cleaning is increasing when compared with no rotation case.

Ford et al.[40] and Peden et al.[41] carried out an experimental study in order to investigate hole cleaning in 21 ft long, 5.4 in by 2.4 and 3.5 in inclined annulus with the inner pipe rotation. They found that pipe rotation does not have any significant effect on the minimum fluid velocity if circulating a lower viscosity fluid, e.g., water. On the other hand, if medium and or highly viscous fluids are used, the minimum fluid velocity considerably decreases. It was also emphasized that the pipe rotation has no significant effects on cuttings transport in concentric annuli. However, the pipe rotation reduced minimum transport velocity in case of +50% eccentricity but there were no noticeable effects of pipe rotation when using -50% eccentricity.

Sifferman and Becker[42] performed an experimental study and found that the variables with significant influence on cuttings bed size were mud annular velocity, mud density, inclination angle, and pipe rotation. Mud rheology, cuttings size and pipe eccentricity have moderate effects on cuttings transport. They stated that the largest cuttings beds occurred with more viscous mud at the lower mud velocity, without pipe rotation. In addition, as the mud velocity is increased, the effect of pipe rotation speed is decreased.

Lockett et al.[43] demonstrated the importance of pipe rotation effects for removing cuttings from the wellbore by using Taylor vortices. However, computer simulations of fluid flow and particle transport were not compared with enough experimental data.

Ribeiro and Podio[44] developed a numerical model in order to determine the effect of rotational speed and eccentricity on annular flows. The analysis revealed that pipe rotation speed and eccentricity of the inner cylinder have significant effect on the pressure loss of flows through annulus.

Gao and Young[45] presented a theoretical analysis and their field experience of the cuttings transport of a pseudo-oil based mud in drilling extended reach wells. It was noticed that axial pipe rotation has little effect on the minimum transport velocity required for the adequate hole cleaning. However, when drill pipe is rotated in an orbital manner, it can significantly improve hole cleaning. Orbital motion and sweeping effect of the drill pipe improve cuttings transport especially in extended reach wells.

Sanchez et al.[46] examined the effect of pipe rotation on hole cleaning during directional well drilling as conducted over 600 tests. The pipe rotation effects are greatest at 90 degrees inclination and they have least effects at 40 degrees inclination. They also observed that drill pipe orbital motion is needed for considerable development in cuttings transport and pipe rotation decreases the time needed to remove the cuttings from the wellbore.

Saasen[47] stated that pipe rotation influences change with the rheology of cuttings bed-fluid mixture. If the bed has been formed in an oil-based drilling fluid which has no gel structure that connects the cuttings particles, pipe rotation has little effect on hole cleaning. However, as a water-based drilling fluid is used including polymers that have a strong gel structure, pipe rotation aids to transport larger volumes of cuttings when compared with oil-based fluids.

Hemphill and Ravi[48] emphasized that the effects of pipe rotation on pressure drop and local velocity with varying pipe eccentricities and pipe rotation can greatly improve hole cleaning when the pipe is eccentric. Besides, Hemphill et al.[49] stated that there exists a positive proportional relationship between pipe rotation speed and annular pressure drop (and equivalent circulating density), i.e., pressure drop increases with increasing rotation speed.

Duan et al.[50] performed an experimental study on transportation of small-size cuttings during pipe rotation in extended reach drilling. They emphasized that smaller cuttings are more difficult to transport than larger cuttings in a horizontal annulus when tested with water. Pipe rotation improves the efficiency of transportation of smaller cuttings when compared with larger-sized cuttings. They also observed that increase in pipe rotation speed cause a decrease in pressure drop due to a reduced bed cross-sectional area which leads to an increase in fluid flow area.

Duan et al.[51] also carried out an experimental investigation of the effect of drill pipe rotation on pressure losses and fluid velocity profile in foam drilling. Drill pipe rotation slightly increases pressure drop for lower quality foams (below 70 % foam quality), no noticeable effect on medium quality foams (70-80 % foam qualities), and slightly decreases pressure drop for higher quality foams (90 % foam quality) in a concentric annulus. Pipe rotation increases pressure drop for foam flow in an eccentric annulus with a given cuttings bed height.

More recently, Duan[52] developed a mechanistic model for foam using exlog approach in order to predict cuttings concentration, bed height and pressure drop in horizontal wells with various pipe rotation speeds. Model was compared with experimental results and it was successful in predicting cuttings bed thickness and total pressure drop with an error less than 15% in most cases.

Ozbayoglu et al.[8] investigated experimentally the effect of pipe rotation on hole cleaning for water-based drilling fluids in horizontal and deviated wells. It was observed that pipe rotation has a significant effect on cuttings transport ability of the fluid. It was also noticed that mud viscosity seems to have some influence on hole cleaning for low rotation speeds. As the rotation speed is increased, this influence diminishes. A direct relation between the hole inclination and pipe rotation speed was not identified. However, no bed development was observed as the inclination moved away from horizontal and pipe was rotated.

1.2.3 Pipe Rotation Effects on Frictional Pressure Loss without Cuttings

Accurate prediction of frictional pressure loss of Newtonian and non-Newtonian fluids in concentric and eccentric annulus prevents occurrence of a number of serious problems such as loss of circulation, kicks, improper rig power selection etc. However, it is a very difficult task to determine proper frictional pressure loss of Newtonian and non-Newtonian fluids in eccentric annuli, especially during pipe rotation. The major factors affecting the frictional pressure loss in annulus may be summarized as fluid properties (density and rheogical properties), fluid velocity, flow regime, eccentricity, pipe rotation speed and annulus geometry.

Numerous studies regarding pipe rotation effects on frictional pressure drop have been conducted over the last 50 years. These studies can be separated into two basic approaches: *i*) experimental and *ii*) numerical.

Yamada[53] conducted an earlier study for water through concentric annuli when inner pipe rotates. Coleman and Noll[54] proposed an exact solution for incompressible flow in a concentric annulus, which is also called helical flow.

Delwiche et al.[55] and Marken et al.[56] investigated pipe rotation effects on pressure loss using real wells and found that frictional pressure loss increases if rotation is applied to the inner cylinder in the annulus. In addition, Marken et al.[56] emphasize that the flow regime and pressure losses are affected by pipe motion, eccentricities and temperature along the length of the annulus.

McCann et al.[57] conducted extensive experimental studies in order to investigate the effects of high speed pipe rotation on pressures in narrow annulus. They pointed out that the pipe rotation speed and eccentricity strongly affect the pressure loss in narrow annuli. It was also observed that for power-law fluids, when the flow regime is turbulent, the pressure loss increases with increasing pipe rotation, and when the flow regime is laminar, pressure drop decreases with increasing pipe rotation.

Hansen and Sterri[58] investigated experimentally pipe rotation effects on frictional pressure loss in an annuli. It was noticed that the pipe rotation increases the frictional pressure loss for low viscosity fluids and decreases frictional pressure loss for high viscosity shear thinning fluids.

Nouri and Whitelaw[59] stated that the rotation had similar effects on the Newtonian and non-Newtonian fluids, with a more uniform axial flow across the annulus and the maximum tangential velocities in the narrowest gap in both cases.

Wei et al.[60] carried out theoretical, experimental, and field data studies about the effects of drillpipe rotation on annular frictional pressure loss for laminar, helical flow of power law fluids. With drillpipe dynamic influence, the annular pressure loss is the combined result of shear-thinning effect and drillpipe dynamic effect. The latter increases the annular pressure loss, and in most cases is the dominant factor. The effect of drillpipe rotation on annular pressure loss is affected by mud properties, flow rate, wellbore geometry and drillpipe rotation speed.

Ooms and Kampman-Reinhartz[61] pointed out that in the case of a concentric drill pipe, rotation does not influence the axial pressure drop for a stationary, fully developed laminar flow of a Newtonian liquid. However, when the drill pipe is placed in an eccentric position, the axial pressure drop increases with increasing rotation speed.

Wang et al.[62] performed an experimental investigation about the effects of high rotation speeds, annular gap and pipe eccentricity on slimhole annular pressure loss. It was emphasized that, contrary to conventional drilling, in slimhole drilling, the annular mud flow regime is not only relied on Reynolds number,but also on Taylor number.

Wan et al.[63] and Escudier et al.[64] investigated numerically the effects of eccentricity and pipe rotation on frictional pressure loss for Newtonian and non-Newtonian fluids. They concluded that combination of inertia and shear thinning effects combination determines the magnitude of frictional pressure loss inside the annulus when the pipe is rotating. The inertia effects tend to increase frictional pressure loss while shear thinning effects diminish pressure drop. Inner-cylinder rotation is to increase axial pressure gradient in eccentric annuli since inertia effects dominate shear thinng effects. For slightly eccentric and concentric annulus, frictional pressure loss decreases as the pipe rotates since shear-thinning effects can counteract inertial effects.

Woo et al.[65] conducted an experimental study of fully developed laminar flows of Newtonian and non-Newtonian fluids through a concentric annulus and inner cylinder rotation. The pressure drop increases as the rotational speed of the inner cylinder increases and the increases in pressure drop depends on the flow regime. Ahmed and Miska[66] carried out an experimental and theoretical study about laminar flows of yield power-law fluids in concentric and fully eccentric annulus with inner cylinder rotation. They adopted Coleman and Noll[54]'s analytical solution for yield power-law fluid. It was emphasized that shear thinning, inertial effects and secondary flows substantially influence frictional pressure loss, when inner pipe rotates. In highly eccentric annuli, pressure drop increases as the pipe rotation does since inertial effects dominate the phenomenon of shear thinning.

1.2.4 Friction Factor Correlations for Newtonian and non-Newtonian Fluids inside Pipe and Annulus

Numerous studies have been conducted to determine the friction factor for turbulent Newtonian flow in pipes and annulus[67-72]. Dodge and Metzner[73] conducted theoretical and experimental study and developed friction factor correlation for turbulent flow of Newtonian and non-Newtonian fluid in annuli.

Kozicki et al.[74] proposed equations to calculate pressure drop for steady, isothermal, laminar flow of non-Newtonian fluids in ducts of arbitrary cross section. They verified friction factor correlations by using experimental data.

Gucuyener and Mehmetoglu[75] presented analytical solutions to the volumetric flow rate for the axial laminar flow of yield-pseudo-plastic fluids in concentric annuli. Moreover, Gucuyener and Mehmetoglu[76] proposed modified Reynolds Number based on the equivalent diameter concept for laminar-turbulent transition of Newtonian and non-Newtonian fluids flows inside pipes and concentric annulus.

Reed and Pilehvari[77] introduced effective diameter concept for predicting pressure gradients of non-Newtonian fluids in all laminar, transitional and turbulent flow regimes. Model predictions were verified experimental data for non-Newtonian fluids flowing in pipes and annulus.

Singhal et al.[78] proposed friction factor correlations for non-Newtonian fluids in turbulent flow regime. Friction factor correlations were compared with experiments and available correlations for Newtonian and non-Newtonian fluids.

McKeon et al.[79] derived a new friction factor for fully developed pipe flow using high Reynolds number pipe flow data.

Avci and Karagoz[80] suggested a friction factor equation for a smooth and rough wall fully developed turbulent flows in pipes.

1.3 Scope of the Study

The aim of this study is to investigate mechanics of analysis for cuttings transport in horizontal and deviated wellbores during pipe rotation and to evaluate drilling fluid performance in the annulus. A mechanistic model will be introduced to predict frictional pressure loss of low viscous fluids in concentric horizontal annulus with and without drillpipe rotation. The performance of the proposed model will be compared with the experimental data obtained from Flow Loop facility at METU-PETE as well as Computational Fluids Dynamics (CFD) code ANSYS. Then, cuttings transport inside horizontal fully eccentric annulus during pipe rotation will be simulated numerically using an Eulerian- Eulerian computational fluid dynamics (CFD) model. CFD model will be tested using cuttings transport experiments. Dimensional analysis will be conducted to properly understand the effect of each drilling parameter on cuttings transport and to develop empirical correlations for frictional pressure loss and cuttings bed thickness. Finally, expressions and charts based on the experimental data will be developed to estimate the friction factor for water and drilling fluids in terms of Reynolds number and stationary cuttings bed thickness.

Geometry and governing equations of proposed mathematical model, dimensional analysis and friction factor equations will be given in chapter 2. In chapter 3, experimental setup used in this study will be presented. In chapter 4, mathematical model predicting pressure loss in concentric annulus will be introduced in details. CFD software solution of cuttings transport inside horizontal annulus with pipe rotation will be given in chapter 5. In chapter 6, results and discussions will be presented. Main conclusions obtained from this study and recommendations will be given in Chapter 7. Derivations of viscosities for power law fluids, flow curves of drilling fluids used in this study, comparison of model and CFD predictions with experimental data and CFD software solution process will be presented in the Appendices.

CHAPTER 2

THEORY

2.1 Geometry and Governing Equations of Mathematical Model

Concentric annular geometry is represented as a narrow slot, i.e., flow through between two parallel plates, in order to simplify and speed-up the calculation process. Schematic diagram of the single phase flow model including pipe rotation is shown in Figure 2.1.

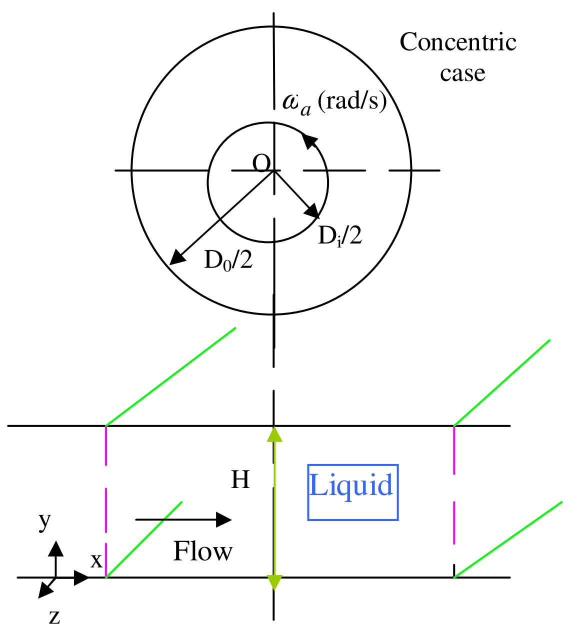

Figure 2.1- Slot equivalent of concentric annuli[81]

For conduit cross sections other than simple circular tubes, it is a common practice to use an effective diameter definition for representing annular geometries, termed as the hydraulic diameter, D_{hyd}, which is defined as

$$D_{hyd} = \frac{4x(cross-\sec tional)area}{wetted-perimeter} \tag{1}$$

Slot representation of annulus gives accurate solution for $D_i / D_o > 0.3$[82]. The wetted perimeter is the perimeter in contact with the fluid[83]. For concentric annulus

$$D_{hyd} = \frac{4\pi(r_o^2 - r_i^2)}{2\pi(r_o + r_i)} = 2(r_o - r_i) = D_o - D_i \tag{2}$$

and hydraulic diameter of parallel plate height is 2H

$$D_{hyd}=2*(2H) \tag{3}$$

Finally, $H = \dfrac{D_o - D_i}{4}$ (4)

The assumptions used in the analysis are:

- Steady state flow;
- Main flow is in +x direction ($u_x=u$, $u_y=\upsilon$, $u_z=w$);
- Fluid is incompressible;
- Fully developed flow (there is no variation of velocity in the axial direction)
- Isothermal system (physical properties are constant).

In this proposed model, Ω is the rotation speed of inner drillpipe (rpm).

Therefore, the angular velocity (ω_a (rad/s)) is defined as:

$$\omega_a = \Omega\left(\frac{2\pi}{60}\right) \tag{5}$$

The equation of continuity is written as

$$\frac{\partial \rho}{\partial t} + \nabla.\rho v = 0 \tag{6}$$

and for incompressible fluid, density is constant, therefore eq.(6) reduces to

$$\nabla.v = 0 \tag{7}$$

and the equation of continuity may be obtained in rectangular coordinates

$$\frac{\partial u}{\partial x} + \frac{\partial \upsilon}{\partial y} + \frac{\partial w}{\partial z} = 0 \tag{8}$$

The equations of motion in terms of stresses is expressed as

$$\rho\frac{Dv}{Dt} = -\nabla p - \nabla.\tau + \rho g \tag{9}$$

where v is the velocity vector, g is the gravity vector, τ is the stress tensor, p is the fluid pressure vector and ∇ means '' the gradient of''.

As an open form, the equation of motion for cartesian coordinates (x,y,z) and turbulent flow is[84,85]:

$$\rho(\frac{\partial u}{\partial t}+u\frac{\partial u}{\partial x}+\upsilon\frac{\partial u}{\partial y}+w\frac{\partial u}{\partial z})=-\frac{\partial p}{\partial x}+\left[\frac{\partial}{\partial x}\tau_{xx}+\frac{\partial}{\partial y}\tau_{yx}+\frac{\partial}{\partial z}\tau_{zx}\right]+$$
$$\rho g_x-\frac{\partial(\rho u'\upsilon')}{\partial y}-\frac{\partial(\rho u'^2)}{\partial x}-\frac{\partial(\rho u'w')}{\partial z}+\rho\omega_a^2 y \tag{10}$$

$$\rho(\frac{\partial \upsilon}{\partial t}+u\frac{\partial \upsilon}{\partial x}+\upsilon\frac{\partial \upsilon}{\partial y}+w\frac{\partial \upsilon}{\partial z})=-\frac{\partial p}{\partial y}+\left[\frac{\partial}{\partial x}\tau_{xy}+\frac{\partial}{\partial y}\tau_{yy}+\frac{\partial}{\partial z}\tau_{zy}\right]+$$
$$\rho g_y-\frac{\partial(\rho u'\upsilon')}{\partial x}-\frac{\partial(\rho \upsilon'^2)}{\partial y}-\frac{\partial(\rho \upsilon'w')}{\partial z} \tag{11}$$

$$\rho(\frac{\partial w}{\partial t}+u\frac{\partial w}{\partial x}+\upsilon\frac{\partial w}{\partial y}+w\frac{\partial w}{\partial z})=-\frac{\partial p}{\partial z}+\left[\frac{\partial}{\partial x}\tau_{xz}+\frac{\partial}{\partial y}\tau_{yz}+\frac{\partial}{\partial z}\tau_{zz}\right]+$$
$$\rho g_z-\frac{\partial(\rho u'w')}{\partial x}-\frac{\partial(\rho \upsilon'w')}{\partial y}-\frac{\partial}{\partial z}w'^2 \tag{12}$$

The constitutive equation of Newtonian fluids is expressed as

$$\tau_{xy}=\tau_{yx}=\mu\left[\frac{\partial \upsilon}{\partial x}+\frac{\partial u}{\partial y}\right] \tag{13}$$

The total shear stress (T_{yx}) can be written as

$$T_{yx}=(\mu+\mu_t)\frac{\partial u}{\partial y} \tag{14}$$

The effective viscosity can be expressed as

$$\mu_e=\mu+\mu_t \tag{15}$$

2.2 Extension of Pipe Flow Equations

Extension of pipe flow equations to annular geometry by modification in the diameter term is used generally to calculate frictional pressure losses in the concentric annuli and Reynolds number. There are different effective diameter definitions in literature for Newtonian fluids. Different frictional pressure losses and Reynolds number is obtained by using different effective diameter. Three expressions given below have been used in practice to represent annular flow.

The hydraulic diameter is defined as

$$D_e = D_{hyd} = D_o - D_i \tag{16}$$

The equivalent circular diameter of a slot flow representation of an annulus is given by

$$D_e = D_{slot} = 0.816(D_o - D_i) \tag{17}$$

The Crittendon's equivalent diameter is defined as

$$D_e = D_{crittendon} = \frac{\sqrt[4]{D_o^4 - D_i^4 - \dfrac{(D_o^2 - D_i^2)^2}{\ln(D_o/D_i)}} + \sqrt{D_o^2 - D_i^2}}{2} \tag{18}$$

Eq.16 is possibly the most widely used in petroleum industry[82].

The fanning friction factor for laminar flow can be written as

$$f = \frac{16}{N_{\mathrm{Re}}} \tag{19}$$

For turbulent flow, Colebrook equation is used

$$\frac{1}{\sqrt{f}} = 4\log(N_{\mathrm{Re}}\sqrt{f}\,) - 0.395 \tag{20}$$

Finally, frictional pressure gradient can be calculated as

$$\frac{\Delta P}{\Delta L} = \frac{2 f\rho V^2}{D_e} \tag{21}$$

2.3 Dimensional Analysis

Cuttings bed thickness is defined as the ratio of area occupied by stationary cuttings in the annulus cross-section to the total flow area

$$A_r = A_{bed} / A_{wellbore} \tag{22}$$

Drilling variables influencing stationary cuttings bed thickness can be summarized as

$$A_r = f(V, C_c, \theta, D_{hyd}, \rho, \mu, \rho_c, d_c, g) \tag{23}$$

where V is the average fluid velocity, C_c is the feed cuttings concentration, θ is the hole inclination, ρ is the fluid density, μ is the fluid viscosity, ρ_c is the cuttings density, d_c is the cuttings diameter and g is the gravity. After applying Buckingham-π theorem, dimensionless groups are determined as follows:

$$\Pi_1 = \frac{\rho\, VD_{hyd}}{\mu_e} \tag{24}$$

$$\Pi_2 = \frac{V^2}{gD_{hyd}} \tag{25}$$

$$\Pi_3 = C_c \tag{26}$$

$$\Pi_4 = \theta \tag{27}$$

$$\Pi_5 = \frac{d_c}{D_{hyd}} \tag{28}$$

$$\Pi_6 = \frac{d_c \rho V}{\mu_e} \tag{29}$$

$$\Pi_7 = \frac{\Omega D_{hyd}}{V} \tag{30}$$

In these groups,

$$D_{hyd} = D_o - D_i \tag{31}$$

$$C_c = \frac{(ROP) D_{bit}^2}{1466.95 R_T Q}(100) \tag{32}$$

$$R_T = \frac{V - V_s}{V} \tag{33}$$

C_c is the feed cuttings concentration[86], ROP is the rates of penetration (ft/hr), Ω is the pipe rotation speed (rpm), D_{bit} is the bit diameter (in), Q is the flow rate (gpm), R_T is the transport ratio, considered as 0.5 in this study and V_s is the slip velocity.

2.4 Friction Factor Correlations for Water-Based Drilling Fluids in Horizontal and Deviated Wells during Pipe Rotation

Frictional pressure gradient inside an annulus for unit length using narrow slot approach can be defined as

$$\frac{\Delta P}{\Delta L} = \frac{f\rho V^2}{21.1(D_o - D_i)} \tag{34}$$

Here, $\Delta P/\Delta L$ is the frictional pressure drop for unit length (psi/ft), f is the Fanning friction factor, ρ is the fluid density (ppg), D_o is the wellbore diameter (in), D_i is the outer pipe diameter (in), and average annular fluid velocity, V (ft/s), is expressed as follows:

$$V = \frac{Q}{2.448(D_o^2 - D_i^2)} \tag{35}$$

where Q is the volumetric flow rate (gpm). Effect of pipe rotation on friction losses will be included by modifying the Reynolds number to contain rotational velocity. Total Reynolds number for the combined axial and rotational flows can be defined as

$$N_{RET} = N_{RE} + N_{RER} \tag{36}$$

In field units, the Reynolds number in the axial direction can be expressed as

$$N_{RE} = \frac{757\rho V(D_o - D_i)}{\mu_e} \tag{37}$$

Reynolds number due to the rotation is described by

$$N_{RER} = \frac{2.025\rho\Omega(D_o - D_i)D_i}{\mu_{eR}} \tag{38}$$

where ρ is ppg, D_o and D_i are in., μ_{eR} is the effective viscosity for radial direction (cp), Ω is the rotation speed (rpm). Viscosities are expressed as

$$\mu = \left(\frac{K(D_o - D_i)^{1-n}}{144V^{1-n}}\right)\left(\frac{2+\frac{1}{n}}{0.0208}\right)^n \tag{39}$$

for axial direction, and

$$\mu_R = K\left(\frac{1}{n}\right)^n (\xi)\left(\frac{1}{\Omega}\right)^{1-n} \tag{40}$$

for radial direction, respectively. K is the consistency index (eq.cp), and n is the Power-Law index. Here,

$$\xi = \left(\frac{D_o^2 - D_i^2}{D_o^2}\right)\left(\frac{15}{\pi}\right)^{1-n}\left(\frac{1}{\left(1-\left(\frac{D_o}{D_i}\right)^{-\frac{2}{n}}\right)}\right)^n \tag{41}$$

Derivations of eq. (39) and eq.(40) are presented in Appendix A.

2.5 Classification of Fluid Behavior

Fluid model describes the flow behavior of a fluid by expressing a mathematical relationship between shear rate and shear stress. Rheological models used in this study to approximate fluid behaviour are 1) Newtonian model, 2) Power law model.

2.5.1 Newtonian Model

Newtonian fluid model is represented by the relationship

$$\tau = \mu\gamma \tag{42}$$

where τ is the shear stress, μ is the fluid viscosity and γ is the shear rate. For a Newtonian fluid, shear stress is directly proportianal to shear rate. Water and several pure organic fluids are Newtonian fluids.

2.5.2 Power Law Model

The Power Law Model is defined by

$$\tau = K(\gamma)^n \tag{43}$$

where K is the consistency index of the fluid, and n is the flow behavior index. Power Law fluid can be used to represent a pseudoplastic fluid ($n<1$), a Newtonian fluid ($n=1$), or a dilatant fluid ($n>1$). For drilling purposes, shear thinning is a very desirable property, and the most drilling fluids are pseudoplastic[82,87]. Drilling fluids used in this study obey Power Law Model. Flow curves related to these drilling fluids are presented in Appendix B.

CHAPTER 3

EXPERIMENTAL STUDY

3.1 Experimental Setup

Cuttings transport and single phase flow experiments are conducted using METU-PETE (Middle East Technical University Petroleum Engineering Department) Flow Loop for numerous drilling fluids including KCl-polymer muds and PAC systems and water. The test facility consists of cuttings collection and injection tanks, liquid tank, shale shaker, pumps, control valve, compressor, annular test section, pipe rotation system, pressure transducer and data acquisition system. A schematic view of the flow loop is presented in Figure 3.1 and a typical view of the portion of the test section is shown in Figure 3.2.

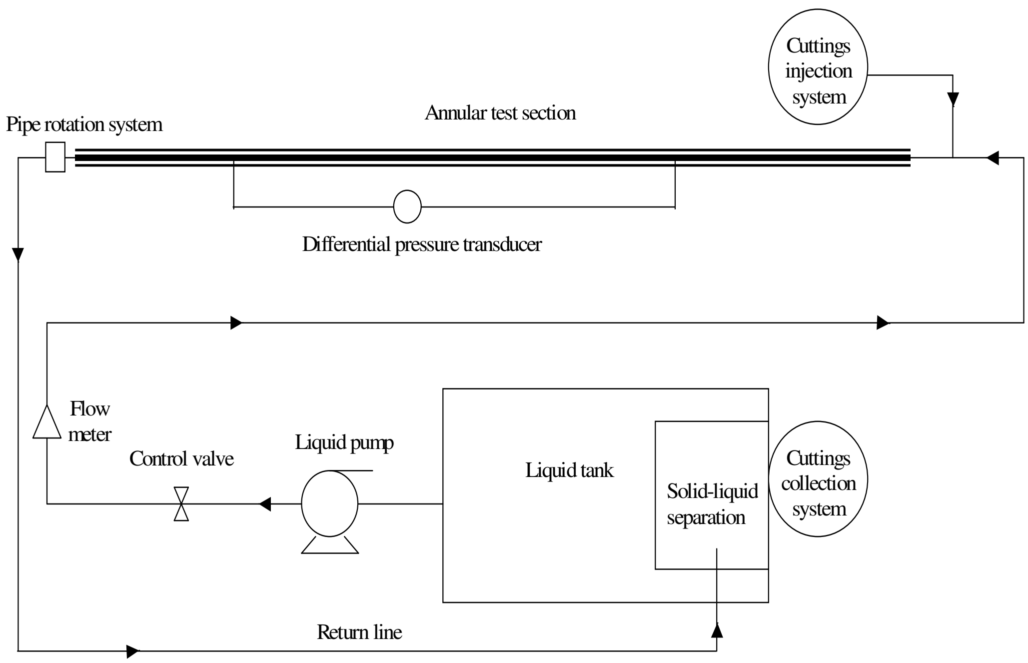

Figure 3.1- METU-PETE Flow Loop[8]

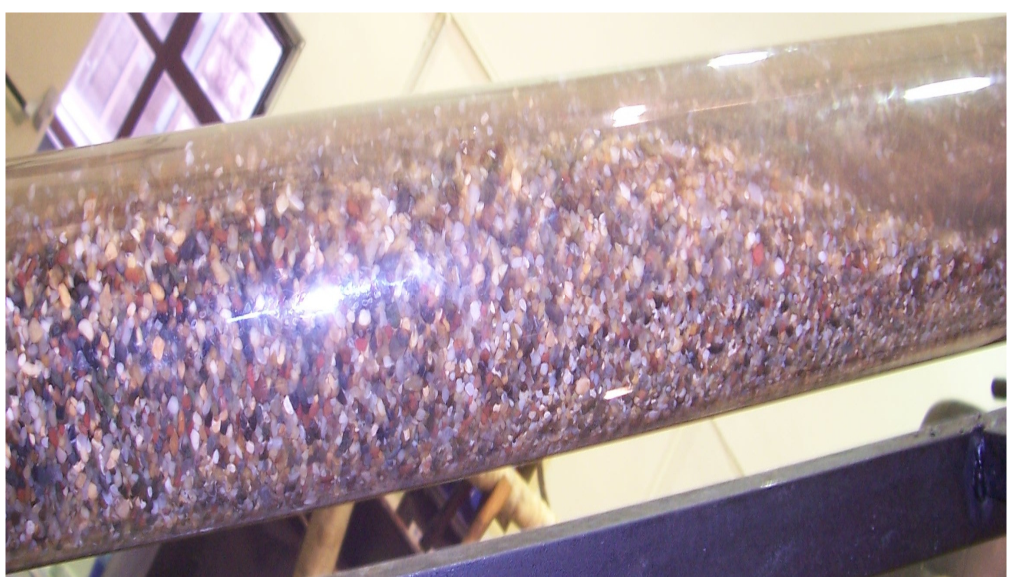

Figure 3.2 A portion of the test section during a cuttings transport experiment

Two centrifugal pumps for liquid injection are mounted with flow capacity of 250 gpm and 150 gpm and they are shown in Figure 3.3. 250 gpm centrifugal pump is used for experiments including high flow rate and 150 gpm centrifugal pump is used for experiments including low flow rate. Flow rate is controlled and measured using a magnetic flow meter and a pneumatic flow controller, as shown in Figure 3.4 and Figure 3.5.

Figure 3.3- Centrifugal pumps

Figure 3.4- Magnetic flowmeter

Figure 3.5- Pneumatic flow controller

Cuttings are injected using a helical screw controlled by a motor assisted by a speed frequency controller in order to adjust the rates of penetration (ROP). ROP is measured by weighing the cuttings injection and collection tanks. The cuttings weight measurement contained load cells, transducers, and remote indicators. To measure the injection and collection tanks weight, the load cells are placed underneath them. Cuttings injection tank is presented in Figure 3.6 and Figure 3.7 and collection tank is shown in Figure 3.8. Cuttings are separated from fluid by using shale shaker. Shale shaker is shown in Figure 3.9.

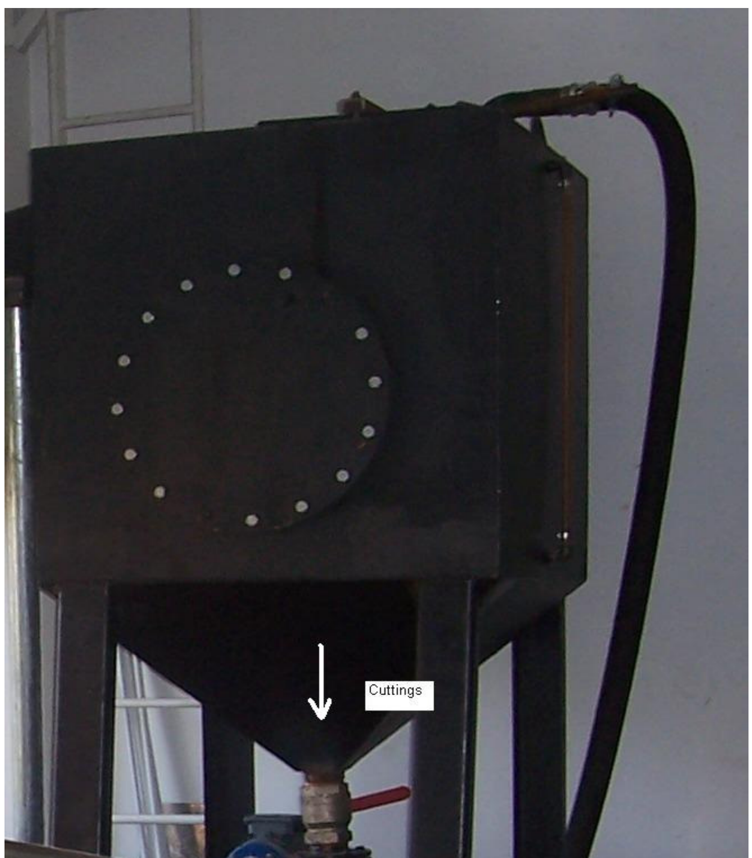

Figure 3.6- The cuttings injection tank-1

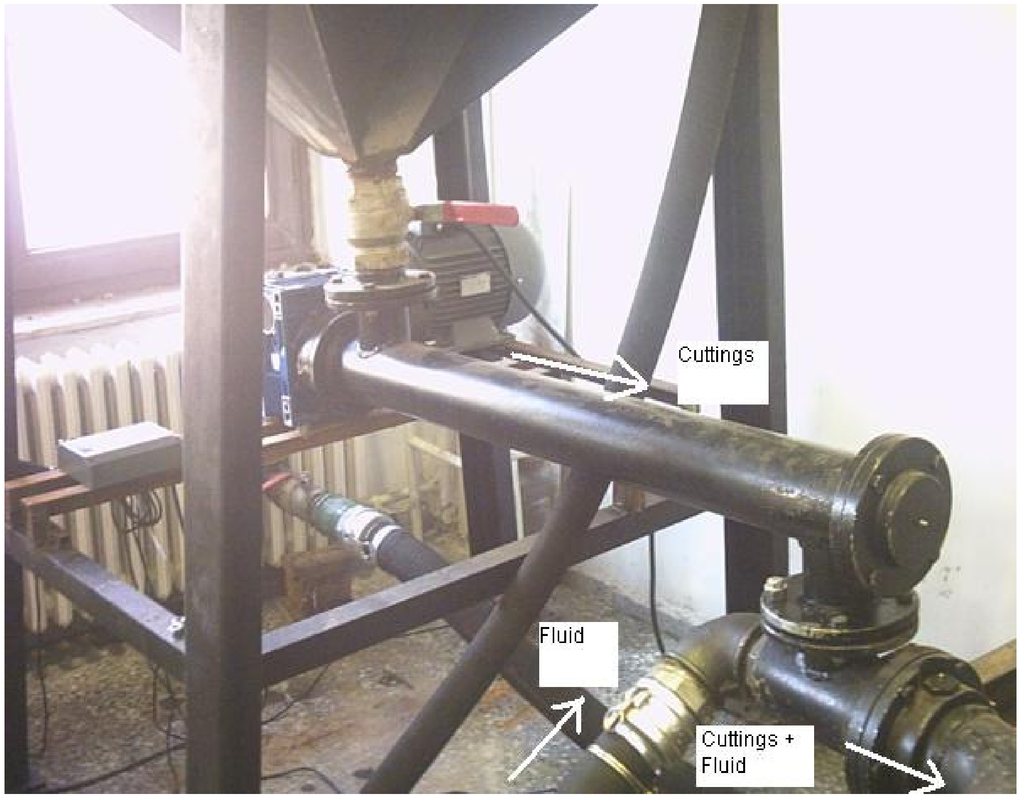

Figure 3.7- The cuttings injection tank-2

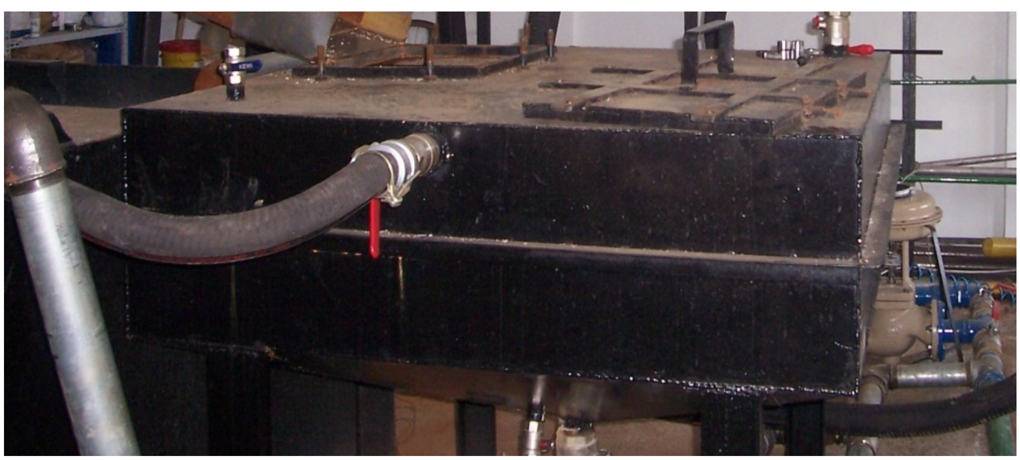

Figure 3.8- The   cuttings collection tank

Figure 3.9- The shale shaker

3.2 Test Section

The test section is 12 ft annular test section that can be set in any inclination from horizontal to vertical and consists of 2.91 in. I.D transparent acrylic casing with 1.8 in. O.D inner drillpipe. The transparent casing allowed the observation of the cuttings movements and developed bed . Also, 1.8 in. O.D inner drillpipe can be rotated up to 200 rpm.

Figure 3.10- Test Section

The determination of the pressure transmitters locations is one of the major concerns in order to collect correct experimental data and eliminate end effects. Therefore, entrance and exit effects are calculated for test section using Eq.44 [91] and Eq.45 [94]. Fully developed region is obtained 0.97 m for annular test section.

$$L_{entrance} = 50 D_{hyd} \tag{44}$$

$$L_{exit} = 4.4 (N_{\mathrm{Re}})^{\frac{1}{6}} D_{hyd} \tag{45}$$

3.3 Test Matrix

Cuttings transport experiments were conducted using pure water as well as water-based drilling fluids consist of different concentrations of xanthan biopolimer, starch, KCl and soda ash, weighted with barite. Flow velocities from 0.64 m/s to 3.05 m/s, rate of penetrations from 0.00127 to 0.0038 m/s, flow rates were between 27 gpm to 150 gpm, and inclinations varied from horizontal to 60°. Average cuttings specific gravity of 2.65 and average cuttings size of 3 mm. Moreover, single phase experiments with water or drilling fluids were performed for various flow rate and drillpipe rotations. Cuttings bed thickness was recorded at four different stations on the test section by visual observation at each station. Inner pipe can be rotated by a rotation system with a rotation speed range of 0-120 rpm. During the flow tests, pressure drop was also measured at a fully developed section on the test section using a digital pressure transducer. Drillpipe was fully eccentric during cuttings transport experiments. Data logger and data acquisition software were used to gather and store the experimental data. Fann viscometer was used to determine the rheological properties (n and K) of drilling fluids. More than 690 experiments have been conducted in this study, including properties of the drilling fluids presented in Table-1.

Table 1 –Properties of the fluids used in this study

	n	K(pa s^n)	density(kg/m^3)
water	1	0.001	997
drilling fluid-1	0.51	0.289	1005
drilling fluid-2	0.47	0.479	1196
drilling fluid-3	0.41	0.806	1077
drilling fluid-4	0.31	1.843	1196

3.4 Flow Loop Frictional Pressure Drop Calibration

Frictional pressure loss calibration is the most important parts of the experimental study. A proper measurement of the pressure drop is critical for the verification of fully developed region in the flow loop and mechanistic model calculations. Figure 3.11 presents that the measured and calculated pressure drop values are good agreement with each other for most cases.

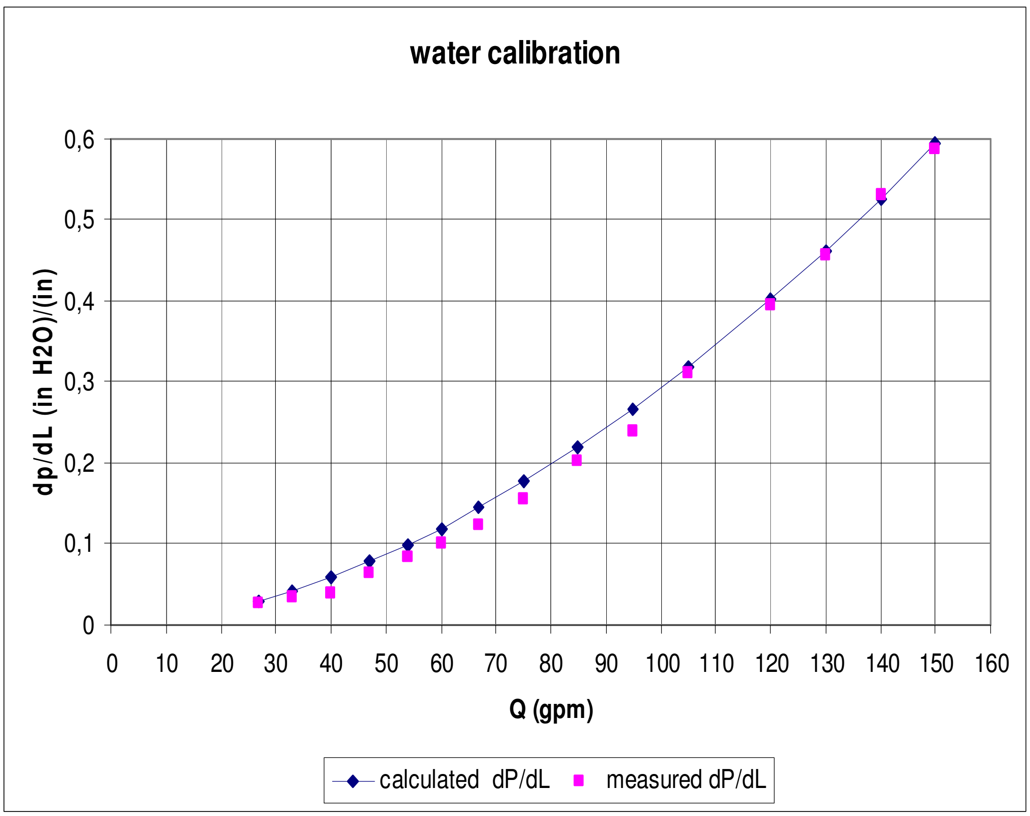

Figure 3.11- Pressure Drop Calibration with water

3.5 Experimental Test Procedure

The experimental procedure of the cuttings transport tests is as follows:

1. The desired test section angle was adjusted.
2. Using the centrifugal pump, the fluid was pumped at a desired flow rate from the liquid collection tank to the flow loop.
3. Once fluid flow rate was stabilized, the cuttings were injected from the injection tank into the system.
4. The desired pipe rotation speed and the rate of penetration were adjusted.
5. When the steady-state conditions were reached, the frictional pressure loss inside the test section and flow rate were recorded using data acquisition systems. Also, the cuttings bed thickness was recorded at four different locations on the test section.

CHAPTER 4

MATHEMATICAL MODEL PREDICTING PRESSURE LOSS IN CONCENTRIC ANNULUS

Accurate prediction of frictional pressure losses within the wellbore, especially inside the annulus, is a major factor in order to determine bottomhole pressure and minimum hydraulic requirements as well as foresee any serious problems such as loss of circulation, improper rig power selection, hole cleaning problems etc. during drilling operations. Thus, in order to identify the frictional pressure loss in an annulus becomes more significant and essential. In this chapter, pressure loss estimation methods and discussion of the model performance are presented in details.

4.1 Simplified Solution Using Mixing Length Approach

In fluid dynamics, the mixing length theory is one of the turbulence models to predict the turbulent viscosity. According to the mixing length model, turbulent viscosity in Eq. (15) can be expressed as

$$\mu_t = l_m^2 \left| \frac{\partial u}{\partial y} \right| \tag{46}$$

The mixing length and damping function are presented as

$$l_m = H\left[0.14 - 0.08\left(1 - \frac{y}{H}\right)^2 - 0.06\left(1 - \frac{y}{H}\right)^4\right] f_\mu \tag{47}$$

$$f_\mu = 1 - \exp(-\frac{y^+}{26}) \tag{48}$$

where $y^+ = \dfrac{yu_*}{\mu}$, $u_* = \sqrt{\dfrac{\tau_w}{\rho}}$ and $\tau_w = -(\dfrac{\partial p}{\partial x} - \rho \omega_a{}^2 H) * H$ (49)

This model can be extended for non-Newtonian fluids by using viscosity, μ in Eq. (15).

$$\mu = \frac{1}{4} K (\frac{D_o - D_i}{2u})^{1-n} \left(\frac{3n+1}{n}\right)^n \tag{50}$$

where u is the axial fluid velocity, K is the consistency index (Pa s^n), and n is the Power-Law index (dimensionless).

4.1.1 Explicit Solution of Governing Equation

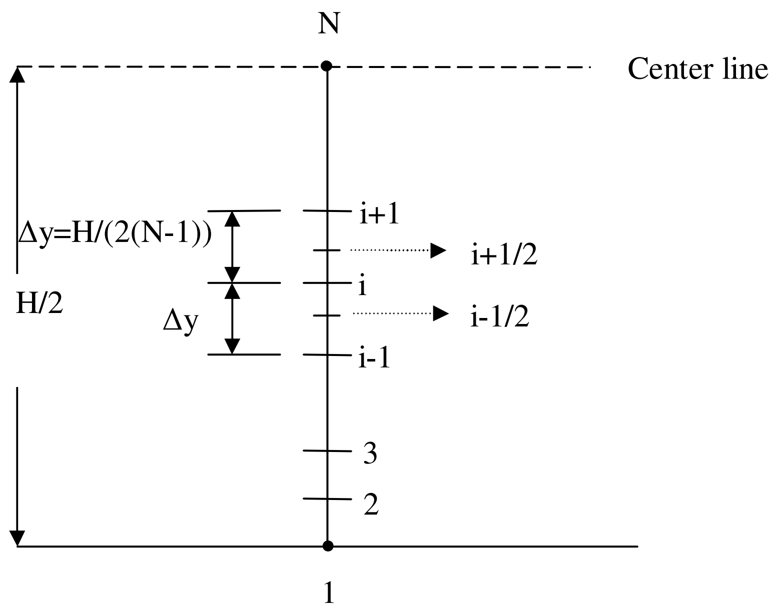

Figure 4.1- Discrete domain by using finite difference technique

BC1=0; Boundary condition at wall, u=0

BC2=0; Boundary condition at centerline, du/dy=0,

Using assumptions, Eq.(10) can be written as

$$\frac{\partial}{\partial y} T_{yx} = \frac{\partial p}{\partial x} - \rho \omega_a^2 y \tag{51}$$

$$M = \frac{\partial p}{\partial x} - \rho \omega_a^2 y \tag{52}$$

for no-rotation case, ω_a =0

$$\frac{\partial}{\partial y} T_{yx} = M \tag{53}$$

By using finite difference approximation, Eq. (53) can be expressed as

$$\mu_{i+1/2}\frac{u_{i+1}-u_i}{\Delta y}-\mu_{i-1/2}\frac{u_i-u_{i-1}}{\Delta y}=(y_{i+1/2}-y_{i-1/2})M \tag{54}$$

$$-A_i u_{i+1}+B_i u_i-C_i u_{i-1}=D_i \tag{55}$$

where $A_i=\dfrac{\mu_{i+1/2}}{\Delta y}$, $B_i=A_i+C_i$, $C_i=\dfrac{\mu_{i-1/2}}{\Delta y}$ and $D_i=(y_{i+1/2}-y_{i-1/2})\dfrac{\partial p}{\partial x}$ (56)

4.2 Flow Chart of Computer Program

A computer code based on the proposed mechanistic model is developed to predict frictional pressure loss inside concentric annulus by using Matlab 7.0.4. The performance of the mathematical model and experimental data analysis are discussed in details in the next section. The flow chart of the computer program used in this study is presented in Figure 4.2.

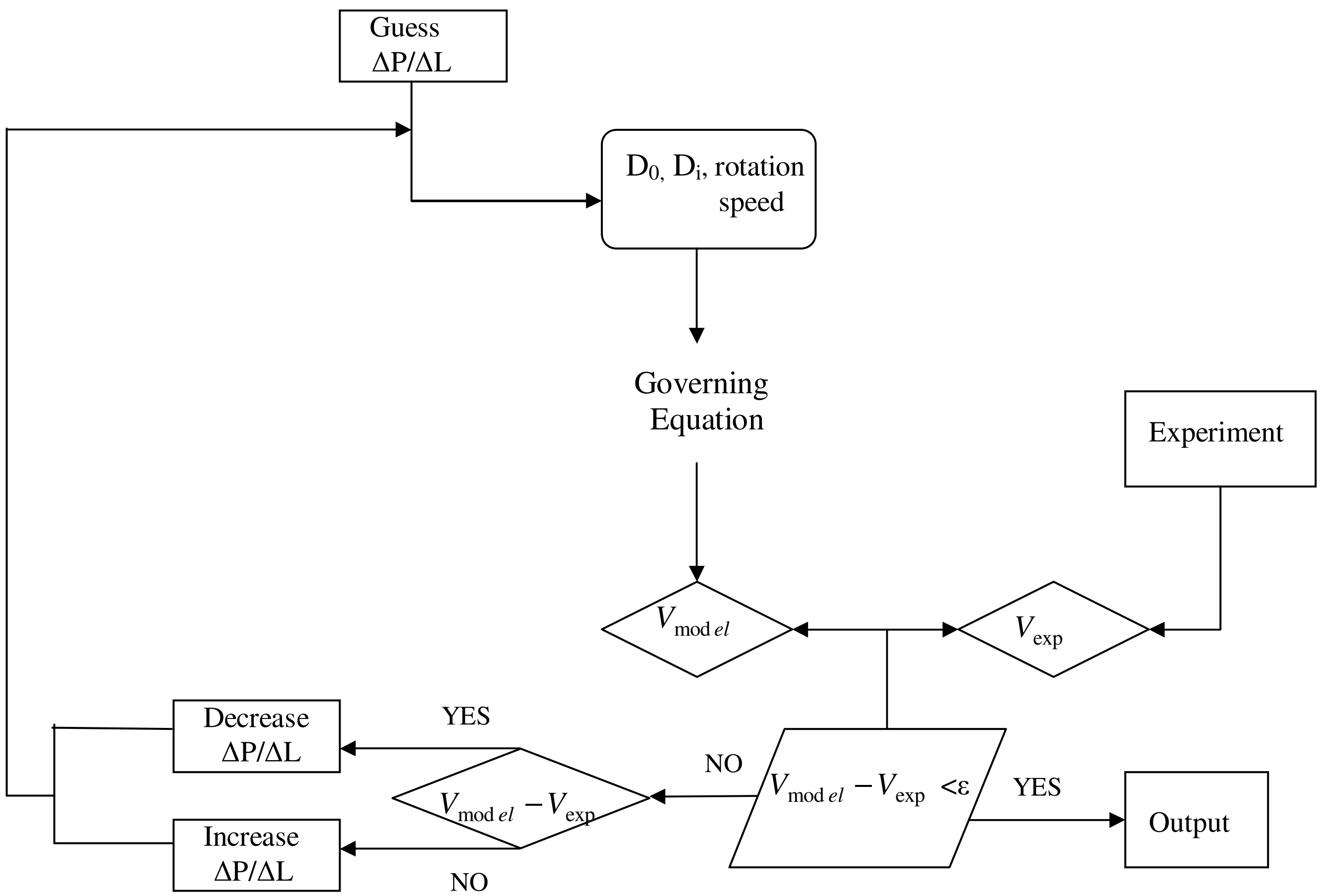

Figure 4.2- Flow chart of MATLAB code for the frictional pressure lossdetermination with drill pipe rotation

4.3 Comparison of Mechanistic Model and Experimental Data

4.3.1 Predicting Pressure Losses of Newtonian Fluids Flow through Horizontal Concentric Annulus

The annular frictional pressure losses are calculated by using proposed mechanistic model as well as widely used extension pipe flow equations such as hydraulic diameter, slot equation and Crittendon's criteria and a software based on finite element model (ANSYS) for various flow rates. The performance of proposed model is also compared with McCann et al.[57] published experimental results and experimental data gathered at Middle East Technical University Cuttings Transport Flow Loop.

Figure 4.3 shows lower values of pressure gradients and the higher values of pressure gradients are presented in Figure 4.4. As seen from these figures, hydraulic diameter approach and Crittendon's empirical correlation and proposed model estimate frictional pressure gradient values with a high accuracy. On the other hand, slot equation (eq.17) give close results to experimental results for lower values of pressure gradients.

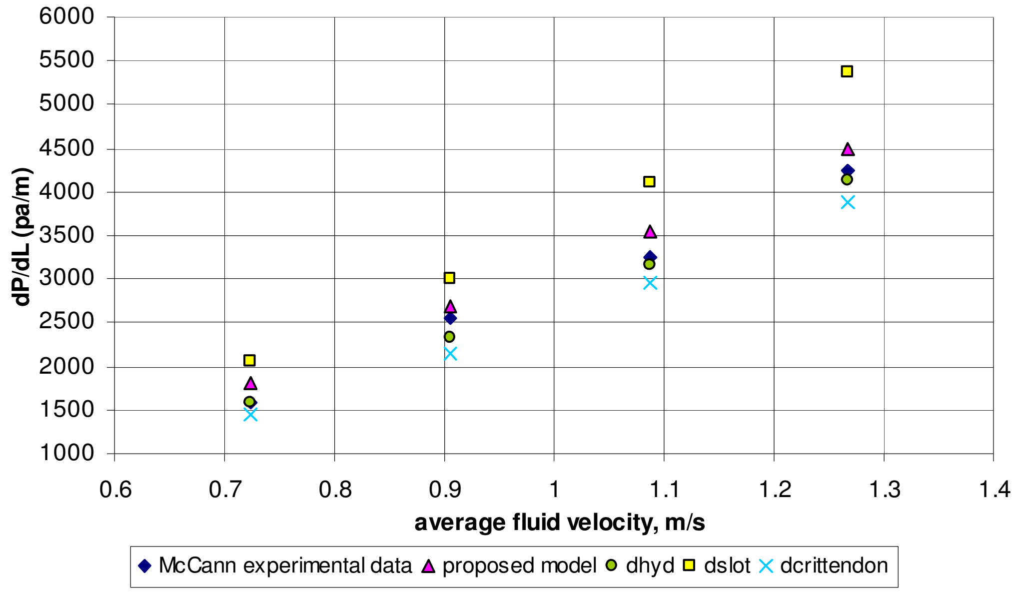

Figure 4.3- Comparison of McCann et al.[57] experimental results with the calculated pressure gradient values for low $\Delta P/\Delta L$

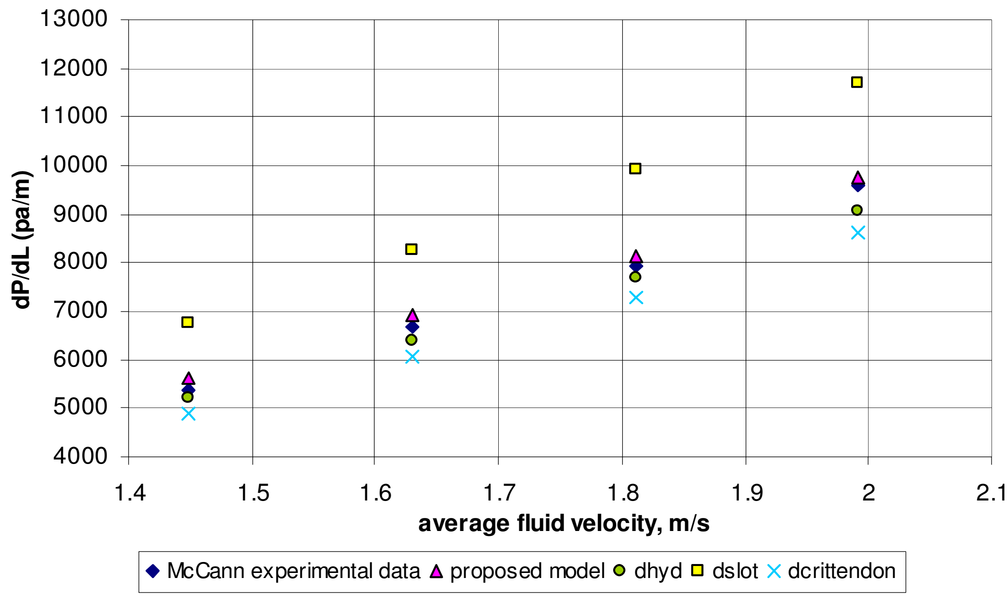

Figure 4.4- Comparison of McCann et al.[57] experimental results with the calculated pressure gradient values for high $\Delta P/\Delta L$

Proposed model predictions compared with experimental data obtained from Middle East Technical University Flow Loop and Computational Fluid Dynamics (CFD) simulation software code ANSYS are presented in Figure 4.5 and Figure 4.6 As seen from these figure, if model is used, pressure gradient values can be estimated correctly. CFD software and proposed model used different shear stress models (k-ε and mixing length theory, respectively) in order to calculate the turbulent eddy-viscosity. Also, they computed pressure loss using diverse models such as finite element and finite difference approximation. Thus, proposed model and CFD software could give slightly different frictional pressure loss results in concentric annuli for fully turbulent flow.

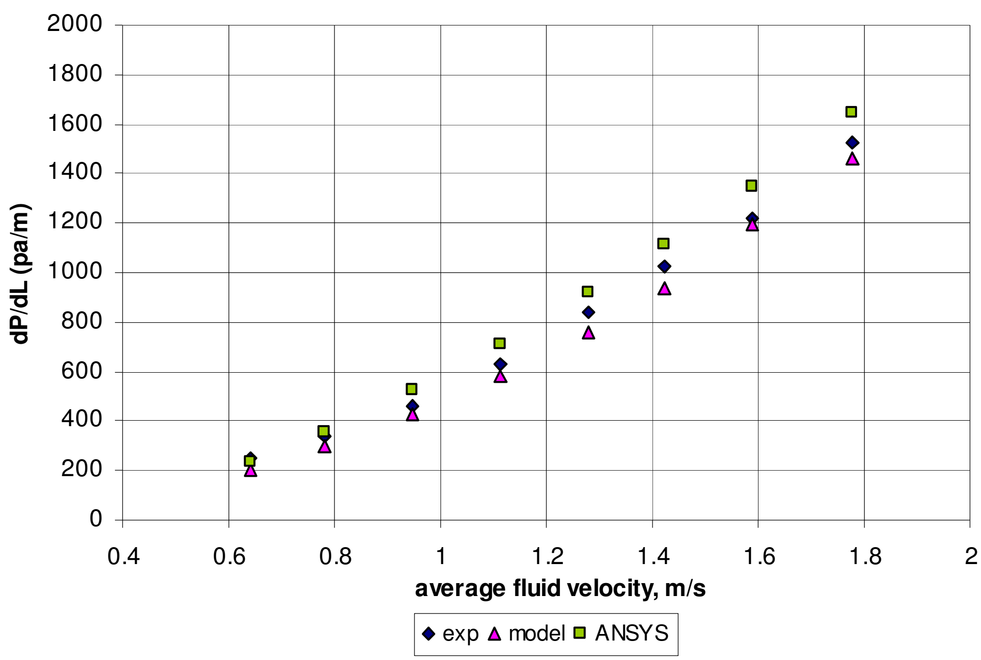

Figure 4.5- Comparison of the experimental data obtained from METU- PETE Flow Loop with the calculated pressure gradient values in annuli for low ΔP/ΔL

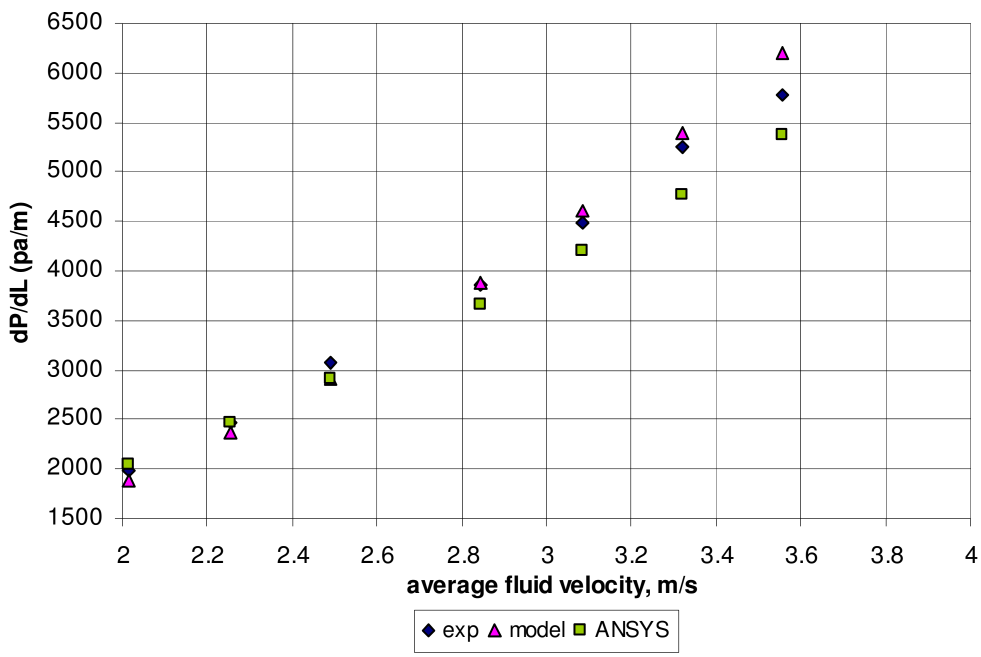

Figure 4.6- Comparison of the experimental data obtained from METU- PETE Flow Loop with the calculated pressure gradient values in annuli for high ΔP/ΔL

The proposed model accuracy can be examined by investigating Figure 4.7 and Figure 4.8, where the experimental results and model predictions for low and high pressure drop are presented. The dashed lines in these figures are in ±20 % and ±10 % error margin, and the solid line represents the perfect match between the experimental frictional pressure gradient values and calculated results for the proposed model and the CFD software. As seen from these figures, all of the data points predicted by the proposed model fall into ± 10 error margins.

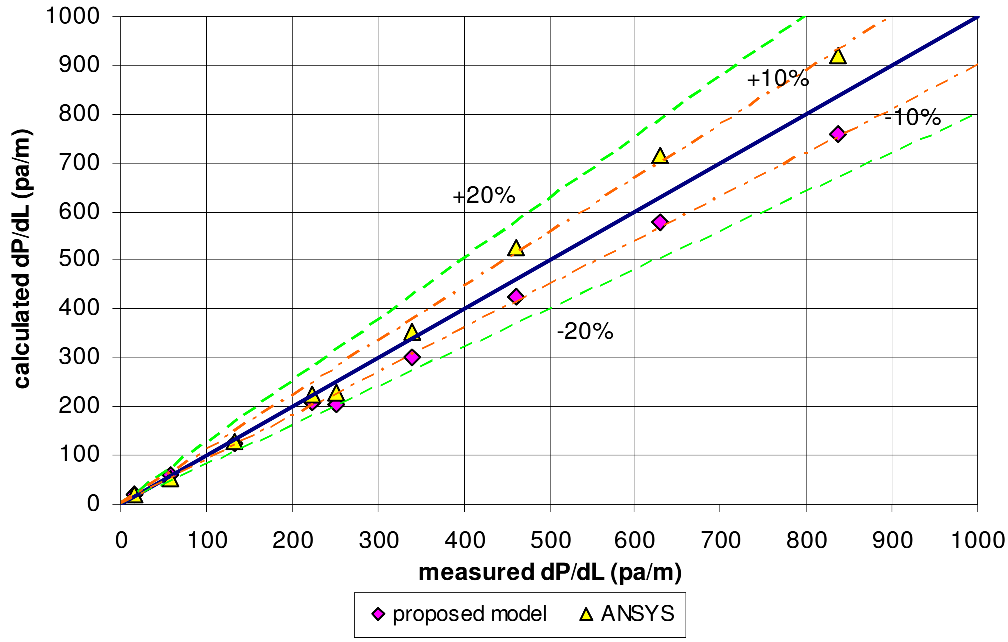

Figure 4.7- Comparison of experimental and calculated frictional pressure gradient values for low $\Delta P/\Delta L$

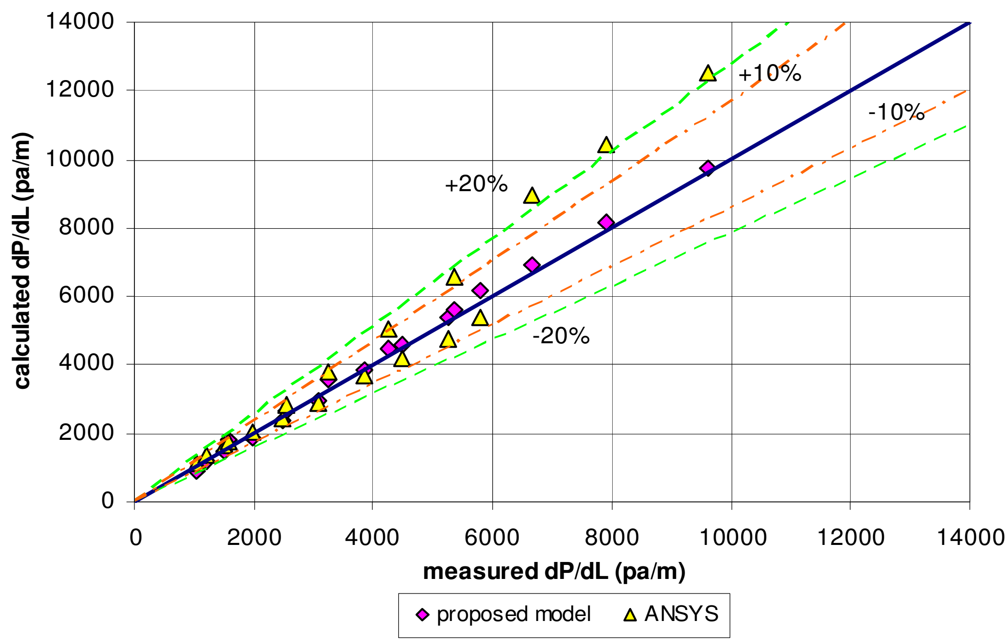

Figure 4.8- Comparison of experimental and calculated frictional pressure gradient values for high $\Delta P/\Delta L$

4.3.2 Estimation of Pressure Losses for Newtonian Fluids in Horizontal Concentric Annulus with Pipe Rotation

In this section, the frictional pressure loss of Newtonian fluid flow through in concentric annulus with pipe rotation is calculated by using proposed mechanistic model and Computational Fluid Dynamics (CFD) code ANSYS. To verify the proposed model, estimated frictional pressure losses are compared with experimental data gathered at METU-PETE Flow Loop as well as Computational Fluid Dynamics (CFD) software.

4.3.2.1 Model Performance

Experimental data obtained from METU-PETE Flow Loop are compared with both mathematical model and CFD simulation for 0- 120 rpm and the results are presented in Figures 4.9- 4.18.

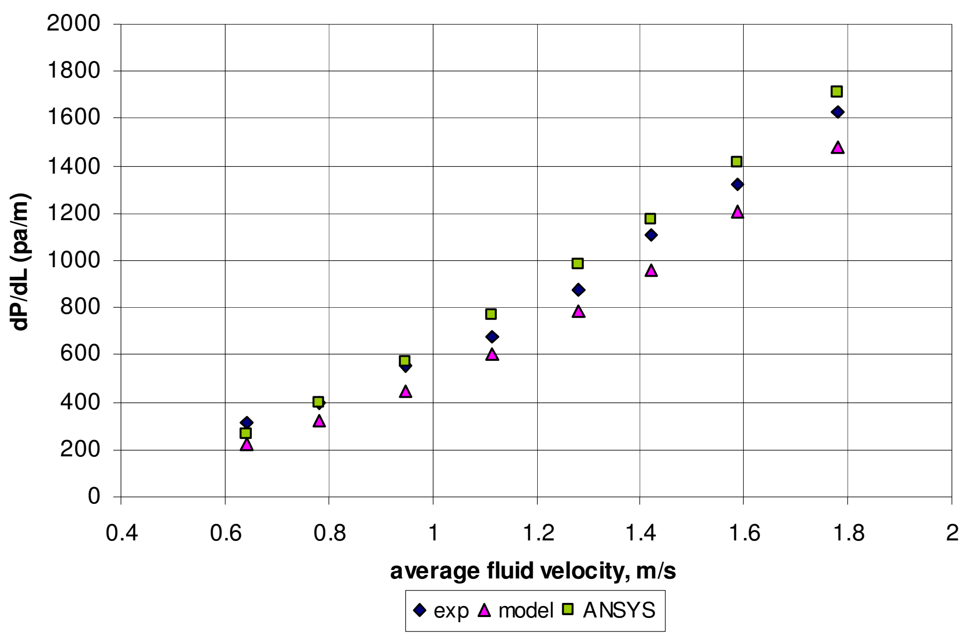

Figure 4.9- Comparison of proposed model and ANSYS with experiment for pipe rotation (rpm)=40 and low ΔP/ΔL

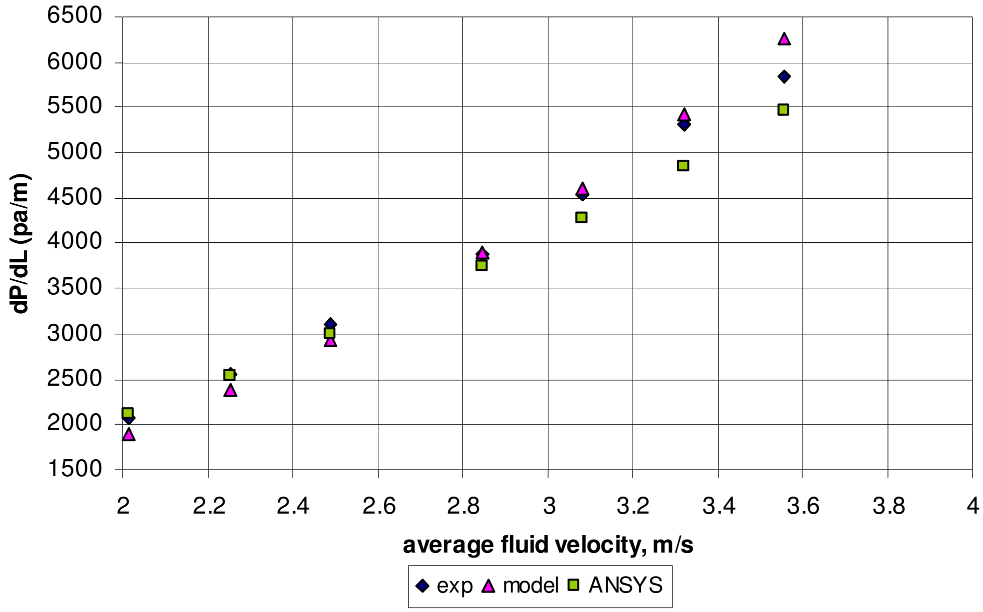

Figure 4.10-Comparison of proposed model and ANSYS with experiment for pipe rotation (rpm)=40 and high ΔP/ΔL

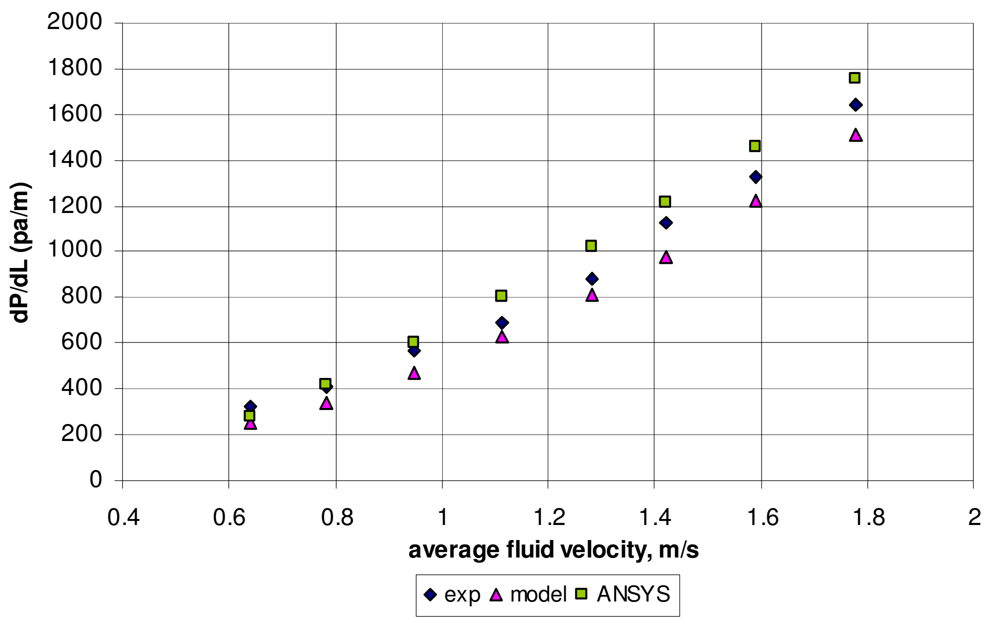

Figure 4.11- Comparison of proposed model and ANSYS with experiment for pipe rotation (rpm)=60 and low ΔP/ΔL

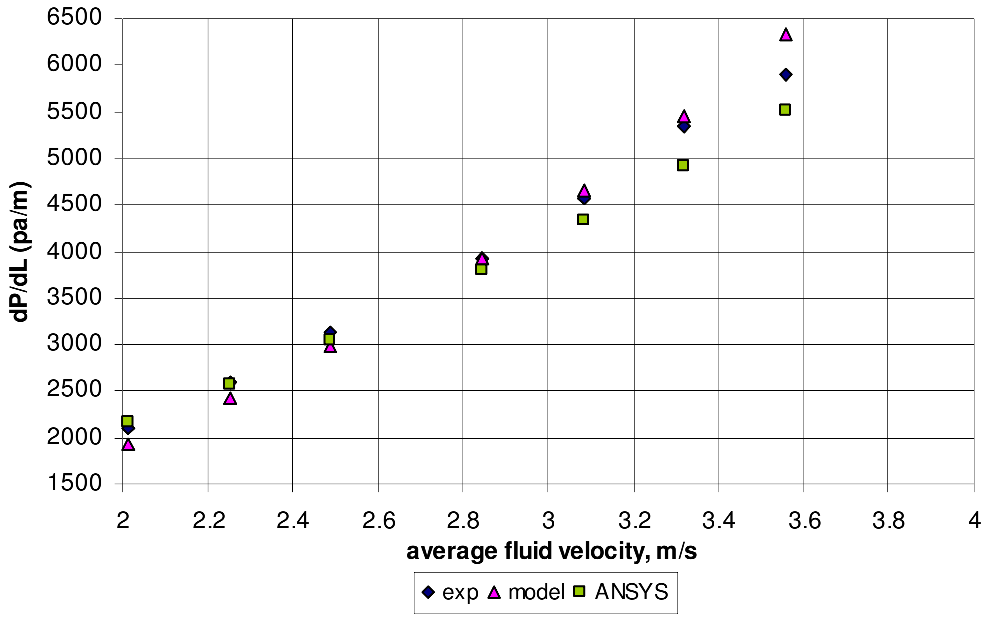

Figure 4.12- Comparison of proposed model and ANSYS with experiment for pipe rotation (rpm)=60 and high ΔP/ΔL

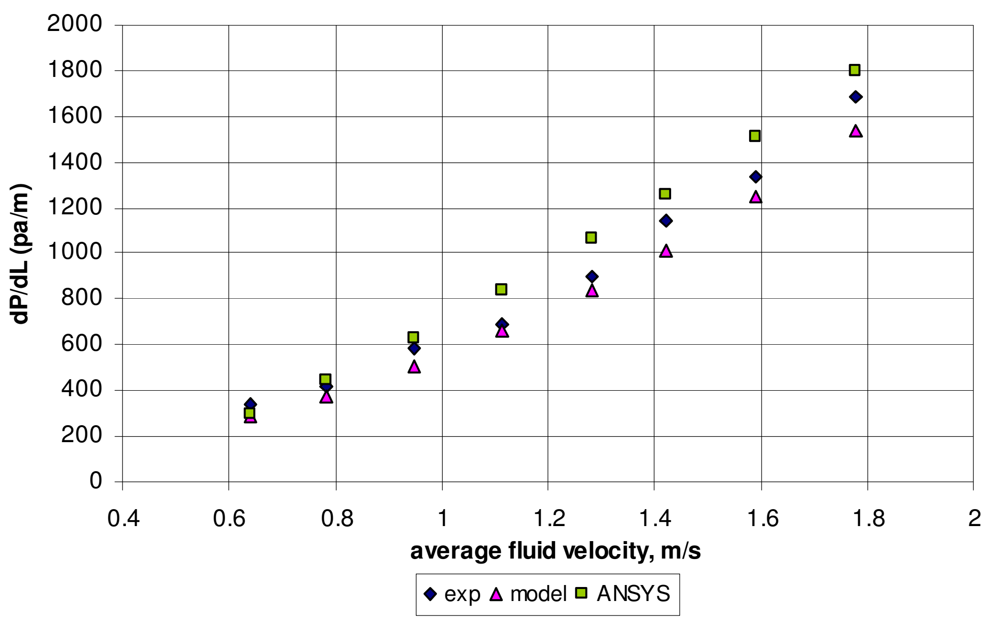

Figure 4.13- Comparison of proposed model and ANSYS with experiment for pipe rotation (rpm)=80 and low ΔP/ΔL

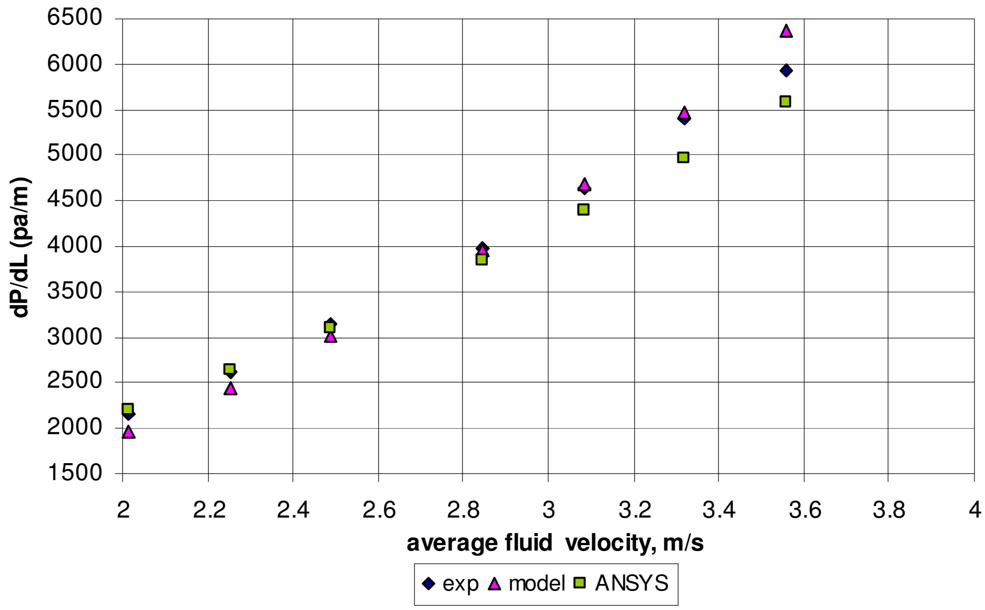

Figure 4.14- Comparison of proposed model and ANSYS with experiment for pipe rotation (rpm)=80 and high ΔP/ΔL

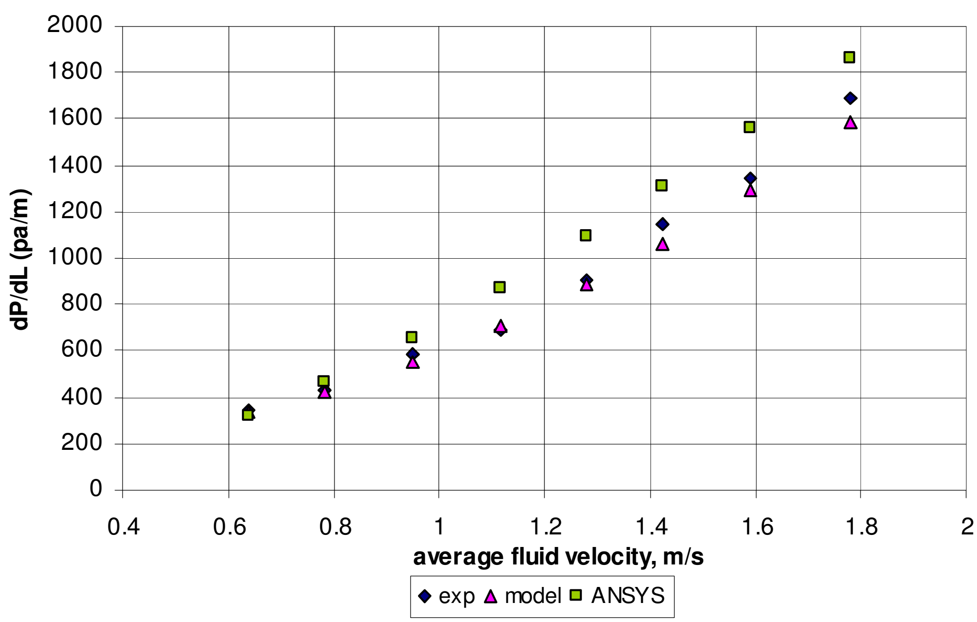

Figure 4.15- Comparison of proposed model and ANSYS with experiment for pipe rotation (rpm)=100 and low ΔP/ΔL

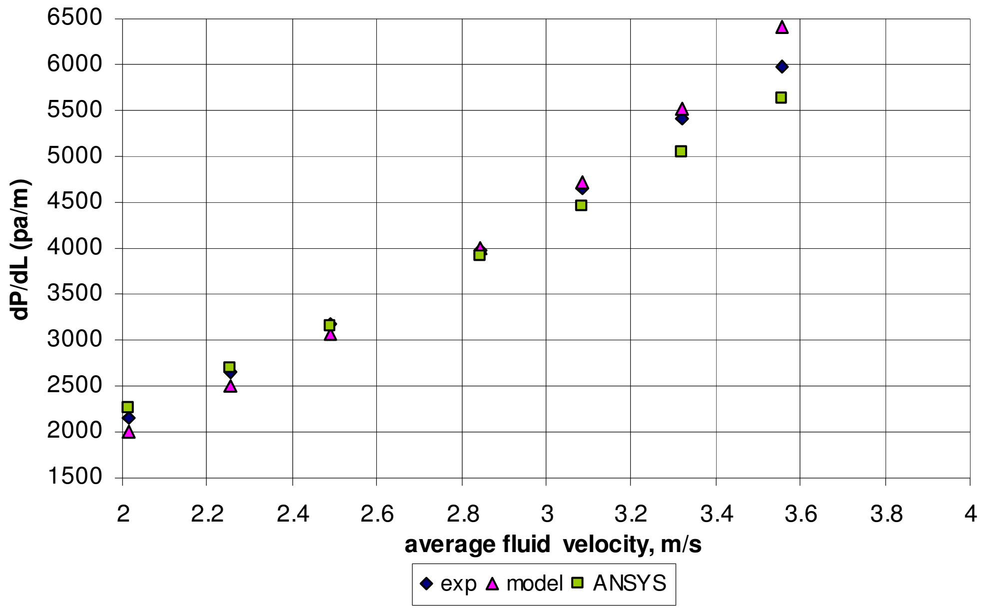

Figure 4.16- Comparison of proposed model and ANSYS with experiment for pipe rotation (rpm)=100 and high ΔP/ΔL

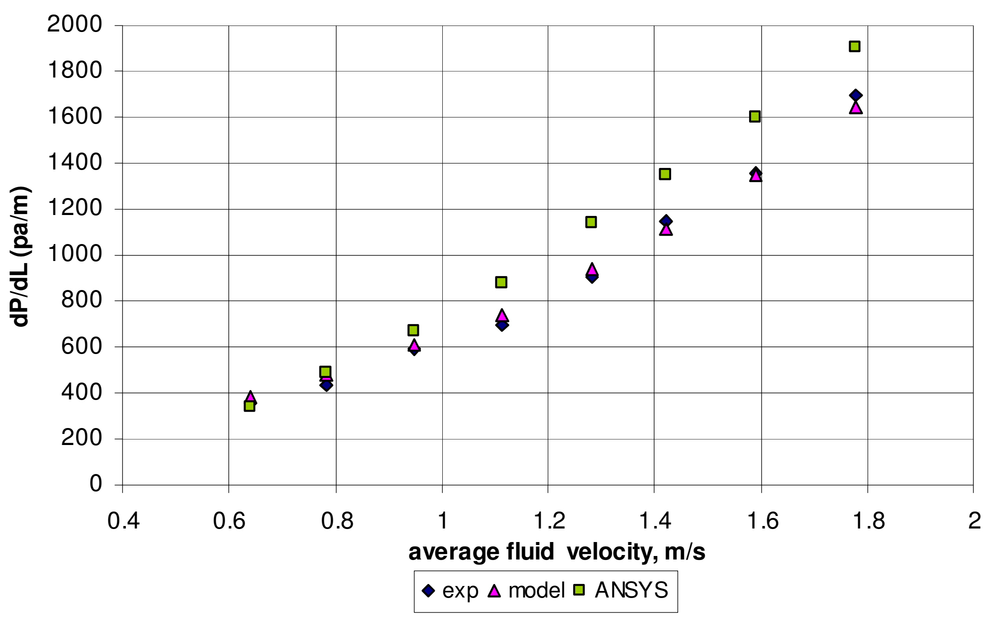

Figure 4.17- Comparison of proposed model and ANSYS with experiment for pipe rotation (rpm)=120 and low ΔP/ΔL

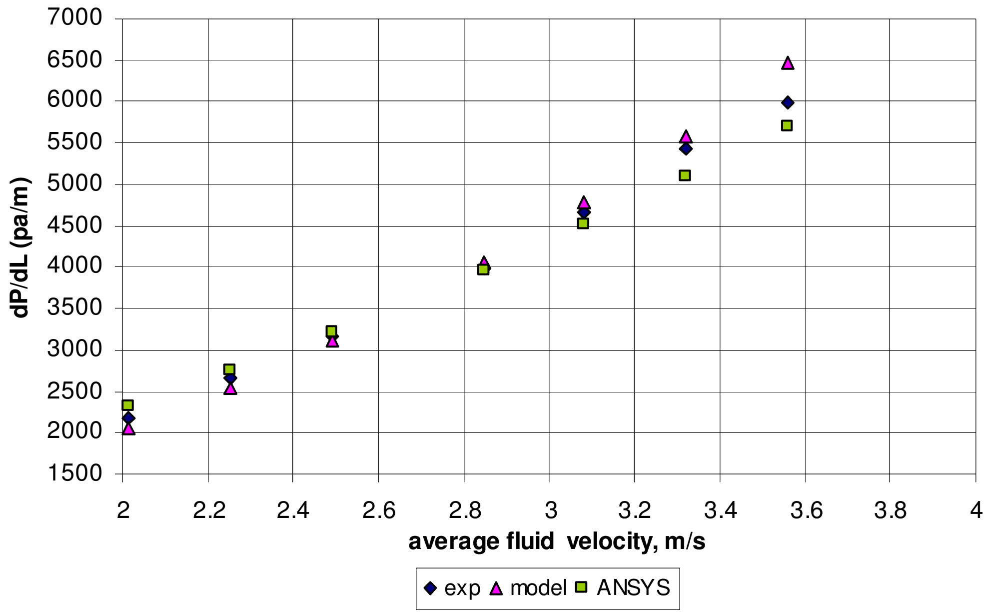

Figure 4.18- Comparison of proposed model and ANSYS with experiment for pipe rotation (rpm)=120 and high $\Delta P/\Delta L$

4.3.2.2 Error Analysis

Experimental results and model predictions for annular frictional pressure losses of Newtonian fluid flow in concentric annulus with drillpipe rotation are presented in Figures 4.19-4.21 in order to demonstrate the accuracy of the models. Solid lines in these figures represent the perfect match between the experimental and calculated values. As seen from these figures, there is a good agreement in most cases between model predictions and experimental data. Additionally, an error analysis is carried out for mathematical model estimations. There are 99 data points for different flow rates and pipe rotations, and the error distribution is presented in Figure 4.21. Figure 4.21 shows that the model can estimate the frictional pressure loss with an error of less than 10% for 78 data points and 12 points that fall into an error range of 20% and only 2 data points showed a deviation in excess of 20% and maximum deviation of 23.6 %.

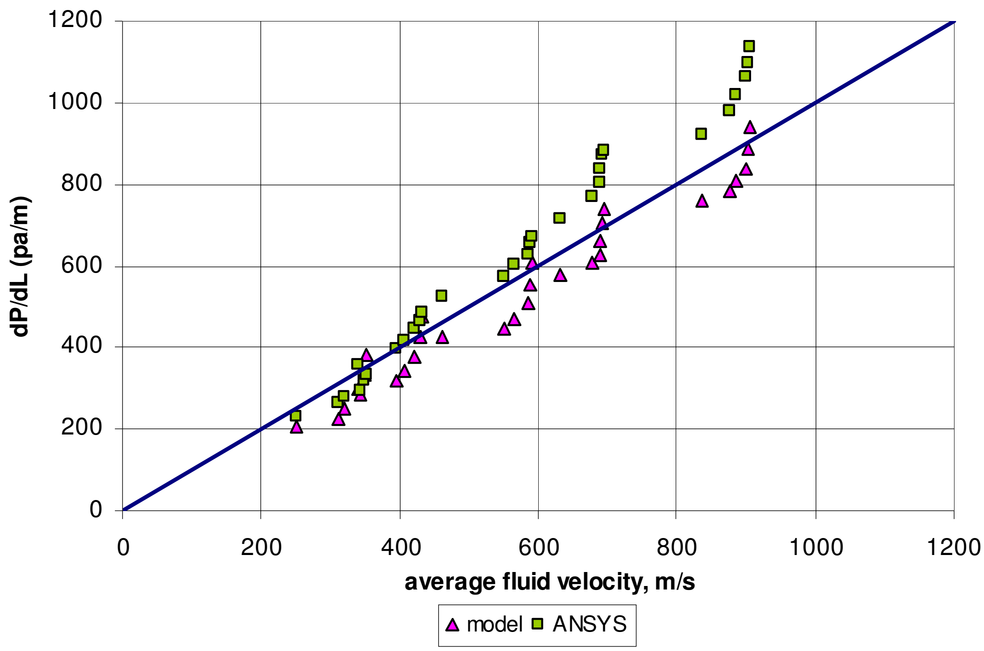

Figure 4.19- Comparison of the model and ANSYS predictions with experiments of pressure gradient values of water through concentric annulus for low ΔP/ΔL

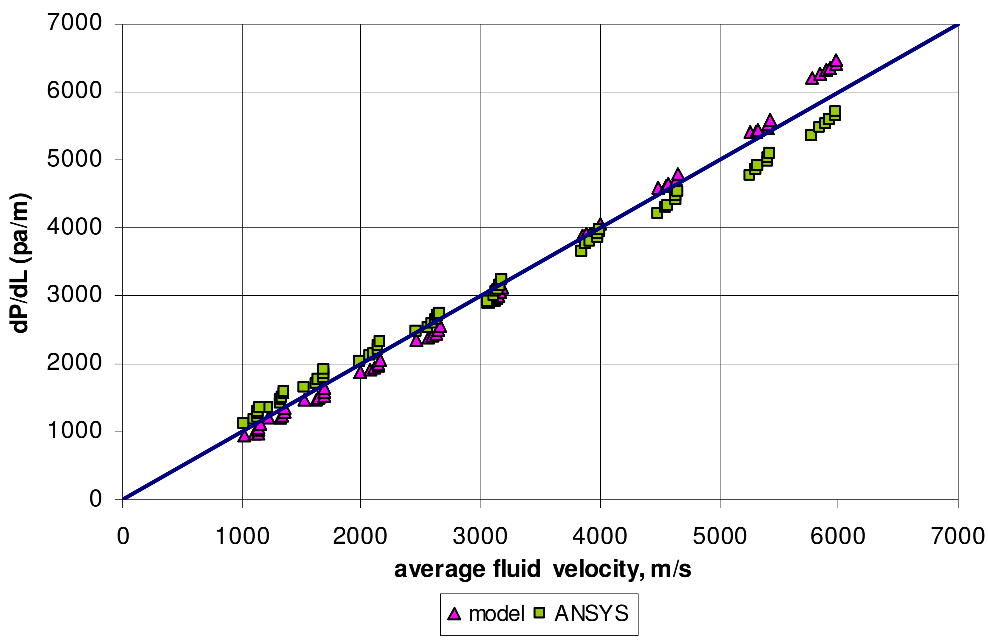

Figure 4.20- Comparison of the model and ANSYS predictions with experiments of pressure gradient values of water through concentric annulus for high ΔP/ΔL

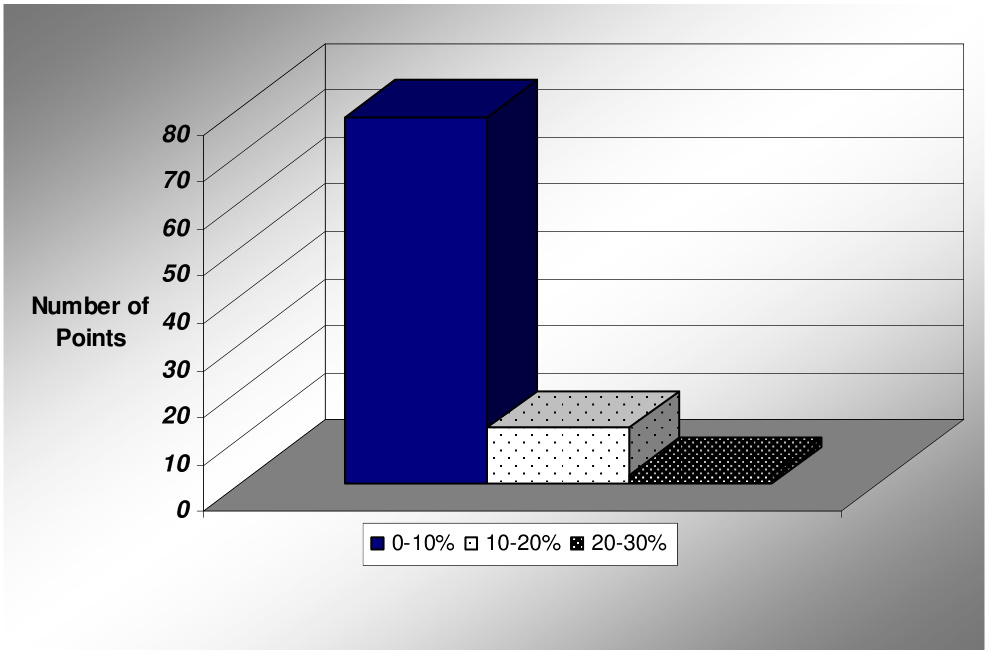

Figure 4.21- Comparison of the performance proposed model as a function of error distribution

CHAPTER 5

COMPUTATIONAL FLUID DYNAMICS SIMULATION

Computational Fluid Dynamics (CFD) software is widely used to set up simulations in many engineering areas such as chemical, mechanical, civil and aerospace engineering. Equations of continuity and momentum are numerically solved by using CFD software. In this study, a commercial software package, Ansys Workbench and Ansys CFX were used to calculate frictional pressure loss of Newtonian fluid flow in annulus with pipe rotation and to simulate cuttings transport in horizontal wellbores. The CFD results were compared with experimental data.

5.1 ANSYS Workbench and ANSYS CFX

Concentric and fully eccentric annulus were created and meshed using Ansys Workbench. Simulations were solved using Ansys CFX. Ansys CFX is a general purpose Computational Fluid Dynamics (CFD) code, combining an advanced solver with powerful pre-and post-processing capabilities and contains CFX Pre, CFX Solver and CFX Post. The flow chart of the CFD codes is given in Figure 5.1. Ansys CFX tools are as follows:

CFX Pre: This package is used to define the simulation, import the mesh and specify a type of simulation and initial values.

CFX Solver: It solves all the solution variables for the simulation for the problem specification generated in Ansys CFX-Pre.

CFX Post: This Ansys CFX tool is used to analyze ANSYS CFX simulation results[90].

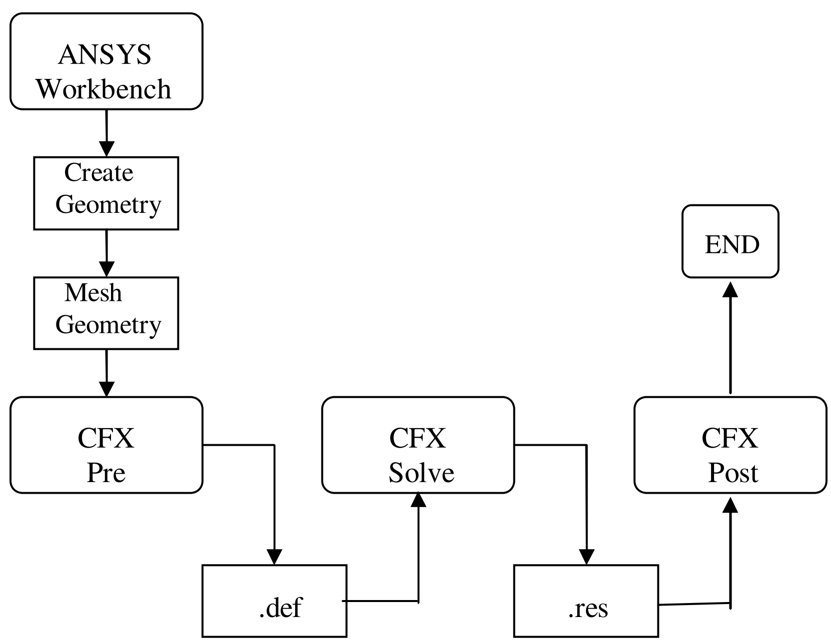

Figure 5.1- Flow chart of ANSYS

In this study, two geometries were created, i.e., they consist of 2.91 x 1.8 in and 1.5 x 1.25 in annulus. The pipe length, L, required to eliminate the end effects and to obtain fully developed flow, selected for simulation greater than the maximum entrance length, L_e[94].

$$L_e = 0.06(D_o - D_i)N_{R_e} \qquad \text{(Laminar flow)} \tag{57}$$

$$L_e = 4.4(D_o - D_i)(N_{R_e})^{\frac{1}{6}} \qquad \text{(Turbulent flow)} \tag{58}$$

When the geometry is created, it should be appropriately meshed to generate the computational grids. Computation speed and accuracy can be improved considerably a well meshed geometry. Number of tetrahedral mesh directly influences accuracy of frictional pressure loss results obtained from CFD. Therefore, in this study, tetrahedral mesh number in geometry was increased until it did not affect pressure loss results in annulus. In this study, for all of the cases, the geometry is divided approximately 2.3 x 10^6 tetrahedral meshes. Tetrahedral meshing sample for fully eccentric annulus is shown in Figure 5.2.

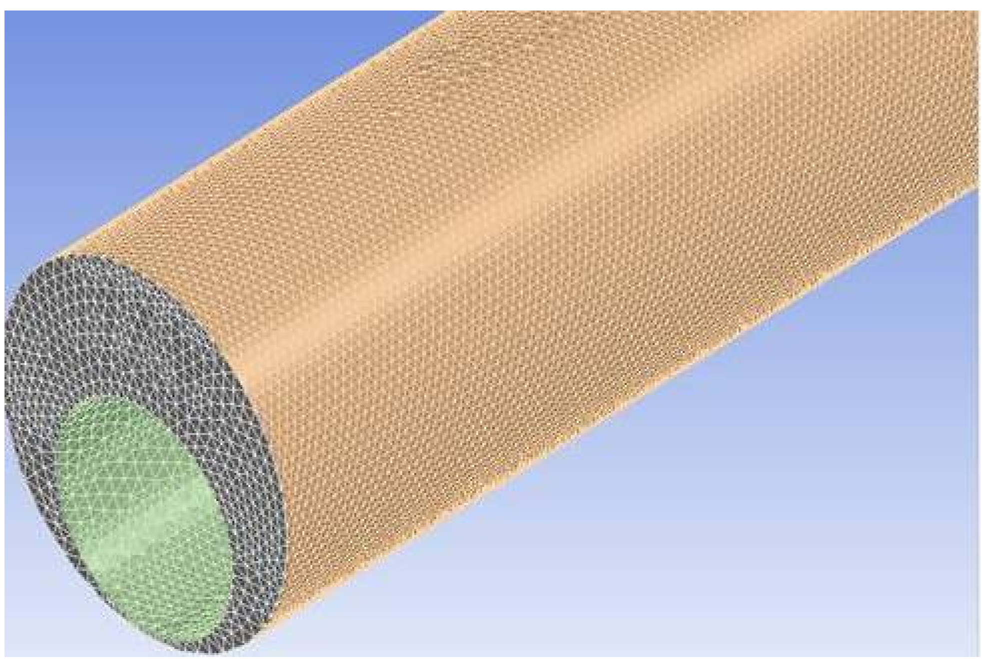

Figure 5.2- Tetrahedral meshing sample for fully eccentric annulus

After the meshed geometry is imported to CFX Pre, the boundary conditions and initial values have to be described. The inlet was defined as an inlet velocity which depends on the average velocity at the inlet. The inner drill pipe was described as a rotational wall depending on the pipe rotation speed. The outlet was specified as atmospheric pressure and the flow was assumed to be steady, incompressible, isothermal and k-ε model used for turbulent flow. Pressure and velocity profile within the annulus were obtained from the CFD simulations.

5.2 Computational Fluid Dynamics (CFD) Software Solution Method

5.2.1 Single Fluid Flow Fundamentals

The equation of continuity (Eq.8) and equation of motion (Eq. 9) are also valid for CFD model simulation of fluid flow in annulus. In this study, $k-\varepsilon$ model is used to calculate the effective viscosity for fully turbulent flow[92].

$$\mu_e = \mu + C_\mu \rho \frac{k^2}{\varepsilon} \tag{59}$$

where C_μ is constant, k is the turbulent kinetic energy and ε is turbulent kinetic energy equation.

Turbulent kinetic energy equation is as follows:

$$\begin{aligned}\frac{\partial \rho k}{\partial t} + \frac{\partial(\rho v_x k)}{\partial x} + \frac{\partial(\rho v_y k)}{\partial y} + \frac{\partial(\rho v_z k)}{\partial z} = \frac{\partial}{\partial x}\left(\frac{\mu_t}{\sigma_k}\frac{\partial k}{\partial x}\right) + \frac{\partial}{\partial y}\left(\frac{\mu_t}{\sigma_k}\frac{\partial k}{\partial y}\right) + \frac{\partial}{\partial z}\left(\frac{\mu_t}{\sigma_k}\frac{\partial k}{\partial z}\right) + \\ \mu_t \Phi - \rho\varepsilon + \frac{C_4 \beta \mu_t}{\sigma_t}\left(g_x \frac{\partial T}{\partial x} + g_y \frac{\partial T}{\partial y} + g_z \frac{\partial T}{\partial z}\right)\end{aligned} \tag{60}$$

where σ_k is 1.0, β is 0 and C_4 is 0.

Dissipation rate equation can be defined as,

$$\frac{\partial \rho \varepsilon}{\partial t}+\frac{\partial(\rho v_x \varepsilon)}{\partial x}+\frac{\partial(\rho v_y \varepsilon)}{\partial y}+\frac{\partial(\rho v_z \varepsilon)}{\partial z}=\frac{\partial}{\partial x}(\frac{\mu_t}{\sigma_\varepsilon}\frac{\partial \varepsilon}{\partial x})+\frac{\partial}{\partial y}(\frac{\mu_t}{\sigma_\varepsilon}\frac{\partial \varepsilon}{\partial y})$$
$$+\frac{\partial}{\partial z}(\frac{\mu_t}{\sigma_\varepsilon}\frac{\partial \varepsilon}{\partial z})+C_{1\varepsilon}\mu_t\frac{\varepsilon}{k}\Phi-C_2\rho\frac{\varepsilon^2}{k}+ \tag{61}$$
$$\frac{C_\mu(1-C_3)\beta\rho k}{\sigma_t}(g_x\frac{\partial T}{\partial x}+g_y\frac{\partial T}{\partial y}+g_z\frac{\partial T}{\partial z})$$

where σ_ε is 1.3, $C_{1\varepsilon}$ is 1.44, C_2 is 1.92, C_μ is 0.09, C_3 is 1.0 and σ_t is 1.0.

5.2.2 CFD Cuttings Transport Model Including Pipe Rotation for Horizontal Wellbores

Proper modeling of cuttings transport mechanism in horizontal wells becomes more critical while predicting frictional pressure loss and transport velocities. In this chapter, solid-liquid flow inside horizontal wellbores is simulated using an Eulerian- Eulerian computational fluid dynamics (CFD) model for various fluid velocities, rates of penetration and pipe rotation speeds.

5.2.2.1 Lagrangian Tracking Implementation

The cuttings displacement is calculated using forward Euler integration of the particle velocity over time step, δt.

$$x_i^n = x_i^o + v_{pi}^o \delta t \tag{62}$$

where the superscripts o and n refer to old and new values respectively a v_{pi} is the particle velocity. In forward integration, the particle velocity calculated at the start of the time step is assumed to prevail over the entire step. At the end of the time step, the new particle velocity can be calculated as

$$v_p = v_f + (v_p^o - v_f)\exp(-\frac{\delta t}{\tau}) + \tau F_{all}(1-\exp(-\frac{\delta t}{\tau})) \quad (63)$$

5.2.2.2 Momentum Transfer

The equation of motion for such a particle was derived by Basset, Boussinesq and Oseen for a rotating reference frame:

$$m_p \frac{dU_p}{dt} = F_D + F_B + F_R + F_{VM} + F_P + F_{BA} \quad (64)$$

which has the following forces on the right hand side:

The drag force acting on the particle is written as

$$F_D = \frac{1}{8}\pi\rho_f d^2 C_D \left|v_f - v_p\right|(v_f - v_p) \quad (65)$$

where C_D is the drag coefficient and the coefficient is calculated in the same way as for Eulerian- Eulerian multiphase flow.

The buoyancy force on particle immersed in a fluid can be defined as

$$F_B = (m_p - m_F)g = m_p(1-\frac{\rho_F}{\rho_P})g = \frac{\pi}{6}d_p^3(\rho_p - \rho_F)g \quad (66)$$

In a rotating frame of reference particles are subject to the two additional forces due to the system rotation

$$F_R = F_{centripetal} + F_{corilois} \quad (67)$$

$$F_R = -m_p\omega^2 r - 2m_p(v_p \times \omega) \quad (68)$$

where v_p is the particle velocity, ω is the angular velocity of the rotating frame, m_p is the particle mass and r is the vector from the axis of rotation to the current particle position.

The virtual or added mass force is written as

$$F_{VM} = \frac{C_{VM}}{2} m_F \left(\frac{dv_F}{dt} - \frac{dv_p}{dt}\right) \quad \text{(virtual or added mass force)} \tag{69}$$

Virtual mass force is caused by the fact that the particle has to accelerate some of the surrounding fluid. Pressure gradient force are defined by

$$F_P = -\frac{m_F}{\rho_F} \nabla p \tag{70}$$

This is the force applied on the particle due to the pressure gradient in the fluid surrounding the particle caused by fluid acceleration. It is only significant when the fluid density is comparable to or greater than the particle density.

F_{BA}: Basset force or history term which accounts for the deviation in flow pattern form a steady state. This term is not implemented in CFD simulation.

5.2.2.3 Turbulence in Particle Tracking

The turbulent velocity is calculated based on the local turbulence properties of the flow.

$$v_f' = \Gamma\left(\frac{2k}{3}\right)^{0.5} \tag{71}$$

where k is local turbulent kinetic energy and Γ is a normally distributed random number which accounts for the randomness of turbulence about a mean value[92].

5.3 Verification of CFD Cuttings Transport Model with Experimental Data

CFD simulations have been conducted for water velocities 0.43-1.3 m/s, rates of penetration 0.001-0.01 m/s and pipe rotation speed 0-120 rpm. Frictional pressure loss of two-phase solid-liquid flow through in fully eccentric horizontal annulus with and without pipe rotation is computed by using CFD model. CFD software predictions of pressure losses are verified with experimental data obtained from METU-PETE Cuttings Transport Flow Loop.

5.3.1 Model Performance

A few examples about the comparison of the experimental and predicted pressure gradients are presented in Figures 5.3-5.7. As seen from these figures, CFD model gives generally good predictions of the frictional pressure loss with and without pipe rotation. The experimental pressure drop is recorded during cuttings transport experiments, and calculated values are obtained from Ansys CFX. Moreover, Figure 5.8 shows cuttings concentration inside annulus for rates of penetration=0.004 m/s. In this study, CFD cuttings transport model is tested over 90 experimental frictional pressure loss values. Experimental data and model estimations are compared in Figure 5.9. As seen from figure, CFD predictions of solid-liquid pressure loss showed good agreement (± 20%) with experiments. Good agreement was achieved.

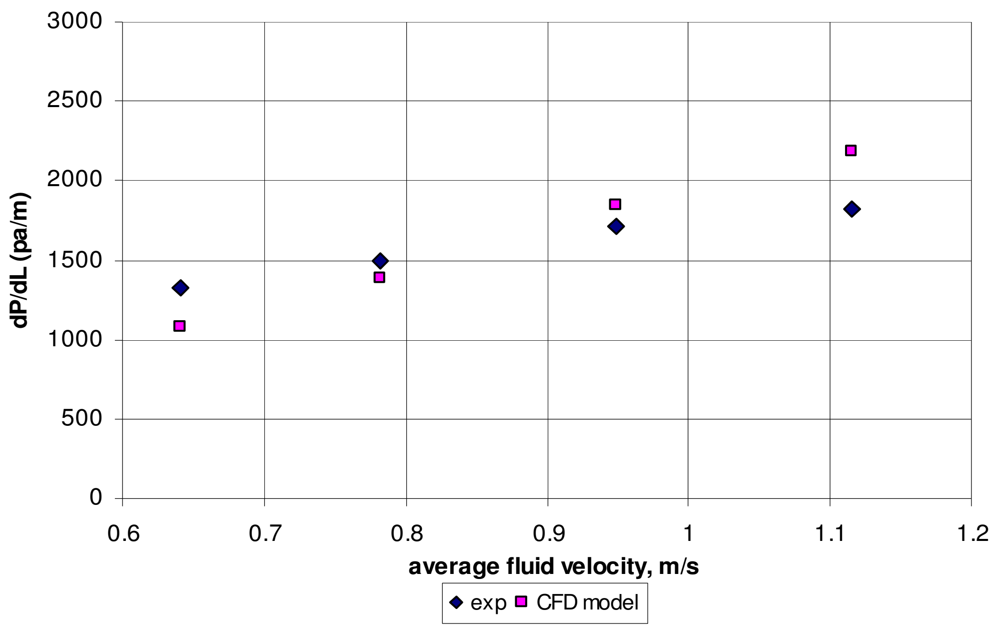

Figure 5.3- Comparison of CFD simulation with experimental data for pipe rotation (rpm)=0 and rates of penetration=0.00127 m/s

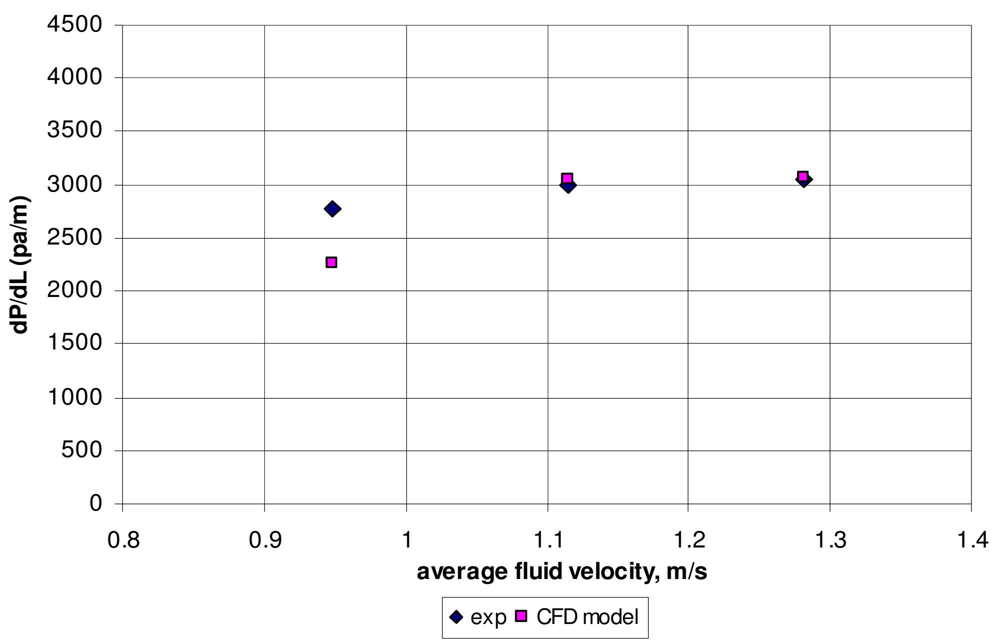

Figure 5.4- Comparison of CFD simulation with experimental data for pipe rotation (rpm)=0 and rates of penetration=0.004 m/s

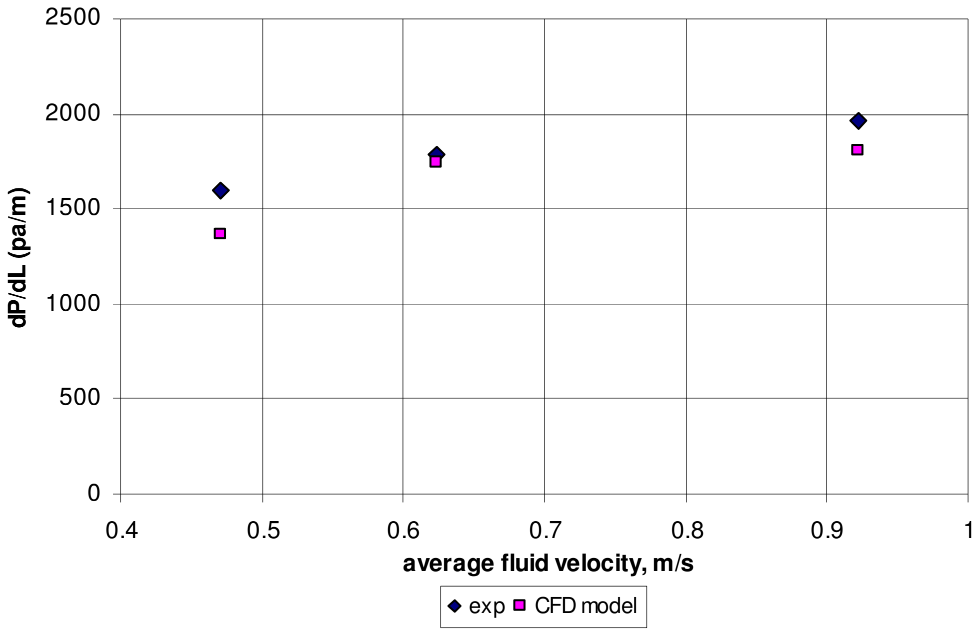

Figure 5.5- Comparison of CFD simulation with experimental data for pipe rotation (rpm)=120 and rates of penetration=0.01 m/s

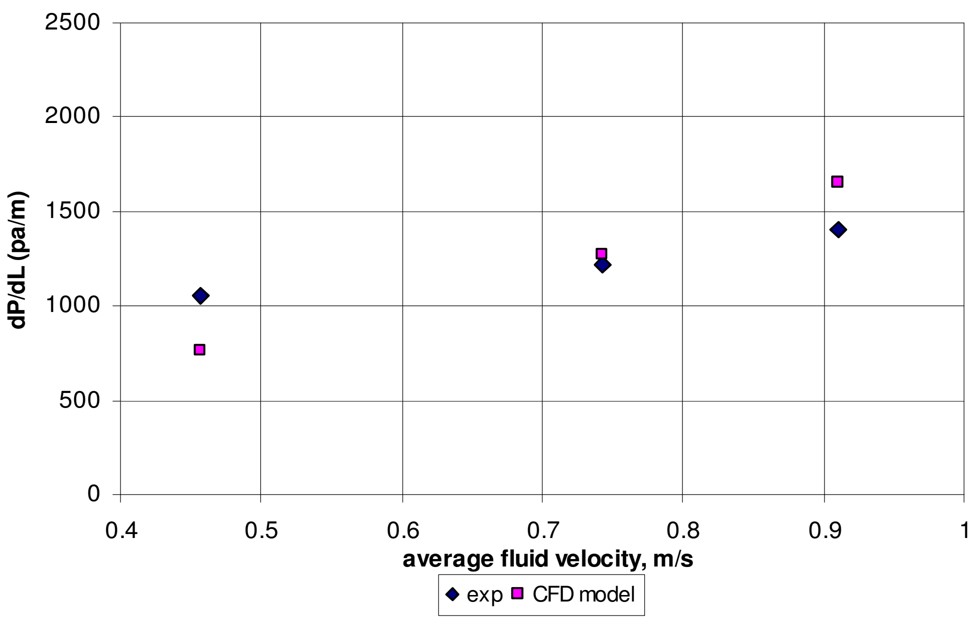

Figure 5.6- Comparison of CFD simulation with experimental data for pipe rotation (rpm)=100 and rates of penetration=0.005 m/s

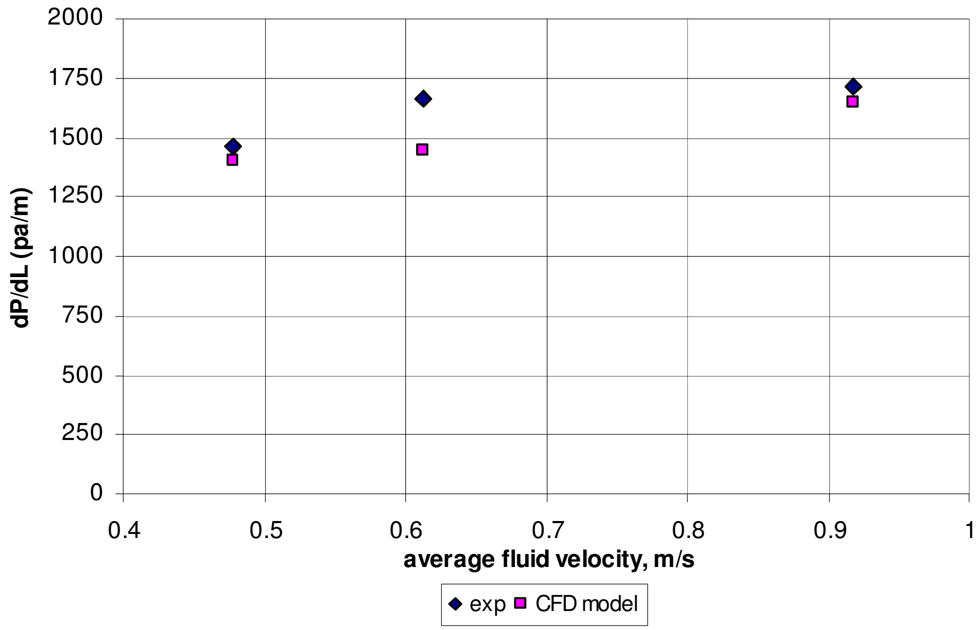

Figure 5.7- Comparison of CFD simulation with experimental data for pipe rotation (rpm)=80 and rates of penetration=0.007 m/s

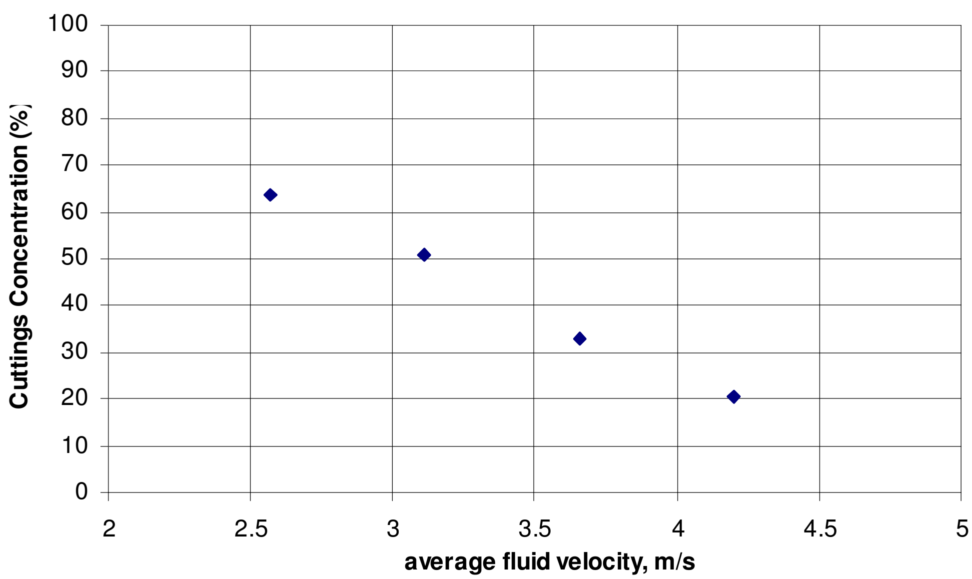

Figure 5.8- Cuttings Concentration inside annulus for pipe rotation (rpm)=0 and rates of penetration=0.004 m/s

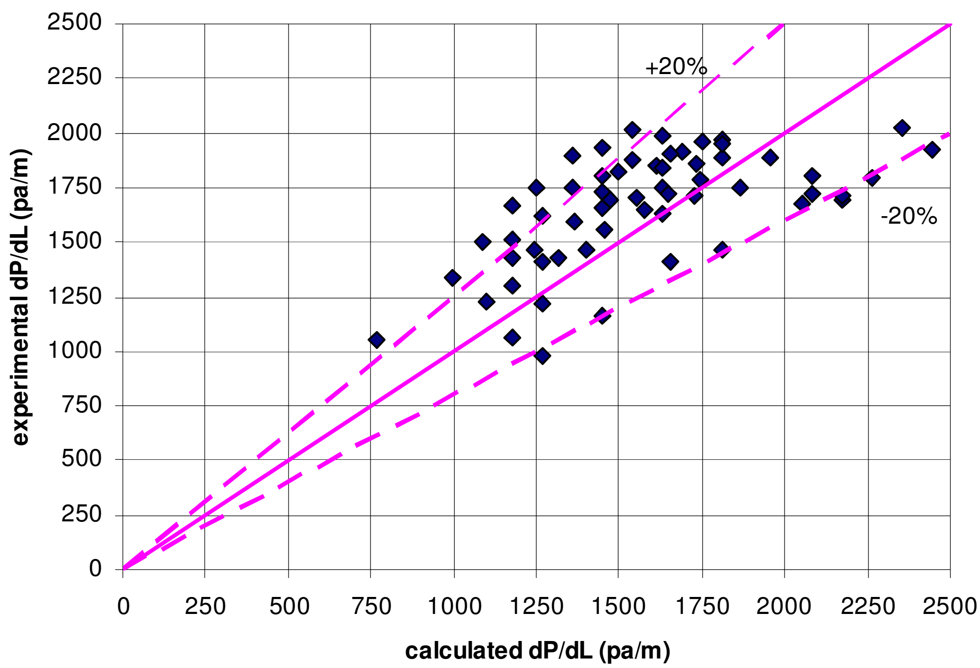

Figure 5.9- Comparison of measured and estimated frictional pressure gradient values

CHAPTER 6

RESULTS AND DISCUSSION

In previous two chapters, a mathematical model to estimate frictional pressure loss inside concentric annulus is verified by using experimental data which were available in the literature and gathered at METU-PETE Flow Loop as well as Computational Fluid Dynamics (CFD) software. Moreover, cuttings transport inside horizontal annulus is simulated using CFD code Ansys Workbench. In this chapter, empirical equations for estimating frictional pressure drop and stationary bed thickness are developed using statistical techniques. Friction factor charts and equations are developed for water and drilling fluids in terms of combined Reynolds number and stationary cuttings bed thickness. A sensitivity analysis is conducted in order to investigate the effects of drilling parameters on cuttings transport. The results and in-depth discussion are given in details in the following sections.

6.1 Cuttings Bed Area and Frictional Pressure Gradient Equations

Cuttings bed thickness within the wellbore is one of the most important parameters to be observed to achieve the hole-cleaning performance and conduct a successful drilling operation. A schematic view of horizontal eccentric annulus with and without cuttings is shown in Fig. 6.1. In this study, the inner pipe was fully eccentric during cuttings transport experiments.

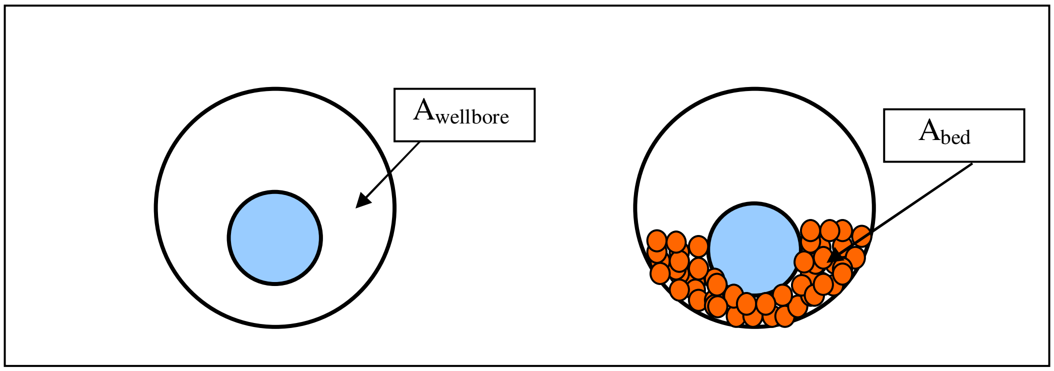

Figure 6.1- Schematic drawing of horizontal eccentric annulus with and without cuttings

Cuttings bed area as a non-linear function using the developed dimensionless groups can be expressed as

$$A_r = a_1\left[(\Pi_1)^{a_2} + (\Pi_2)^{a_3} + a_4(\Pi_3) + a_5(\Pi_4) + a_6(\Pi_7)\right] \tag{72}$$

Also, an attempt is conducted for estimating pressure drop as a function of some of the dimensionless groups and the bed area calculated using Eq.72. In this study, pressure gradient is estimated using

$$\frac{\Delta P}{\Delta L} = b_1\left[b_2\left(\frac{\Pi_1}{10000}\right) + b_3(\Pi_3) + b_4(\Pi_4) + b_5\left(\frac{\Pi_7}{10}\right) + b_6\left(\frac{A_{bed}}{A_{wellbore}}\right)\right] \tag{73}$$

In Eq.73, b_1 has the same unit with the pressure gradient, i.e., $(m/(Lt^2))/L$.

Using the database developed from the experimental work, the constants of Eq.72 and Eq.73 are determined using statistical software, STATISTICA®. Cuttings bed area for inclinations from horizontal to 60 degrees can be estimated as;

$$A_r = 0.517\left[(\Pi_1)^{-5.195} + (\Pi_2)^{-0.625} + 0.089(\Pi_3) + 0.002(\Pi_4) - 0.11(\Pi_7)\right] \quad (74)$$

Here, R^2 of best fit is 0.88, which indicates satisfactory correlation for A_r in spite of large number of independent variables involved in the analysis. As seen from Eq.74, an increase in Reynolds Number (Π_1), Froude Number (Π_2) significantly decreases cuttings bed area. It can be seen that both dimensionless groups include fluid velocity, increasing annular fluid velocity give rise to erode cuttings bed thickness inside the wellbore. Additionally, as the pipe rotation (Π_7) increases, cuttings bed area also decreases. If the amount of cuttings (Π_3) increase in the annulus, more cuttings will accumulate in the wellbore. Furthermore, it can be concluded that no considerable relation exists between hole inclination (Π_4) and the cuttings bed area. The performance of the proposed equation is tested using the actual data obtained from the experiments and presented in Fig. 6.2. In Fig. 6.2, the *x*-axis is the actual bed area, and *y*-axis is the calculated stationary cuttings bed area using the proposed model. The solid line represents the perfect match, and dashed lines represent ±20 % error margin. It is observed that almost all points are within this error margin.

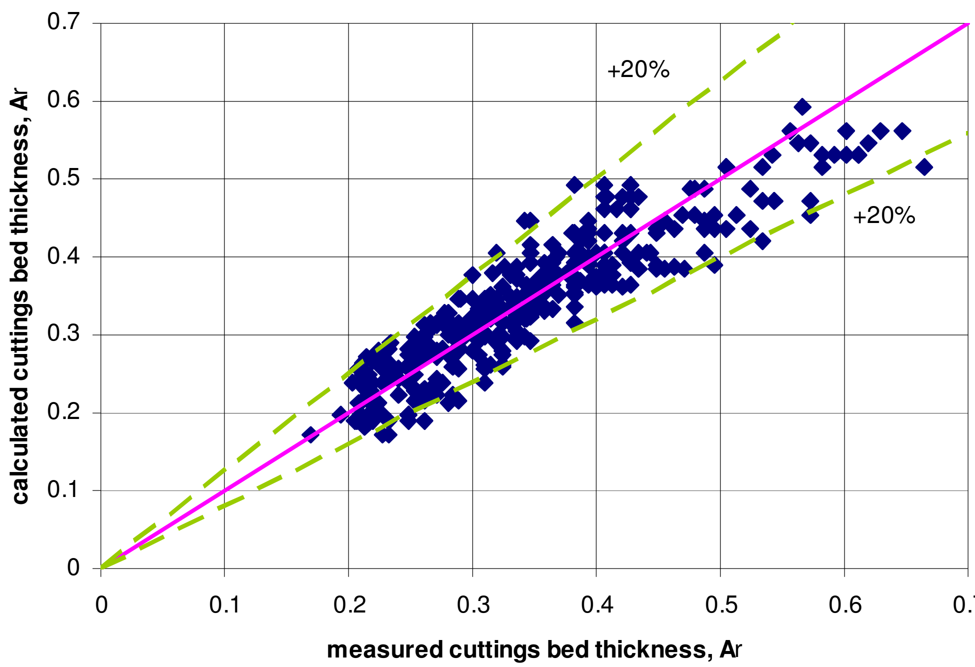

Figure 6.2- Comparison of measured and estimated stationary bed area using Eq. 74

Proposed frictional pressure gradient equation (valid for horizontal to 60 degrees) are presented as

$$\frac{\Delta P}{\Delta L} = 0.2\left[0.182\left(\frac{\Pi_1}{10000}\right) + 0.249(\Pi_3) - 0.19(\Pi_4) + 0.185(\frac{\Pi_7}{10}) + 0.11(A_r)\right] \quad (75)$$

As seen from equation constants of Eq. 75, Π_1 (Reynolds number), Π_3 (cuttings concentration) and pipe rotation speed (Π_7) increase the frictional pressure loss, even though Π_1 gives rise to a reduce in the bed area, which leads to a decrease in the pressure drop. Although an increase in the inclination seems to have a negative effect on pressure drop according to the sign of the constant, such a behavior could not be verified properly from the experiments, since the effect of inclination on pressure drop differs as the conditions are varying. Comparison of predicted pressure loss using Eq.75 with experiments is shown in Fig. 6.3.

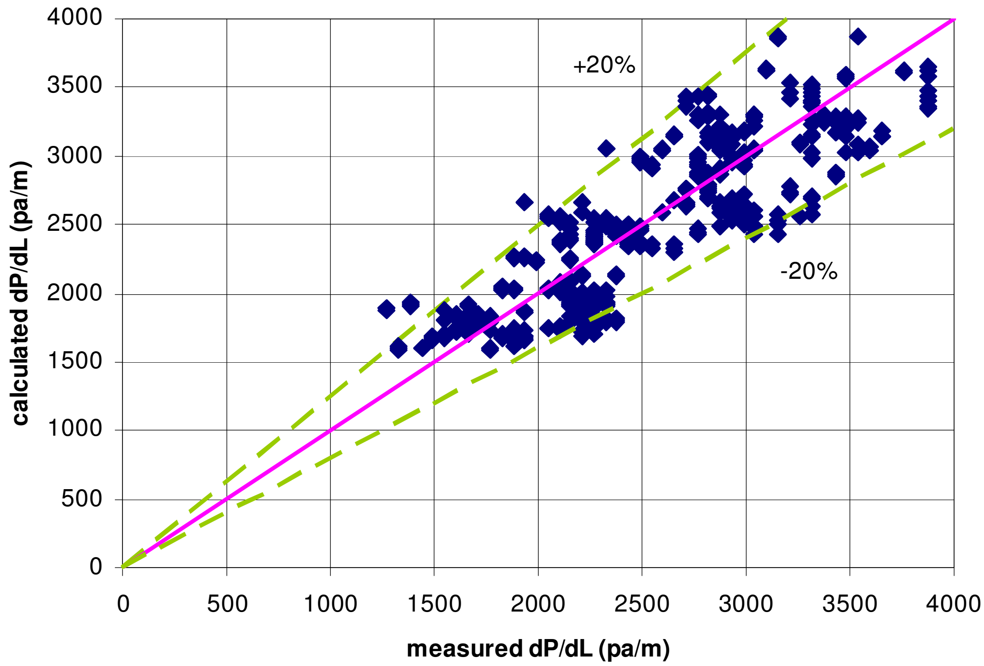

Figure 6.3- Comparison of measured and estimated pressure gradient using Eq. 75

6.2 Development of Friction Factor Correlations and Charts for Water-Based Drilling Fluids in Horizontal and Deviated Wells during Pipe Rotation

In this section, the friction factor correlations and charts for two-phase flows (fluid and cuttings) are proposed. A generalized form based on classical friction expressions for water and drilling fluids is proposed as

$$f = \beta N_{RET}^{-\alpha} \tag{76}$$

Here, β and α both are functions of cuttings bed thickness. Friction factor charts obtained from the experimental data for water and drilling fluids are presented in Fig. 6.4 and Fig. 6.5, respectively. The data set is divided into four groups as A_r<20%, 20%≤A_r<30%, 30%≤A_r<40% and 40%≤A_r<70%. Best fit curves for each group in the form of Eq. (76) are obtained and shown on the figures.

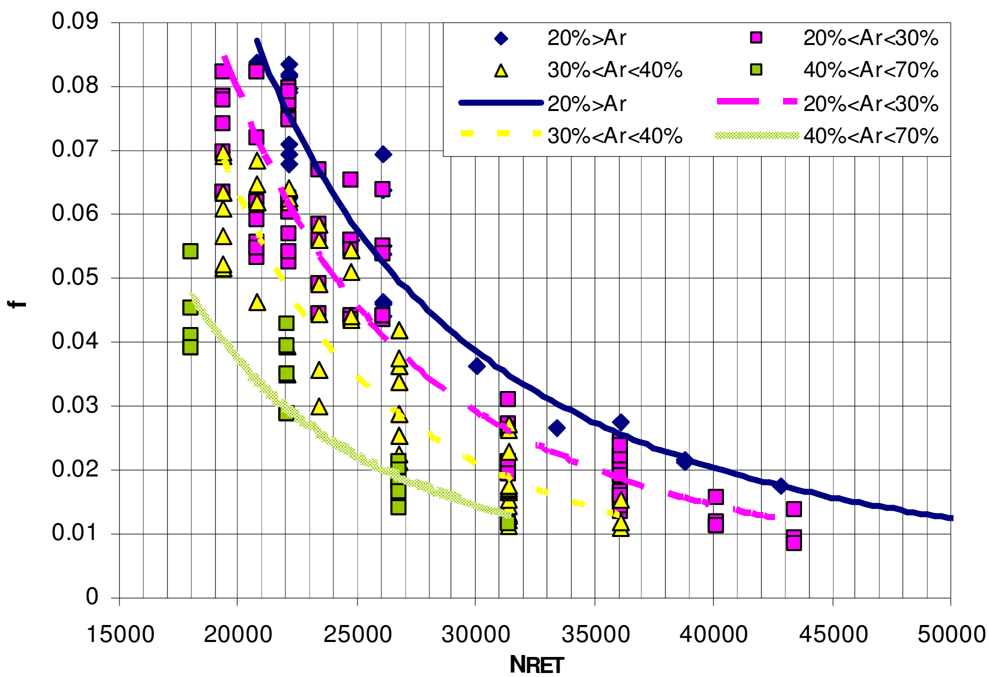

Figure 6.4- Friction factor chart obtained from experimental work for water

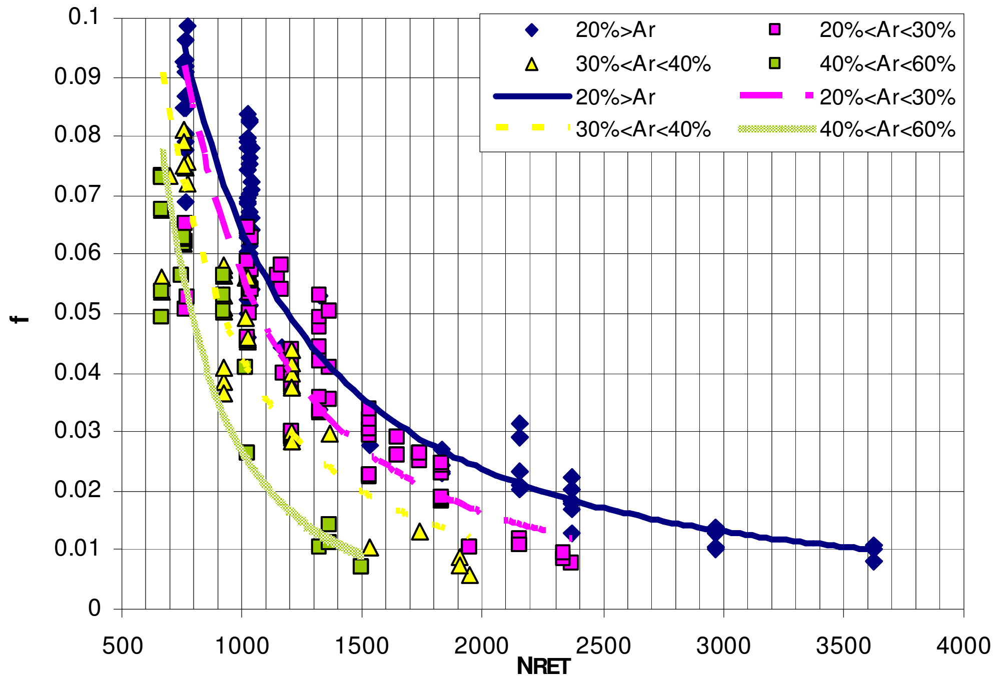

Figure 6.5- Friction factor chart obtained from experimental work for drilling fluids

Initial β and α values are obtained from this best fit operation for each individual data set. In the second step, a simple expression is defined for β as function of A_r from the initial values of β obtained from the four data groups. Then, using function $\beta(A_r)$ corresponding α values are obtained for each data point. The newly obtained α values are plotted as function of A_r (Fig. 6.6) and a best fit function $\alpha(A_r)$ is obtained. In the next cycle of iteration, $\alpha(A_r)$ is assumed known and $\beta(A_r)$ is re-evaluated from the data set to improve the correlation between the data and the best fit function of β. The functions $\alpha(A_r)$ and $\beta(A_r)$ shown in Fig. 6.6 and Fig.6.7 respectively, are the final optimized parameters producing the best-fit curves for the complete experimental data (without any grouping) in the form given by Eq.(76).

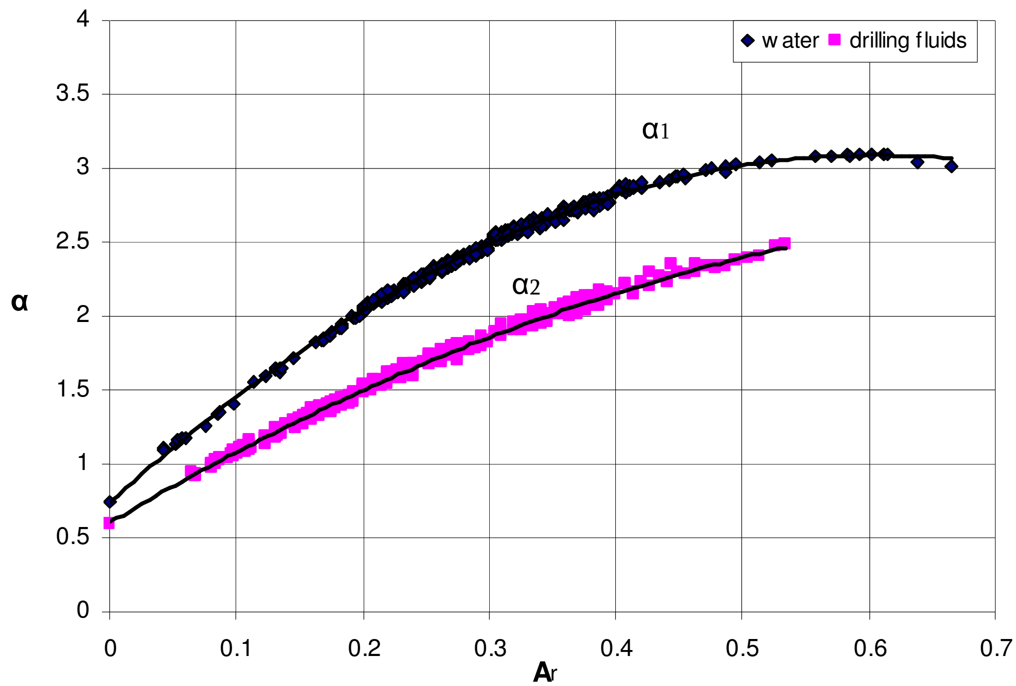

Figure 6.6- α values as a function of dimensionless cuttings bed thickness

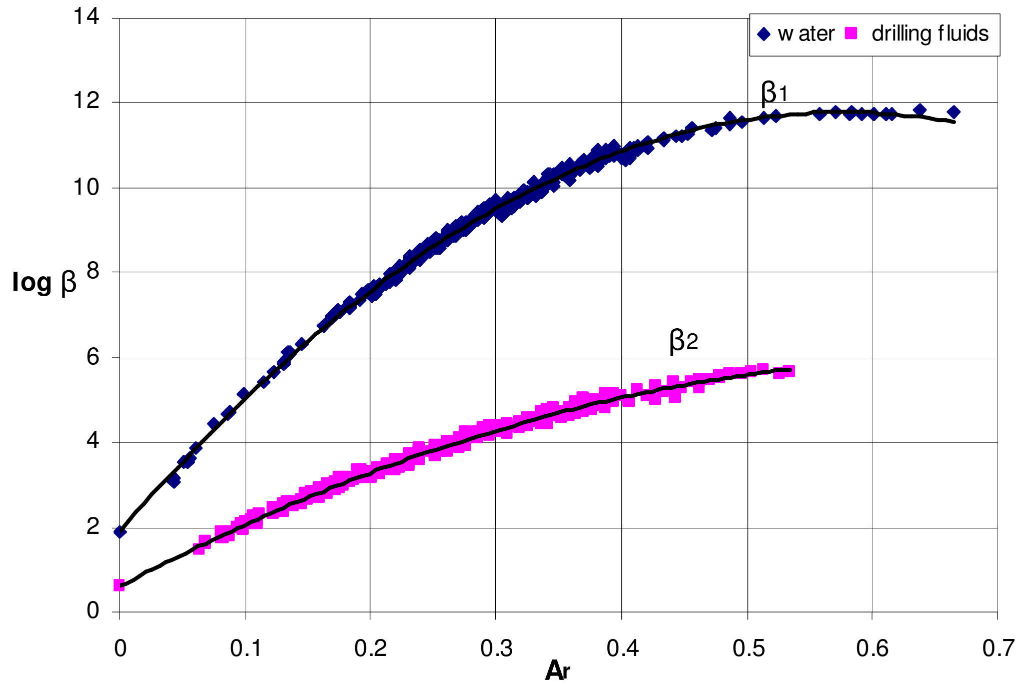

Figure 6.7- Log β values as a function of dimensionless cuttings bed thickness

The final expression of β and α are written for the water as

$$\alpha_1 = -6.43 A_r^{\ 2} + 7.78 A_r + 0.74 \tag{77}$$

$$\beta_1 = 10^{\left(-29.75 A_r^{\ 2} + 34.3 A_r + 1.9\right)} \tag{78}$$

and for the drilling fluids

$$\alpha_2 = -2.92 A_r^{\ 2} + 5.05 A_r + 0.6 \tag{79}$$

$$\beta_2 = 10^{\left(-11.45 A_r^{\ 2} + 15.7 A_r + 0.6\right)} \tag{80}$$

Finally, friction factor for water and drilling fluids can be computed using β and α obtained from Eq. 77~80 and the total Reynolds number from Eq. (36) by inserting into Eq.(76). Friction factor charts reproduced from the above equations are shown in Fig. 6.8 and 6.9 for various cuttings bed thicknesses.

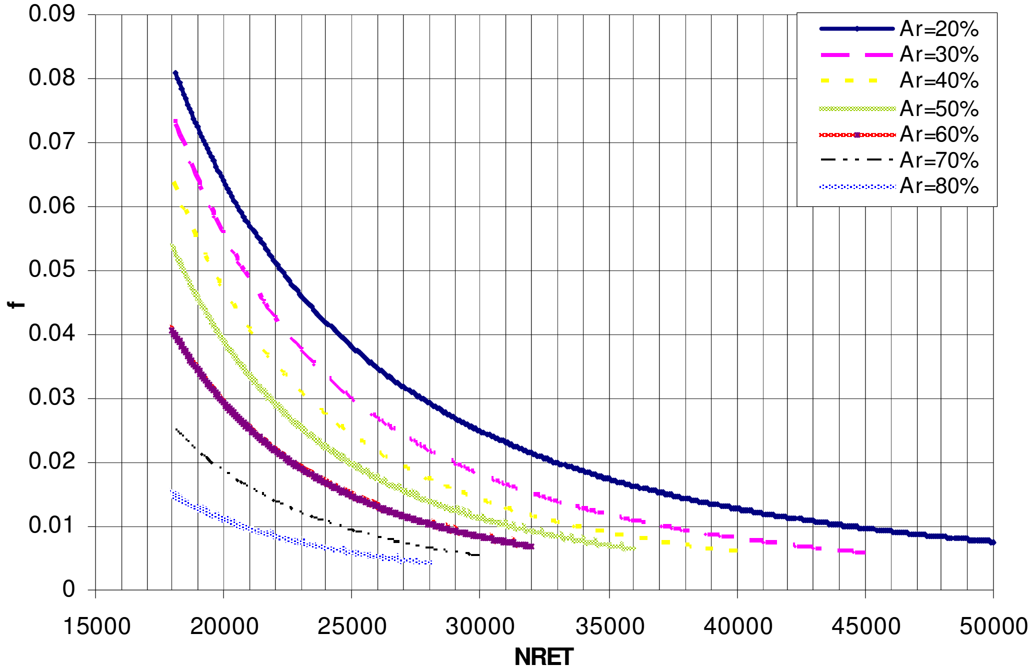

Figure 6.8- New Friction factor chart for water and various cuttings bed thickness

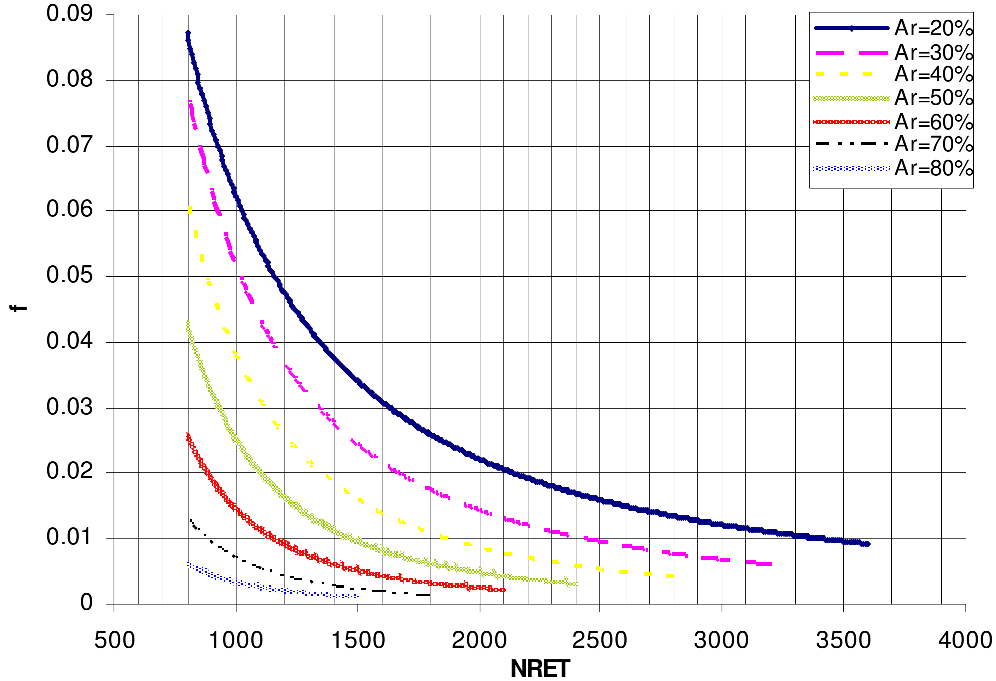

Figure 6.9- New Friction factor chart for drilling fluids and various cuttings bed thickness

Fig.6.10 and Fig.6.11 demonstrate the calculated friction factor versus experimental data for water and drilling fluids fluids, respectively. The solid lines in these figures represent the perfect match between the experimental and calculated results and dashed lines represent ±20 % error margin. A total of 352 pairs of data points were compared in Fig.6.10. As seen from this figure, in most of the cases, proposed empirical correlations for water (Eqs. 76-77-78) estimates frictional pressure loss accurately with and without pipe rotation. Fig. 6.10 shows a total of 338 pairs of data for drilling fluids. From this figure, it can be observed that friction factor for drilling fluids can also be predicted with a high accuracy. Moreover, proposed empirical correlations can also estimate friction factors accurately for various pipe rotation speeds. It should be noted that the friction factor equations for water and drilling fluids result in an overestimation of the pressure losses, when the cuttings bed area inside the annulus approaches to zero.

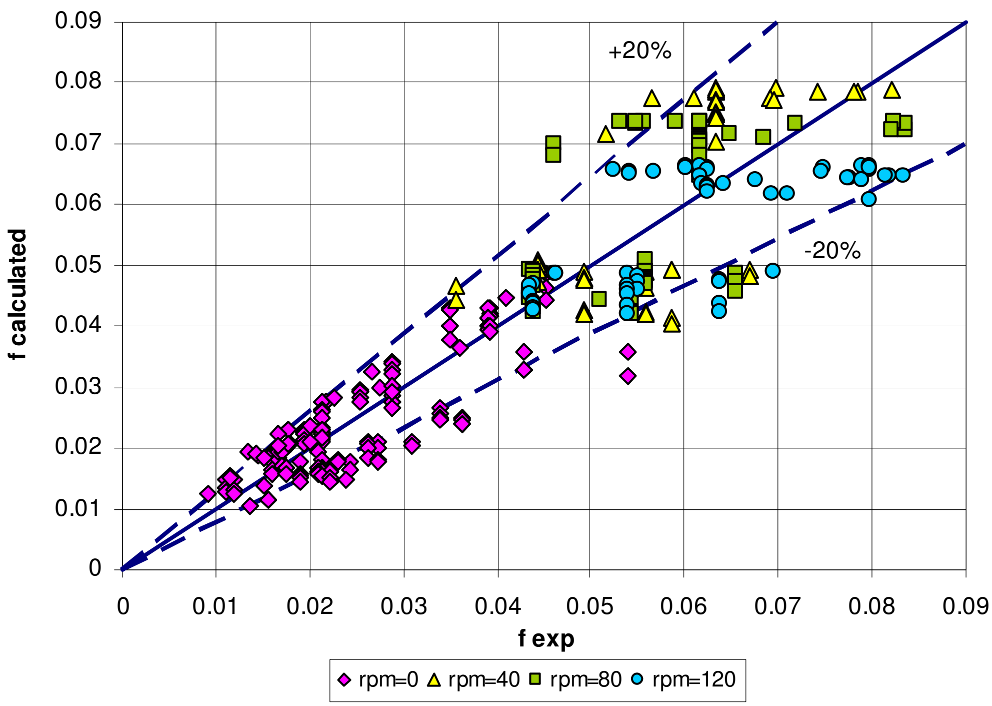

Figure 6.10- Comparison of the calculated and experimental friction factor for water

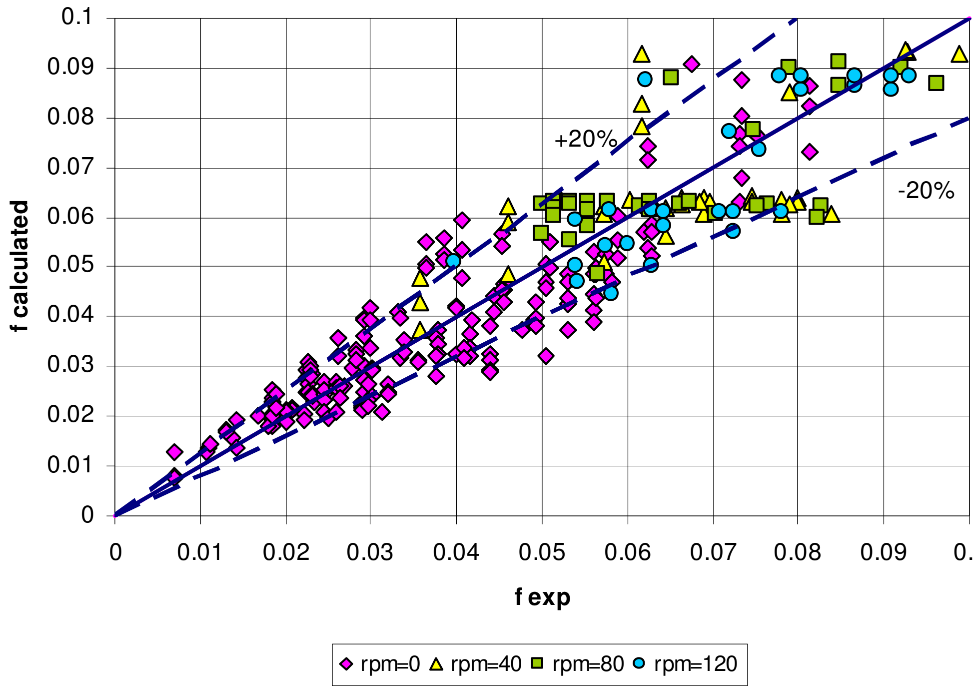

Figure 6.11- Comparison of the calculated and experimental factor factor for drilling fluids

Fig.6.12 represents the measured and predicted frictional pressure loss values with ±20 % error margins. It is observed that more than 90% of the data points are within the error margins.

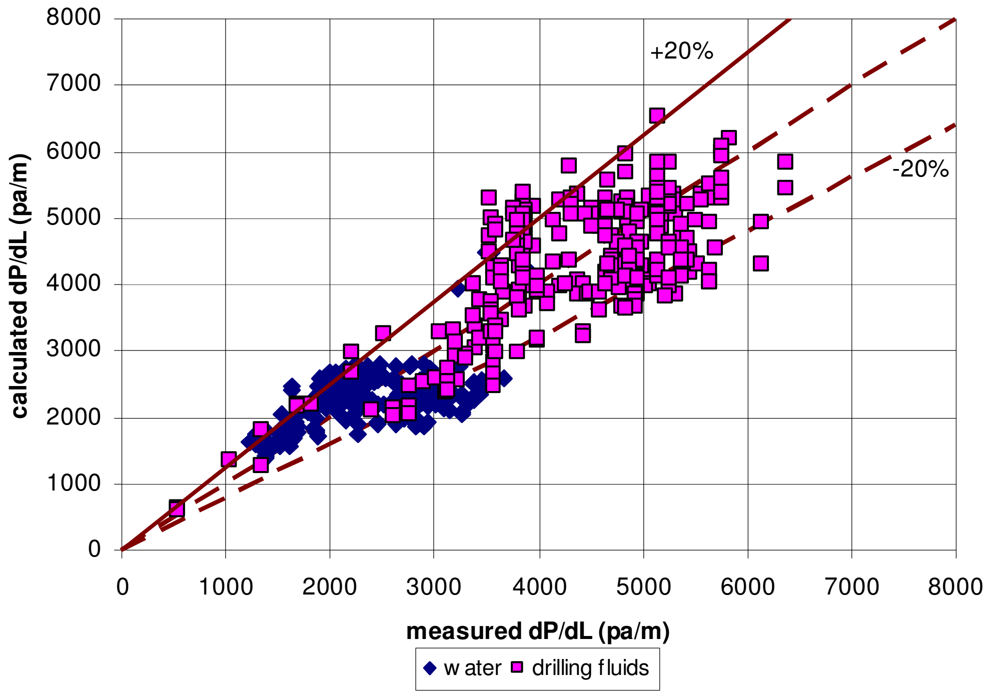

Figure 6.12- Comparison of calculated and measured pressure gradient values

6.3 Sensitivity Analysis on Hole Cleaning for Drilling Parameters

In this section, the effects of different parameters on cuttings transport are investigated. A sensitivity analysis based on the experimental data has been carried out.

6.3.1 Fluid Velocity Effects on Hole Cleaning

Figure 6.13 represents the fluid velocity vs. cuttings bed thickness for water and drilling fluid-1 and drilling fluid-2 in horizontal annulus without pipe rotation. As seen from this figure, as the fluid velocity increases, stationary cuttings bed thickness decreases drastically for all drilling muds. Also, after a certain fluid velocity, stationary bed is removed from the wellbore. From the experimental observations, it can be concluded that the annular fluid velocity is a dominant parameter affecting hole cleaning.

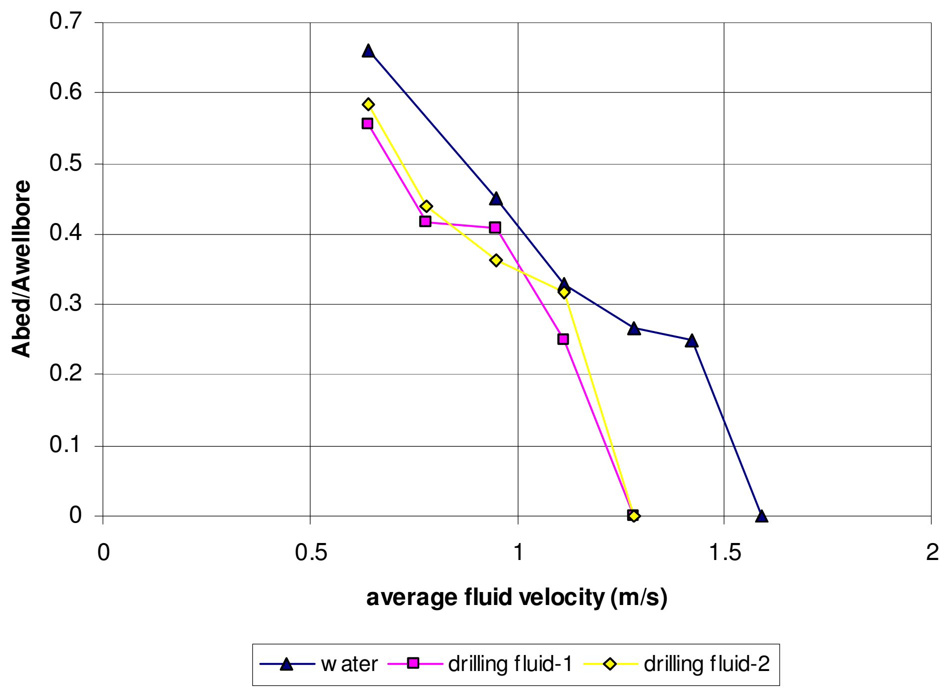

Figure 6.13- Fluid velocity effects on cuttings bed thickness for water, drilling fluid-1 and drilling fluid-2

6.3.2 Fluid Viscosity Effects on Hole Cleaning

The effect of fluid viscosity on hole cleaning without pipe rotation is also analyzed. In figure 6.14, the comparison of drilling fluid-1, drilling fluid-2, drilling fluid-3 which have different viscosities are demonstrated during fluid viscosity 0.64 m/s, rate of penetrations 0.004 m/s, and hole inclination of 90 degrees. As seen from this figure, as the fluid viscosity increases, reynolds number decreases. Therefore, cuttings transport performance of drilling fluids decreases for horizontal case and without pipe rotation.

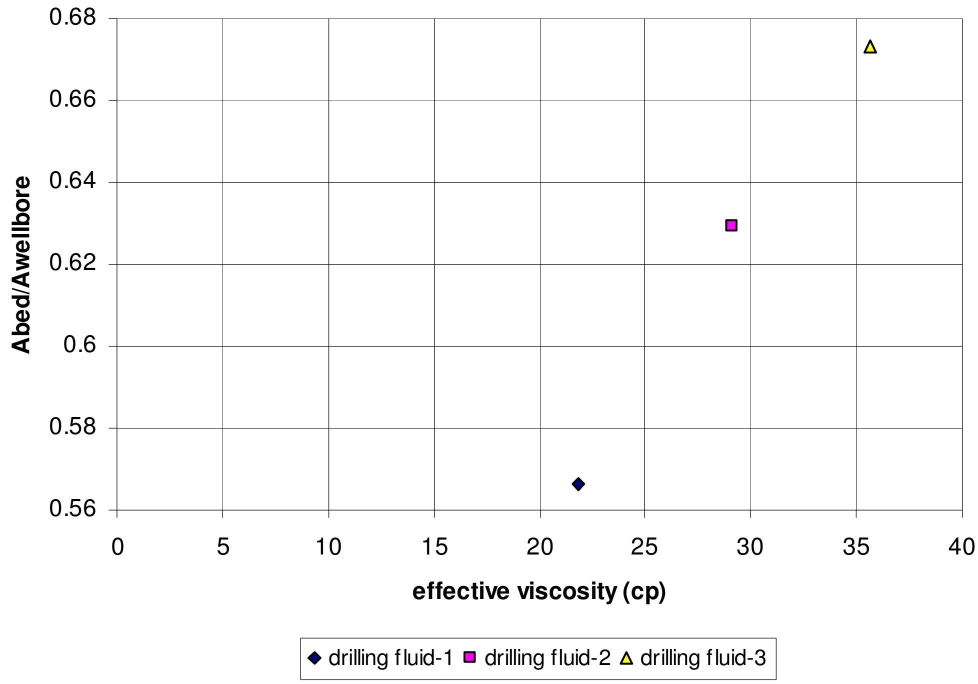

Figure 6.14- Fluid viscosity effects on cuttings bed thickness inside horizontal annulus

6.3.3 Rate of Penetration Effects on Hole Cleaning

Figure 6.15 demonstrates the comparison of rate of penetration effects on hole cleaning for different drilling fluids when the fluid velocity is 0.95 m/s and flow horizontal annulus. For all mud systems, no significant change in cuttings bed thickness is observed as the rate of penetration is increased. For example, for mud

4, although rate of penetration is increased three times, stationary cuttings bed thickness only increased 12%.

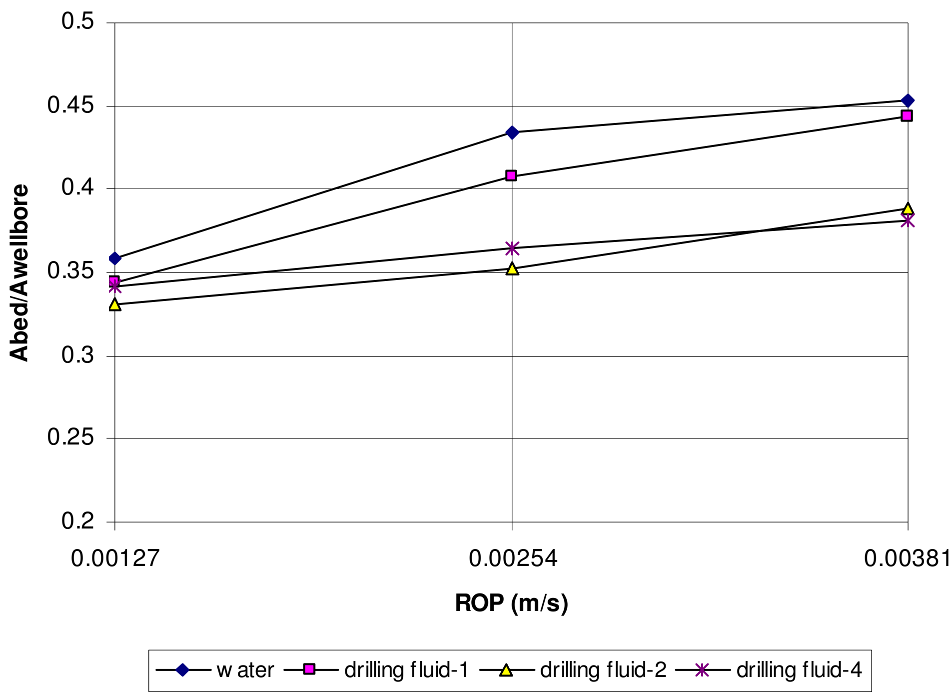

Figure 6.15- Rate of Penetration effects on cuttings bed thickness inside horizontal annulus

6.3.4 Hole Inclination Effects on Hole Cleaning

As seen from figure 6.16, hole inclination has a slight effect on cuttings bed thickness inside annulus between 60 degrees to 90 degrees for all mud systems without pipe rotation. In this figure, all drilling muds are flowing with 0.78 m/s and rate of penetration is 0.00381 m/s.

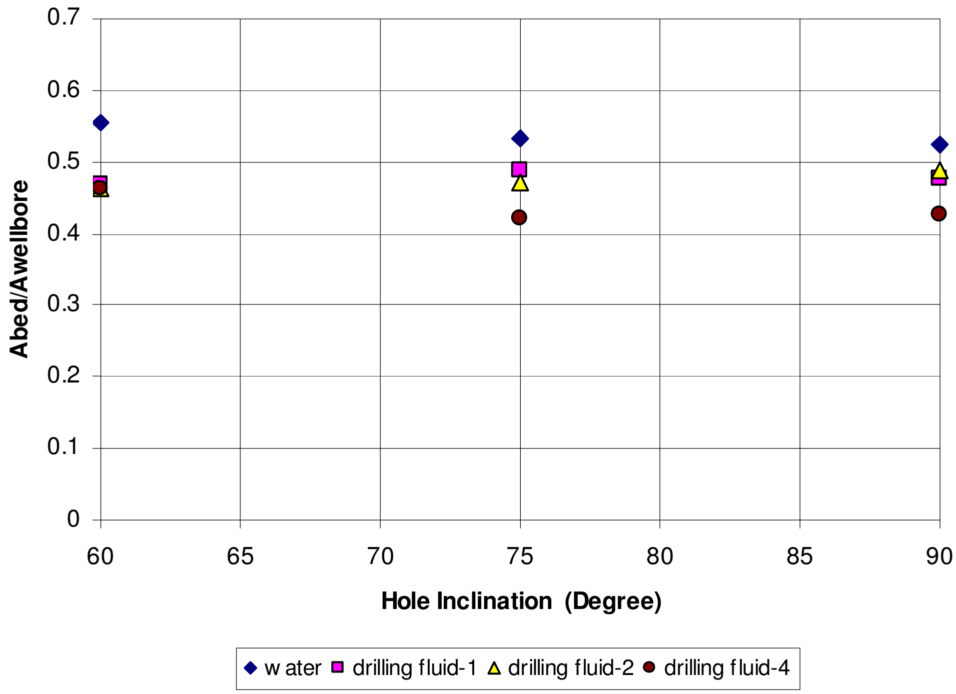

Figure 6.16- Hole inclination effects on cuttings bed thickness inside annulus

6.3.5 Pipe Rotation Effects on Hole Cleaning

Pipe rotation is a significant parameter affecting proper hole cleaning during drilling in horizontal and inclined wells. In this section, the effects of pipe rotation on different drilling variables are analyzed based on the experimental observations.

First of all, the influence of pipe rotation on cuttings bed thickness for four different drilling fluids is discussed. As seen from Figure 6.17- Figure 6.19, at 0.78 m/s fluid velocity and hole inclinations 60 to 90 degrees, pipe rotation significantly reduced cuttings bed development for all muds. As pipe rotation started, a significant decrease in cuttings bed thickness is observed. However, after a certain rotation speed, pipe rotation effects on hole cleaning are negligible. Also, drilling fluid-4 shows a better performance for all hole inclinations when compared with other muds. A possible cause is that drilling fluid-4 has higher viscosity than other muds. It means that as the fluid viscosity increases, pipe rotation effects on carrying capacity of drilling fluids significantly increase.

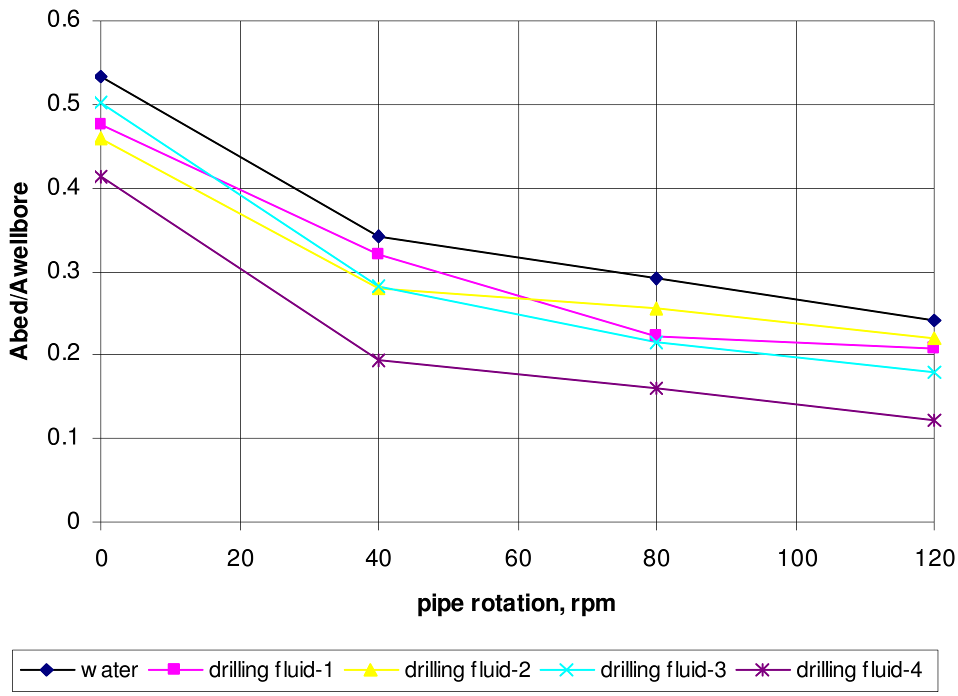

Figure 6.17- Effect of pipe rotation on cuttings bed thickness for different drilling fluids in horizontal wellbores

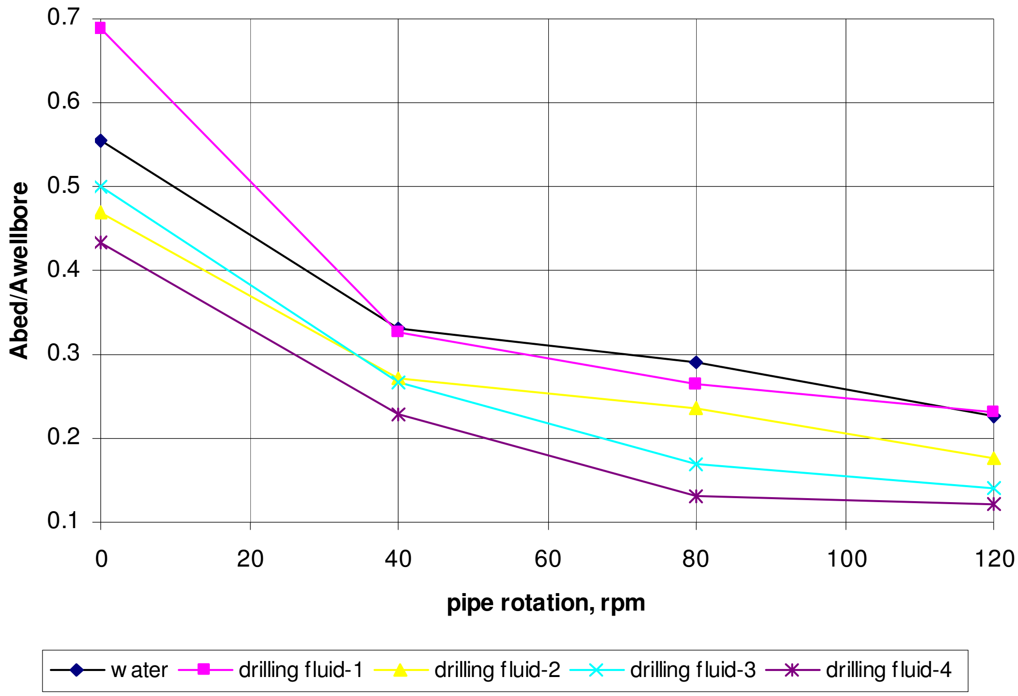

Figure 6.18- Effect of pipe rotation on cuttings bed thickness for different drilling fluids and hole inclination 75 degree

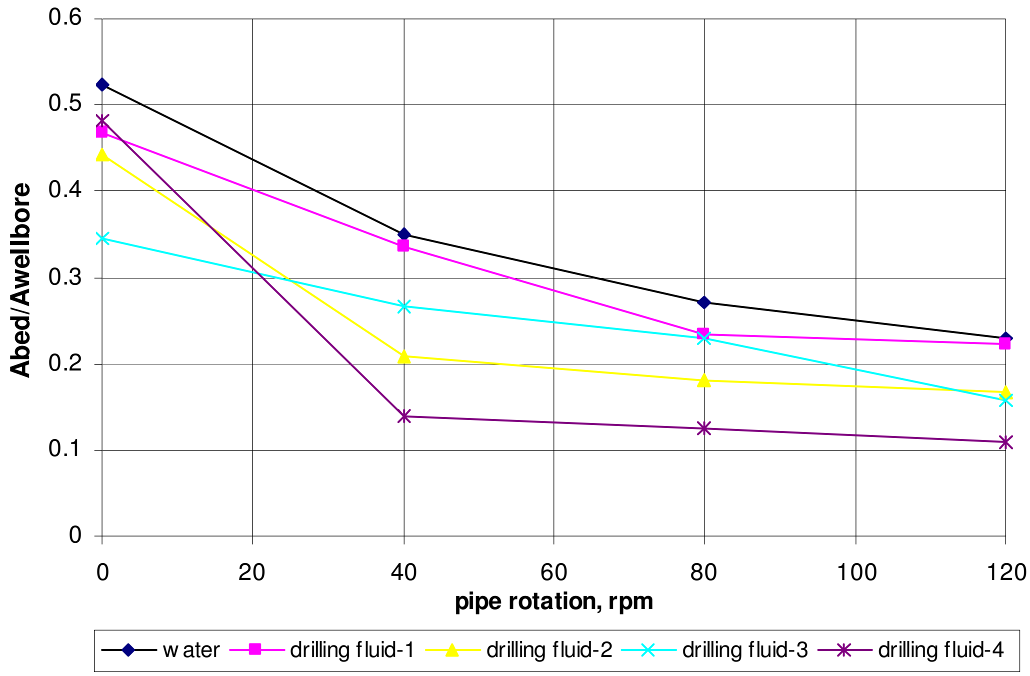

Figure 6.19- Effect of pipe rotation on cuttings bed thickness for different drilling fluids and hole inclination 60 degree

One of the effects of pipe rotation on cuttings transport is to decrease critical fluid velocity, which is a minimum velocity for removing cuttings from the wellbore. Figure 6.20 and Figure 6.21 show pipe rotation effect on critical fluid velocity for water and mud 2. As seen from these figures, pipe rotation considerably decreases critical average fluid velocity. Moreover, as the pipe rotation is increased, stationary bed thickness decrease for the same fluid velocity.

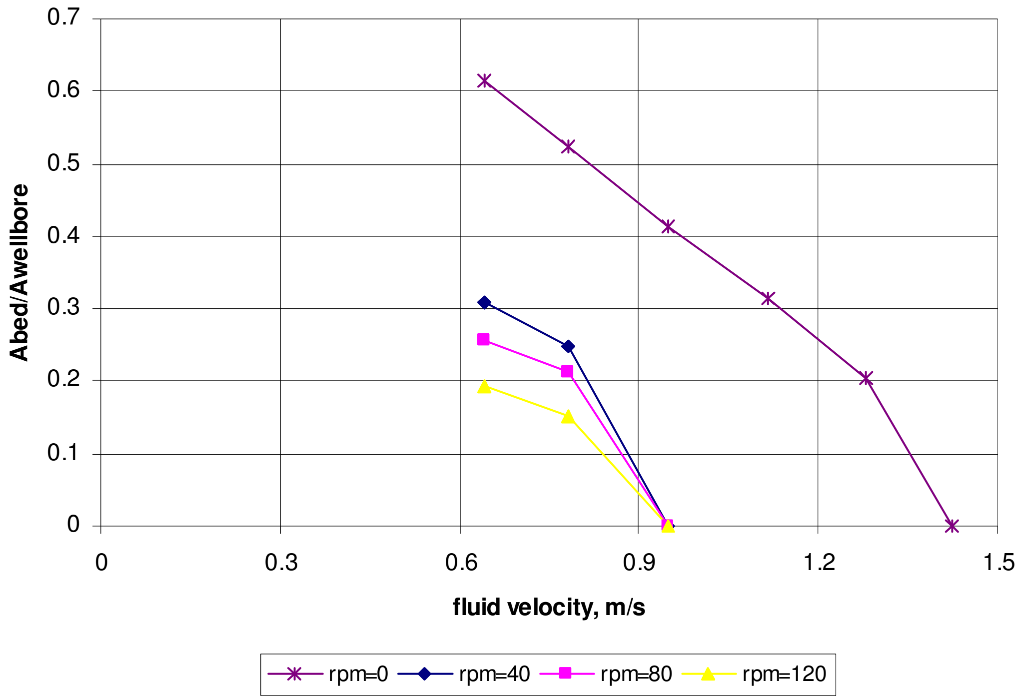

Figure 6.20- Effect of pipe rotation on critical fluid velocity (water, horizontal)

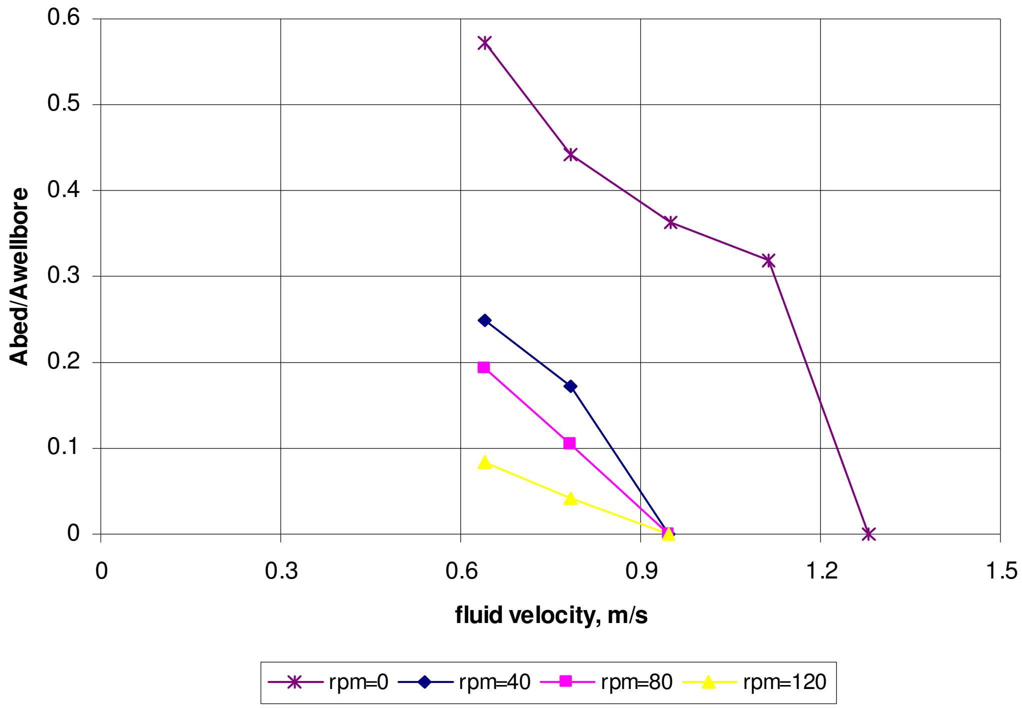

Figure 6.21- Effect of pipe rotation on critical fluid velocity (drilling fluid- 2, horizontal)

Experimental observations in this study showed that pipe rotation significantly increases frictional pressure gradient, particularly at lower flow rates and eccentric annulus, if no cuttings exist in the wellbore. As an example, the effect of pipe rotation on frictional pressure gradient inside fully eccentric and concentric annulus for fluid velocities are 0.64 m/s and 3.55 m/s are presented in Figure 6.22 and Figure 6.23, respectively. If these figures are analyzed, it can be seen that as the pipe rotation is introduced, frictional pressure gradient inside fully eccentric annulus significantly increase at low fluid velocity. At 0.64 m/s fluid velocity, when the pipe rotation increases from 0 to 40 rpm, the pressure gradient increases by 21%. However, after a certain pipe rotation speed, no noticeable effect of pipe rotation on pressure gradient is observed. What is more, pipe rotation has minor effect on pressure gradient for high fluid velocity. An example is shown in Figure 6.3.5.7. As seen from this figure, pressure gradient increases only 3 % for 3.56 m/s while pipe rotation increases 0 to 40 rpm. Moreover, for concentric annulus, pipe rotation has no noticeable influence on pressure gradient.

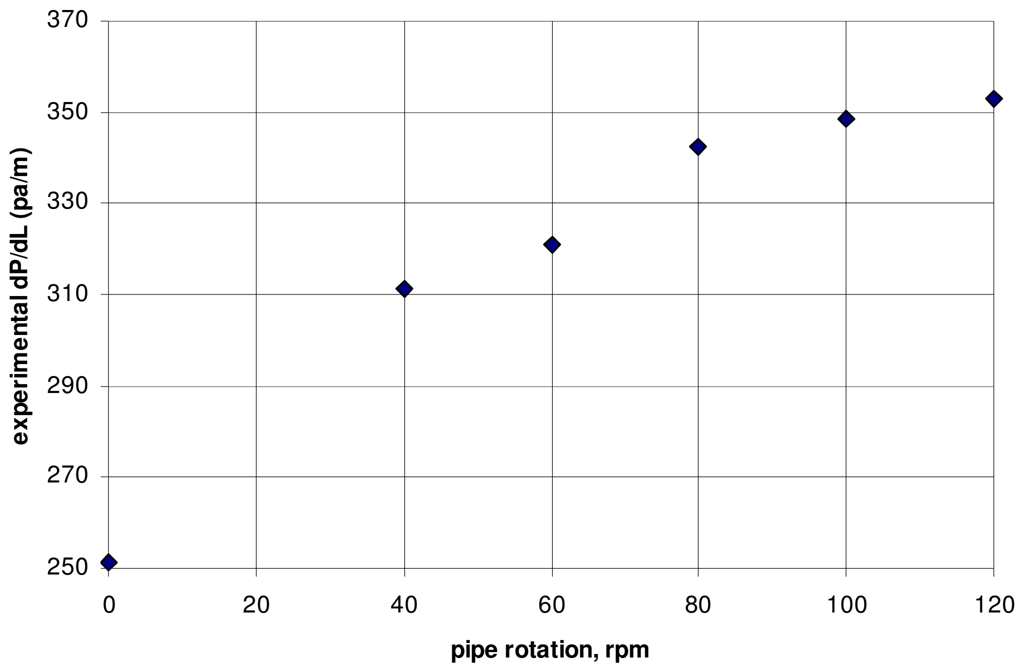

Figure 6.22- Pipe rotation effects on frictional pressure gradient inside fully eccentric annulus for axial velocity 0.64 m/s

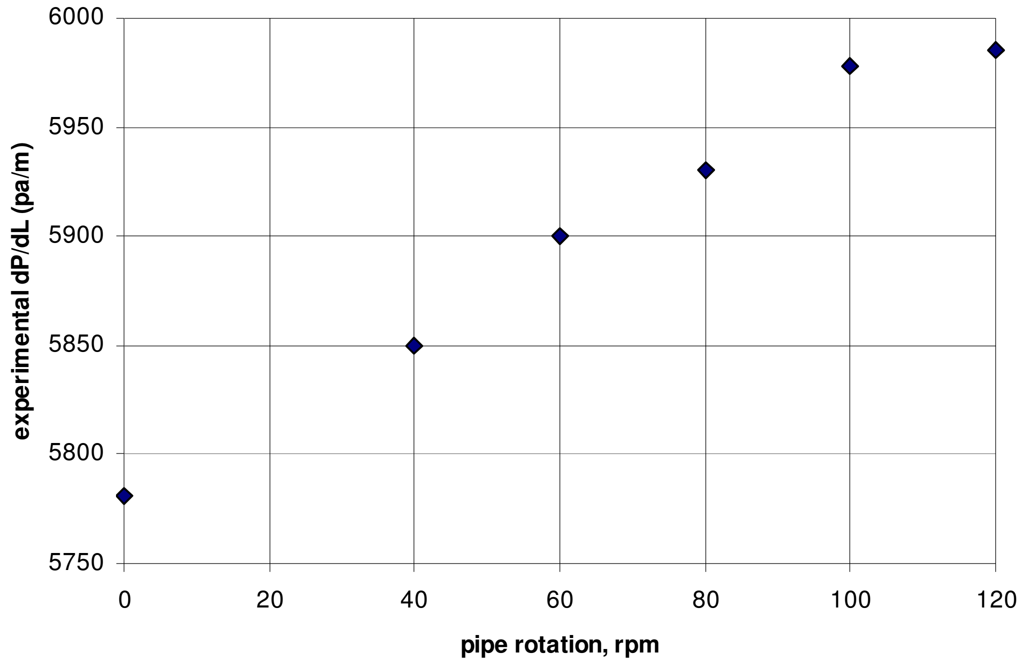

Figure 6.23- Pipe rotation effects on frictional pressure gradient inside fully-eccentric annulus for axial velocity 3.56 m/s

Figure 6.24 shows the influence of pipe rotation on pressure gradient with cuttings during a fluid velocity of 0.64 m/s, rate of penetrations of 0.00127-0.00381 m/s and hole inclination of 90 degrees. As seen from this figure, when the pipe is rotated, frictional pressure loss shows a decrease due to considerable reduction in cuttings bed in the annulus, especially if the pipe is making an orbital motion in eccentric annulus.

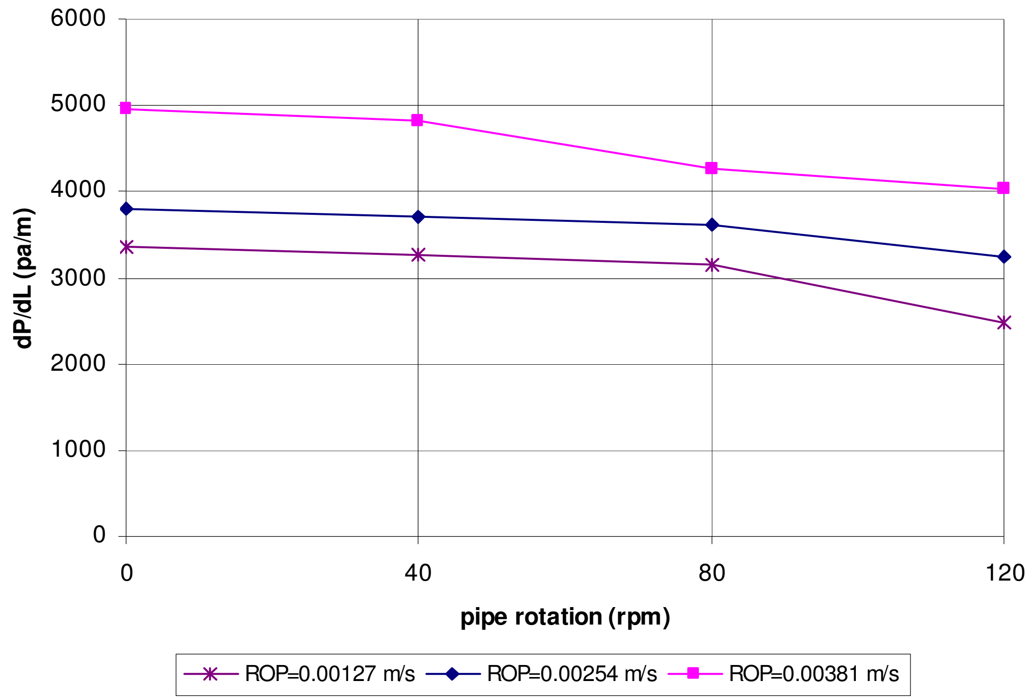

Figure 6.24- Effect of pipe rotation on frictional pressure gradient of drilling fluid-3 with presence of cuttings

CHAPTER 7

CONCLUSIONS AND RECOMMENDATIONS

In this study, frictional performance of drilling fluids inside annulus and cuttings transport mechanism in horizontal and deviated wellbores with and without pipe rotation are investigated. For this purpose, extensive experiments with water and various drilling fluids were conducted at METU-PETE for various inclinations, pipe rotation speeds, flow rates and rate of penetrations. A mathematical model for estimating frictional pressure loss of Newtonian fluids in concentric horizontal annulus with and without drillpipe rotation is proposed. Additionally, a numerical study for estimating frictional pressure loss inside horizontal fully eccentric annulus with pipe rotation and presence of cuttings are conducted by using commercial software program ANSYS Workbench 10.0 instead of using empirical correlations. Based on the experimental data, empirical correlations that can be used easily at the field are developed by using statical techniques for estimating stationary bed thickness and frictional pressure loss in horizontal and highly-inclined wellbores. Moreover, charts and expressions to calculate friction factor for water and drilling fluids are introduced as function of total Reynolds number and cuttings bed thickness. Mechanistic model and empirical correlations are validated by experimental data obtained from this study and previous published experimental data. The following conclusions can be drawn:

1. Fluid velocity is the dominant drilling variable on cuttings transport.

2. From the experimental studies, it has been seen that the rate of penetration and hole inclinations have a slight effect on the stationary cuttings bed thickness.

3. Pipe rotation has a significant influence on cuttings transport ability of the fluid. As the pipe is rotated, an improvement in hole cleaning is observed.

4. Pipe rotation also significantly decrease cuttings bed thickness and critical fluid velocity required to prevent stationary bed development for both water and drilling fluids, especially if the pipe is fully eccentric position. However, after a certain pipe rotation speed, no additional contribution of pipe rotation is observed on critical velocity.

5. For no-rotation and low rotation case, an increase in mud viscosity decreases reynolds number and the carrying capacity of drilling fluids. However, as the pipe rotation speed is increased, this effect diminishes.

6. When there are no cuttings present, the frictional pressure losses inside eccentric annulus increase as the pipe rotation speed is increased. However, as the cuttings are introduced, due to the reduction in the stationary cuttings bed area, frictional pressure losses decreases as the pipe rotation is increased, when compared with no-rotation case.

7. It is observed that the pipe rotation has no noticeable effect on annular frictional pressure loss of Newtonian fluid in concentric annuli. However, for fully eccentric annulus, pipe rotation drastically increases the frictional pressure loss, particularly at lower flow rates, most probably due to the orbital motion of the eccentric drillstring. Up to a point, as the pipe rotation increases, the frictional pressure losses also increase. As the flow rates are increased, the effect of pipe rotation on frictional pressure losses diminishes. Also, after a certain pipe rotation speed, no additional contribution of the pipe rotation on the frictional pressure loss is observed.

8. Expressions and charts for friction factor are proposed as function of total Reynolds number and cuttings bed thickness. This form of friction factor expressions can be used to predict the pressure losses for the cases of pipe rotation and even with the presence of a cuttings bed. When the cuttings bed thickness, i.e., ratio of the cuttings bed area and total flow area within the wellbore, is greater than 0.2, the empirical correlations proposed for estimating friction factor give predictions with error less than 20% in most cases. However, the friction factor is overestimated when the cuttings bed thickness is less than 0.2.

9. CFD software is capable of giving predictions of frictional pressure loss for two-phase solid-liquid flow through in horizontal annulus with and without pipe rotation.

10. The proposed model can estimate accurately the frictional pressure loss in laminar and turbulent flow of Newtonian fluid for concentric with and

without pipe rotation. The model is easy to use and gives more accurate results than empirical correlations widely used in the petroleum engineering such as crittendon, hydraulic, equivalent diameter to represent annular flow. The frictional pressure losses calculated using the proposed model are mostly within a $\pm$ 10% error interval in most cases when compared with the experimental results.

The recommendations for field applications and future works are as follows.

1. Pipe rotation for efficient removal of cuttings from the wellbore is highly recommended during drilling operations.

2. In this study, water based drilling fluids were used in the cuttings transport experiments. Experiments using oil based muds with drillpipe rotation can be conducted for hole inclinations ranging from 50 to 90 degrees in order to investigate cuttings transport performance of oil based muds.

REFERENCES

1. Short J.A. (1993): Introduction to Directional and Horizontal Drilling. Tulsa, Oklahoma: PenWell Publishing Company.

2. Naudri, S., “Managed Pressure Drilling Candidate Selection”, PhD Dissertation, Texas A&M University, Texas (2009).

3. Brown, N.P., Bern P.A. and Weaver A.,: “Cleaning Deviated Holes: New Experimental and Theoretical Studies”, paper SPE/IADC 18636 presented at the 1989 SPE/IADC Drilling Conference, New Orleans, Louisiana, 28 February – 3 March.

4. Bardley, W.B., Jarman, F., Plott, R.S., Wood, R.D., Schofield, T.R., Auflick, R.A., Cocking, D., “A Task Force Approach to Reducing Stuck Pipe Costs”, paper SPE 21999, presented at Amsterdam, 11-14 March 1991.

5. Tomren, P.H., A.W. Iyoho And J.J. Azar: “An Experimental Study of Cuttings Transport in Directional Wells”, SPE Drilling Engineering, Feb. 1986, pp. 43-56.

6. Ozbayoglu M.E., Sorgun M., Saasen A., Svanes K., “Hole Cleaning Performance of Light-Weight Drilling Fluids During Horizontal Underbalanced Drilling”, Journal of Canadian Petroleum Technology, 49, No.4, 21-26, 2010.

7. Kjosnes I., Loklingholm G., Saasen A., Syrstad S.O., Agle A., and Solvang K.A.; “Successful Water Based Drilling Fluid Design for Optimizing Hole Cleaning and Hole Stability”, SPE 85330, Presented at SPE/IADC Middle East Drilling Techology Conference and Exhibition, Abu Dhabi, UAE, 20-22 October, 2003.

8. Ozbayoglu M.E., Saasen A., Sorgun M., Svanes K., “Effect of Pipe Rotation on Hole Cleaning for Water-Based Drilling Fluids in Horizontal and Deviated Wells”, paper SPE 114965 presented at the 2008 IADC/SPE Asia Pacific Drilling Technology Conference & Exhibition in Jakarta, Indonesia , 25–27 August.

9. Lake L.W and Mitchell R.F.: Petroleum Engineering Handbook Volume II, Society of Petroleum Engineers, 2006.

10. Zeidler, H.U.,’’ An Experiment Analysis of the Transport of Drilled Particles’’, paper SPE 3064 presented at the SPE 45th Annular Meeting, Houston, 4-7 October , 1970.

11. Sifferman T.R., Myers G.M., Haden E.L and Wahl H.A.,”Drill Cuttings Transport in Full Scale Vertical Annuli”, paper SPE 4514 presented at the SPE 48th Annular Meeting, Las Vegas, Sept. 30-Oct. 3, 1973.

12. Tomren, P.H., A.W. Iyoho And J.J. Azar: “An Experimental Study of Cuttings Transport in Directional Wells”, SPE Drilling Engineering, Feb. 1986, pp. 43-56.

13. Seeberger M.H., Matlock R.W., and Hanson, P.M.,”Oil Muds in Large Diameter, Highly Deviated Wells”, paper SPE/IADC 18635 presented at the

1989 SPE/IADC Drilling Conference, New Orleanss, Lousiana, Feb. 28 - March 3.

14. Becker, T.E., Azar J.J., and Okrajni S., “Correlations of Mud Rheology Properties with Cuttings Transport Performance in Directional Drilling”, paper SPE 19535 presented at 1989 SPE Annular Technical Conference and Exhibition in San Antonio, October 8-11.

15. Hemphill T., Larsen T.I., ’’Hole Cleaning Capabilities of Water and Oil Based Drilling Fluids: A Comparative Experimental Study’’ SPE 26328 presented at the 1993 SPE Annular Technical Conference and Exhibition in Houston, October 3-6.

16. Luo Y., Bern P.A., Chambers B.D., Kellingray D.S., ‘’Simple Charts to Determine Hole Cleaning Requirements in Deviated Wells’’ paper IADC/SPE 27486 presented at the 1994 Drilling Conference, Dallas, 15-18 February.

17. Saasen A., Eriksen N.H., Han L., Labes P., and Marken C.D., “Is Annular Friction Loss the Key Parameter?”, Oil Gas European Magazine, (1)1998, pp.22-24.

18. Saasen A. And Loklingholm G., “The Effect of Drilling Fluid Rheological Properties on Hole Cleaning”, SPE 74558, Presented at IADC/SPE Drilling Conference, Dallas TX, 26-28 February, 2002.

19. Ozbayoglu M.E, Miska S.Z, Reed T., Takach N., ” Analysis of the Effects of Major Drilling Parameters on Cuttings Transport Efficiency for High Angle Wells in Coiled Tubing Drilling Operations” paper SPE 89334

presented at the SPE/ICoTA Coiled Tubing Conference and Exhibition, Houston, 23-24 March 2004.

20. Yu, M., D. Melcher, N. Takach, S.Z. Miska, R. Ahmed: “A New Approach to Improve Cuttings Transport in Horizontal and Inclined Wells”, SPE Paper 90529 presented at the SPE Annual Technical Conference and Exhibition, Houston, Texas,USA., Sept. 26-29, 2004.

21. Mirhaj S.A., Shadizadeh S.R., and Fazaelizadeh M., ‘’Cuttings Removal Simulation for Deviated and Horizontal Wellbores’’, SPE 105442 presented at the SPE Middle East Oil & Gas Show and Conference, Bahrain, 11-14 March 2007.

22. Ozbayoglu M.E., Saasen A., Sorgun M., Svanes K., “Critical Fluid Velocities for Removing Cuttings Bed Inside Horizontal and Deviated Wells”, Petroleum Science and Technology, 28:594-602, 2010.

23. Yu M., Takach N.E., Nakamura D.R., and Shariff M.M,’’ An Experimental Study of Hole Cleaning Under Simulated Downhole Conditions’’, SPE 109840 presented at the 2007 SPE Annular Technical Conference and Exhibition, California, USA, 11-14 November 2007.

24. Bilgesu H.I, Mishra N., and Ameri S.,“ Understanding the Effects of Drilling Parameters on Hole Cleaning in Horizontal and Deviated Wellbores Using Computational Fluid Dynamics”, paper 111208 presented at the 2007 SPE Eastern Regional Meeting, Lexington, Kentucky, 17-19 October.

25. Nazari, T., Hareland G., Azar J.J.,’’ Review of Cuttings Transport in Directional Well Drilling: Systematic Approach’’, paper 132372 presented

at the SPE Western Regional Meeting, Anaheim, California, USA, 24-27 May 2010.

26. Doron, P., Granica, D., and Barnea D.,“ Slurry Flow in a Horizontal Pipes-Experimental and Modeling”, Int.J. Multiphase Flow, 13, 1987, 535-547.

27. Gavignet, A.A. and Sobey I.J., “Model Aids Cuttings Transport Predictions”, Jour. of Pet. Tech., Sep. 1989, pp. 916-22.

28. Doron, P. and Barnea D., ’’Slurry Flow in Horizontal Pipes- A Three-Layer Model for Solid-Liquid Flow in Horizontal Pipes’’, Intl. Jour. of Multiphase Flow, 19, 1993, pp. 1029-43.

29. Doron, P., Simkhis M., and Barnea D.,’’ Flow of Solid-Liquid Mixtures in Inclined Pipes, Intl. Jour. of Multiphase Flow, 23, 1997, pp. 313-23.

30. Kenny, P., Sunde, E., Hemphill, T.,” Hole Cleaning Modelling: What’s “n” Got To Do With It?” paper IADC/SPE 35099 presented at the 1996 Drilling Conference, New Orleans, Louisina, 12-15 March.

31. Kamp, A.M. and Rivero M. : “Layer Modeling for Cuttings Transport in Highly Inclined Wellbores”, SPE 53942, SPE Latin American and Carribean Petroleum Engineering Conference, Caracas, Venezulea, April 21-23/1999.

32. Larsen, T.I., A.A. Pilehvari And J.J. Azar: “Development of a New Cuttings Transport Model for High-Angle Wellbores Including Horizontal Wells”, SPE Drilling&Completion, Jun. 1997, pp. 129-35.

33. Nguyen, D. and Rahman S.S.: "A Three-Layer Hydraulic Program for Effective Cuttings Transport and Hole Cleaning in Highly Deviated and Horizontal Wells", SPE Drilling & Completion, Sep. 1998, pp. 182-9.

34. Cho, H., Shah S.N., Osisanya S.O., : "A Three-Segment Hydraulic Model for Cuttings Transport in Horizontal and Deviated Wells", SPE 65488, presented at 2000 SPE/ Petroleum Society of CIM International Conference on Horizontal Well Technology, Calgary, Alberta, Canada, November 6-8, 2000.

35. Masuda Y., Doan Q., Oguztoreli M., Naganawa S., Yonezawa T., Kobayashi A., Kamp A.,"Critical Cuttings Transport Velocity in Inclined Annulus: Experimental Studies and Numerical Simulation", SPE 65502, 2000 SPE/Petroleum Society of CIM International Conference on Horizontal Well Technology, Calgary, Alberta, Canada, 6-8 November 2000.

36. Ozbayoglu M.E, ''Cuttings Transport with Foam in Horizontal and Highly-Inclined Wellbores'', PhD Dissertation, U. of Tulsa, Oklahoma(2002).

37. Ramadan A., Skalle P., Saasen A.,'' Application of a three-layer modeling approach for solids transport in horizontal and inclined channels'', Chemical Engineering Science, 60 (2005), 2557-2570.

38. Clark, R. K. And Bickham, K. L.: "A Mechanistic Model for Cuttings Transport", SPE 28306, 69th Annular Technical Conference and Exhibition,New Orleans-Louisiana,September 25-28,1994.

39. Ramadan A., Skalle P., Johansen S.T, Svein J., Saasen A.,'' Mechanistic model for cuttings removal from solid bed in inclined channels'', Journal of Petroleum Science and Engineering, 30 (2001), 129-141.

40. Ford, J.T., Peden, J.M., Oyeneyin, M.B., Gao, E., and Zarrough, R.: "Experimental Investigation of Drilled Cuttings Transport in Inclined Boreholes," paper SPE 20421 presented at the 1990 SPE Annual Technical Conference and Exhibition, New Orleans, Louisiana, 23-26 September.

41. Peden, J.M., Ford, J.T., and Oyeneyin, M.B.: "Comprehensive Experimental Investigation of Drilled Cuttings Transport in Inclined Wells Including the Effects of Rotation and Eccentricity", paper SPE 20925 presented at the 1990 European Petroleum Conference, Hague, Netherlands, 22-24 October.

42. Sifferman, T.R. and Becker T.E.: "Hole Cleaning in Full-Scale Inclined Wellbores", paper SPE 20422 presented at the 1990 SPE Annual Technical Conference and Exhibition, New Orleans, Louisiana, 23-26 September.

43. Lockett, T.J., Richardson, S.M. and Worraker, W.J.: "The Importance of Rotation Effects for Efficient Cuttings Removal During Drilling", paper SPE 25768 presented at the 1993 SPE/IADC Drilling Conference, Amsterdam, Netherland, 22-25 February.

44. Ribeiro P.R. and Podio A.L., ''The Effect of Rotational Speed and Eccentricity on Annular Flows with Application to Slim Hole Drilling Hydraulics'' paper SPE 26958 presented at the 1994 Latin American Petroleum Conference, Argentina, 27–29 April.

45. Gao, E., and Young, A.C., ''Hole Cleaning in Extended Reach Wells-Field Experience and Theoretical Analysis Using a Pseudo-Oil(Acetal) Based Mud'', paper SPE 29425 presented at the 1995 SPE/IADC Drilling Conference, Amsterdam, Netherlands, 28 February- 2 March.

46. Sanchez, R.A., J.J. Azar, A.A. Bassal, and A.L. Martins: Effect of Drillpipe Rotation on Hole Cleaning During Directional-Well Drilling, *SPE Journal*, Jun. 1999, pp. 101-108.

47. Saasen, A.: "Hole Cleaning During Deviated Drilling - the Effects of Pump Rate and Rheology", paper SPE 50582 presented at the 1998 SPE European Petroleum Conference in The Hague, Netherlands, 20-22 October.

48. Hemphill, T. and Ravi, K.,''Pipe rotation and Hole Cleaning in Eccentric Annulus'' paper SPE 99150 presented at the 2006 IADC/SPE Drilling Conference in Miami, February 21-23.

49. Hemphill, T., Bern P., Rojas J.C., and Ravi, K.,''Field Validation of Drillpipe Rotation Effects on Equivalent Circulating Density'' paper SPE 110470 presented at the 2007 IADC/SPE Drilling Conference in California, November 11-14.

50. Duan, M., Miska, Z.S., Yu, M., Takach, N., Ahmed, R., and Zettner, C.: "Transport of Small Cuttings in Extended Reach Drilling," paper SPE 104192 presented at the 2006 SPE International Oil & Gas Conference and Exhibition in China, Beijing, China, 5–7 December.

51. Duan, M., Miska, Z.S., Yu, M., Takach, N., Ahmed, R., and Hallmann, J.: "The Effect of Drillpipe Rotation on Pressure Losses and Fluid Velocity in

Foam Drilling'', SPE 114185 presented at the 2008 SPE International Oil & Gas Conference and Exhibition in USA, California, 31 March-2 April.

52. Duan M., ''Study of Cuttings Transport Using Foam With Drillpipe Rotation Under Simulated Downhole Conditions'', PhD Dissertation, U. of Tulsa, Oklahoma(2007).

53. Yamada, Y.,''Resistance of a flow through an annulus with an inner rotating cylinder,'' Bull. JSME, 5, No. 18, 1962, 302-310.

54. Coleman, B.D. and Noll, W.''Helical Flow of General Fluids,'' J. of App. Phy., 1959, Vol. 30, Issue 10, 1508-1512.

55. Delwiche, R.A., Stratabit D.B., Lejeune, M.W.D., Mawet, P.F.B.N., Vighetto, R. "Slimhole Drilling Hydraulics", paper SPE 24598, presented at the SPE Annual Technical Conference and Exhibition, Washington, 4-7 October, 1992.

56. Marken, C. D., He X. and Saasen A. ''The Influence Of Drilling Conditions on Annular Pressure Losses'', paper SPE 24598 presented at 1992 SPE Annular Technical Conference, Washington, 4-7 October, 1992.

57. McCann, R.C., Quigley, M.S., Zamora M., and Slater K.S.: "Effects of High-Speed Pipe Rotation on Pressures in Narrow Annuli", paper SPE 26343 presented at the 1993 SPE/IADC Drilling Conference, Houston, 3-6 October.

58. Hansen, S.A., Sterri, N.,''Drill Pipe Rotation Effects on Frictional Pressure Losses in Slim Annuli'', paper SPE 30488 presented at the 1995 SPE Annular Technical Conference, Dallas, 22-25 October.

59. Nouri J. M., Whitelaw J. H., ''Flow of Newtonian and Non-Newtonian Fluids in an Eccentric Annulus with Rotation of the Inner Cylinder'', Int.J.Heat and Fluid Flow 18: 236-246, 1997.

60. Wei, X., Miska S.Z., Takash N.E., Bern P., Kenny P., ''The Effect of Drillpipe Rotation on Annular Frictional Pressure Loss'', Journal of Energy Resources Technology 120:61-66, 1998.

61. Ooms G., Kampman-Reinhartz B.E.,''Influence of Drill Pipe Rotation and Eccentricity on Pressure Drop over Borehole During Drilling'', paper SPE 56638, presented at the 74th Annual Technical Conference and Exhibition, Houston, USA, 3-6 October 1999.

62. Wang, H., Su, Y., Bai, Y., Gao, Z., and Zhang, F., ''Experimental Study of Slimhole Annular Pressure Loss and Its Field Applications'', paper IADC/ SPE 59265 presented at the 2000 IADC/SPE Annular Technical Conference, New Orleans, 23-25 February.

63. Wan, S., Morrison, D., Bryden, I.G., ''The Flow of Newtonian and Inelastic Non-Newtonian Fluids in Eccentric Annuli with Inner-Cylinder Rotation'', Theoretical Computational Fluid Dynamics (2000) 13: 349-359.

64. Escudier, M.P., Oliveira, P.J. Pinho, F.T. ''Fully Developed Laminar Flow of Purely Viscous Non-Newtonian Liquids Through Annuli, Including The

Effects of Eccentricity and Inner-Cylinder Rotation'', Int. J. Heat and Fluid Flow. (2002) 23, 52-73.

65. Woo, N., Kim, Y., Hwang, Y., ''Experimental Study on the Helical Flow in a Concentric Annulus with Rotating Inner Cylinder'', Journal of Fluids Engineering Vol.128, 2006, 113-117.

66. Ahmed, R., Miska S., ''Experimental Study and Modeling of Yield Power-Law Fluid Flow in Annuli with Drillpipe Rotation'' paper SPE 112604 presented at the 2008 IADC/SPE Drilling Conference in Orlando, March 4-6.

67. Drew, T.B., Koo, E.C, and McAdams, W.H., 1932. The Friction Factors for Clean Round Pipes. Trans AIChE, Vol. 28, pp.56.

68. Colebrook, C. F., 1939. Turbulent Flow in Pipes With Particular Reference to the Transition Region Between the Smooth and the Rough Pipe Laws. J. Inst. 11, pp.133-156.

69. Moody, L.F., 1944. Friction Factors for Pipe Flow, presented at the Semi-Annual Meeting, American Society of Mechanical Engineering, 19-22 June.

70. Meter, D.M., and Bird, R.B. Turbulent Newtonian Flow in Annuli", AIChE J. 7:41-45, 1961.

71. Chen, N.H. An Explicit Equation for Friction Factor in Pipe, Ind. Eng. Chem. Found, Vol. 18, No.3, 296-297, 1979.

72. Jones, O.G., Jr., Leung, J.C.M. An Improvement in the Calculation of Turbulent Friction in Smooth Concentric Annuli", Journal of Fluid Engineering, Vol. 103, 1981.

73. Dodge, D., and Metzner A., ''Turbulent Flow of Non-Newtonian Systems", AIChE J. 5:189-204., 1959.

74. Kozicki, W., Chou, C.H., and Tiu, C.," Non-Newtonian Flow in Ducts of Arbitrary Cross-Sectional Shape'', Chemical Engineering Science, Vol.21, 665-679, 1966.

75. Gucuyener, H.I., and Mehmetoglu T.,'' Flow of Yield-Pseudoplastic Fluids Through a Concentric Annulus'', AIChE J. 38, 1139-1143, 1992.

76. Gucuyener, H.I., and Mehmetoglu T.,'' Characterization of flow regime in concentric annuli and pipes for yield-pseudoplastic fluids'', Journal of Petroleum Science and Engineering 16, 45-60, 1996.

77. Reed, T.D., and Pilehvari, A.A., '' A New Model for Laminar, Transitional, and Turbulent Flow of Drilling Muds'', SPE paper 25456, presented at the Production Operations Symposium in Oklahoma City, OK, USA, 21-23 March, 1993.

78. Singhal N., Shah S.N., Jain S.,'' Friction Pressure Correlations for Newtonian and Non-Newtonian Fluids in Concentric Annuli'', SPE paper 94280 presented at the 2005 SPE Conference, Oklahoma, USA , 17-19 April.

79. McKeon B.J, Zagarola M.V., and Smits A.J.,'' A new friction factor relationship for fully developed pipe flow''. J. Fluid Mech., Vol.538, pp. 429-443, 2005.

80. Avci A., Karagoz I.,'' A Novel Explicit Equation for Friction Factor in Smooth and Rough Pipes'', Journal of Fluids Engineering, Vol.131, 061203: 1-4, 2009.

81. Iyoho, A.W. and Azar, J.J.,''An Accurate Slot-Flow Model for Non-Newtonian Fluid Flow Through Eccentric Annuli,'' Society of Petroleum Engineers Journal, 21: 565-572,1981.

82. Bourgoyne A.T., Millheim K.K., Chenevert M.E.,Young F.S (1991): Applied Drilling Engineering. Richardson, Texas: SPE Text Book Series, pp 113-189.

83. Munson B.R., Young F.D., Okiishi T.D., Huebsch W.W.(2009): Fundamentals of Fluid Mechanics, John Wiley & Sons, Inc., NJ.

84. Bird R.B., Stewart W.E., Lightfoot E.N.: Transport Phenomena, John Wiley & Sons, Inc., NJ, 2002.

85. Muralidhar K., and Biswas G.: Advanced Engineering Fluid Mechanics, Alpha Science, 2005.

86. Ozbayoglu, M.E., Miska, Z.S., Reed, T., and Takach, N.,'' Using foam in horizontal well drilling: A cuttings transport approach'', J.Petrol.Sci.Eng. 46(4):267-282, 2005.

87. Whittaker A.: Theory and Application of Drilling Fluid Hydraulics, Exlog Series of Petroleum Geology and Engineering Handbooks.

88. Tosun I.: Modelling in Transport Phenomena: a conceptual approach, Elsevier Science B.V., 2005.

89. Harley C., Faghri A.,'' Two-Dimensional Rotating Heat Pipe Analysis'', Journal of Heat Transfer, Vol. 117,1995.

90. Song F., Ewing D., Ching C.Y,'' Fluid Flow and Heat Transfer Model for High-Speed Rotating Heat Pipes'', International Journal of Heat and Mass Transfer, 46(2003), 4393-4401.

91. Knudsen, J.G., Katz, D.L.,'' Fluid Dynamics and Heat Transfer'', McGraw-Hill Book Co. Inc., New York City (1959).

92. ANSYS, Inc. Theory. Release 5.7.

93. ANSYS CFX, Release 10.0: Theory

94. ANSYS CFX 8.0, Tutorial, Section Laminar to Turbulent Flow.

APPENDIX A

DERIVATIONS OF VISCOSITIES FOR POWER LAW FLUIDS

A.1 Axial Direction

If annular geomety is represented as a " narrow slot'' for a Newtonian fluid, frictional pressure gradient can be determined as;

$$\frac{\Delta P}{\Delta L} = \frac{48V\mu}{(D_o - D_i)^2} \tag{A.1}$$

For a Power Law fluid, frictional pressure gradient can be derived as

$$\frac{\Delta P}{\Delta L} = K\left(V\left(\frac{2n+1}{n}\right)\right)^n \left(\frac{4}{D_o - D_i}\right)^{1+n} \tag{A.2}$$

Solving (A.1) and (A.2) for μ yields

$$\mu = K\left(\frac{D_o - D_i}{V}\right)^{1-n} \left(\frac{2n+1}{n}\right)^n \left(\frac{2^{2n}}{12}\right) \tag{A.3}$$

In field units, (A.3) becomes

$$\mu = \left(\frac{K(D_o - D_i)^{1-n}}{144V^{1-n}} \right) \left(\frac{2 + \frac{1}{n}}{0.0208} \right) \tag{39}$$

A.2 Rotational Direction

Moment at any point r in annular geometry can be defined as

$$M = \tau 2\pi r^2 L \tag{A.4}$$

where L is the length of segment, and $r_i \le r \le r_o$. If the system is in equilibrium, at any point between r_i and r_o, moments must be equal, i.e., $M_1 = M_2$. Considering Figure A.1,

$$\tau_1 2\pi r_1^2 L = \tau_2 2\pi r_2^2 L \tag{A.5}$$

Rearranging yields

$$\tau_2 = \tau_1 \frac{r_1^2}{r_2^2} \tag{A.6}$$

Let

$$y = \frac{r}{r_i} \tag{A.7}$$

Then, equation (A.6) can be expressed as

$$\tau = \tau \frac{1}{y^2} \tag{A.8}$$

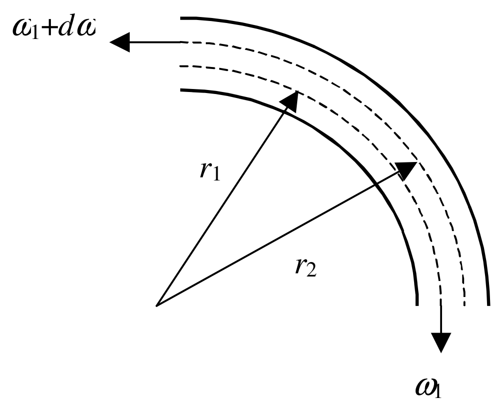

Figure A.1- Annular geometry for rotational motion representation

Shear rate can be defined as

$$\frac{dV}{dr} = \frac{V_2 - V_1}{r_2 - r_1} \tag{A.9}$$

Angular velocity can be expressed in terms of rotation speed as

$$V = \omega r \tag{A.10}$$

Inserting (A.10) into (A.9) yields

$$\frac{dV}{dr} = r\frac{d\omega}{dr} + \omega_1 + d\omega_1 \tag{A.11}$$

When right hand side of (A.11) is analyzed, it can be observed that only the first term is representing the change in velocity with shear rate. Thus, shear rate can be defined as

$$\gamma = f\left(\tau_i \frac{1}{y^2}\right) = \frac{dV}{dr} = r\frac{d\omega}{dr} = y\frac{d\omega}{dr} \tag{A.12}$$

Solving for $d\omega$ and integrating yields

$$\omega = \frac{2\pi\Omega}{60} = \int_0^{\frac{D_o}{D_i}} f\left(\tau_i \frac{1}{y^2}\right)\frac{1}{y}\,dy \tag{A.13}$$

For a Power Law Fluid,

$$\gamma = f\left(\tau_i \frac{1}{y^2}\right) = \left(\frac{\tau_i}{Ky^2}\right)^{\frac{1}{n}} \tag{A.14}$$

Therefore, shear stress can be written as

$$\tau_i = K\left(\frac{\pi\Omega}{15n}\left(\frac{\left(\frac{D_o}{D_i}\right)^{\frac{2}{n}}}{\left(\frac{D_o}{D_i}\right)^{\frac{2}{n}}-1}\right)\right)^n \qquad \text{(A.15)}$$

Considering a Newtonian fluid, using Navier-Stokes equations, shear stress can be

$$\tau_i = -\mu r \frac{d}{dr}\left(\frac{V}{r}\right) \qquad \text{(A.16)}$$

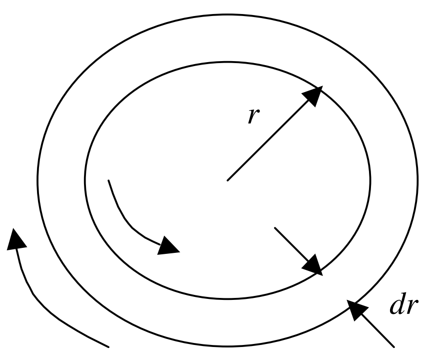

Figure A.2 – Moments acting on a ring element

When the moment distribution inside $(\tau 2\pi r L)$ and outside $((\tau + d\tau) 2\pi (r + dr) L)$ of a ring element is analyzed as shown in Figure A.2,

$$2\tau + r\frac{d\tau}{dr} = 0 \tag{A.17}$$

Therefore, combining (A.16) and (A.17), and solving for V yileds

$$V = \frac{c_1}{2} r + \frac{c_2}{r} \tag{A.18}$$

Applying the boundary conditions

$$r = r_i \qquad V = r_i \omega_i$$

$$r = r_o \qquad V = r_o \omega_o$$

Equation constants in (A.18) can be found as

$$c_1 = \frac{\omega_o r_o^2 - \omega_i r_i^2}{r_o^2 - r_i^2} \tag{A.19}$$

and

$$c_2 = \frac{r_o^2 r_i^2 (\omega_i - \omega_o)}{r_o^2 - r_i^2} \tag{A.20}$$

Since $\omega_2 = 0,$ after inserting (A.19) and (A.20) into (A.18) yileds

$$V = \frac{r_i^2 \omega_i}{r_o^2 - r_i^2}\left(\frac{r_o^2}{r} - r\right) \tag{A.21}$$

Using (A.21) in (A.16) with $r \to r_i$ leads to

$$\tau_i = \frac{2\mu r_o^2 \omega_i}{r_o^2 - r_i^2} = \frac{\pi N}{15}\frac{\mu D_o^2}{\left(D_o^2 - D_i^2\right)} \tag{A.22}$$

Equalizing (A.15) and (A.22), and solving for μ in field units yield

$$\mu_R = K\left(\frac{1}{n}\right)^n (\xi)\left(\frac{1}{\Omega}\right)^{1-n} \tag{40}$$

where

$$\xi = \left(\frac{D_o^2 - D_i^2}{D_o^2}\right)\left(\frac{15}{\pi}\right)^{1-n}\left(\frac{1}{\left(1-\left(\frac{D_o}{D_i}\right)^{-\frac{2}{n}}\right)}\right)^n \tag{41}$$

APPENDIX B

FLOW CURVES OF DRILLING FLUIDS USED IN THIS STUDY

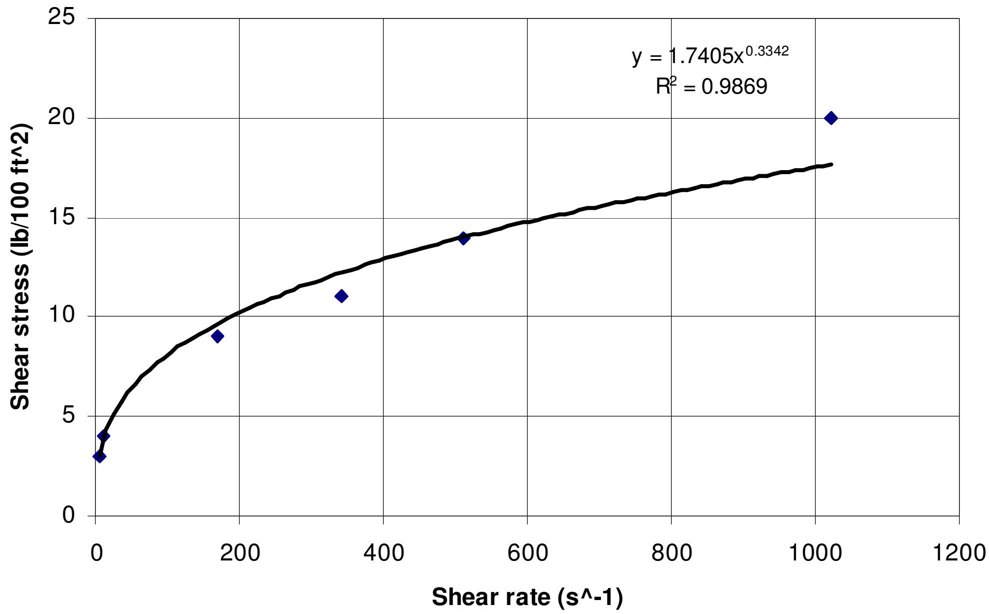

Figure B.1- Flow curves of drilling fluid-1

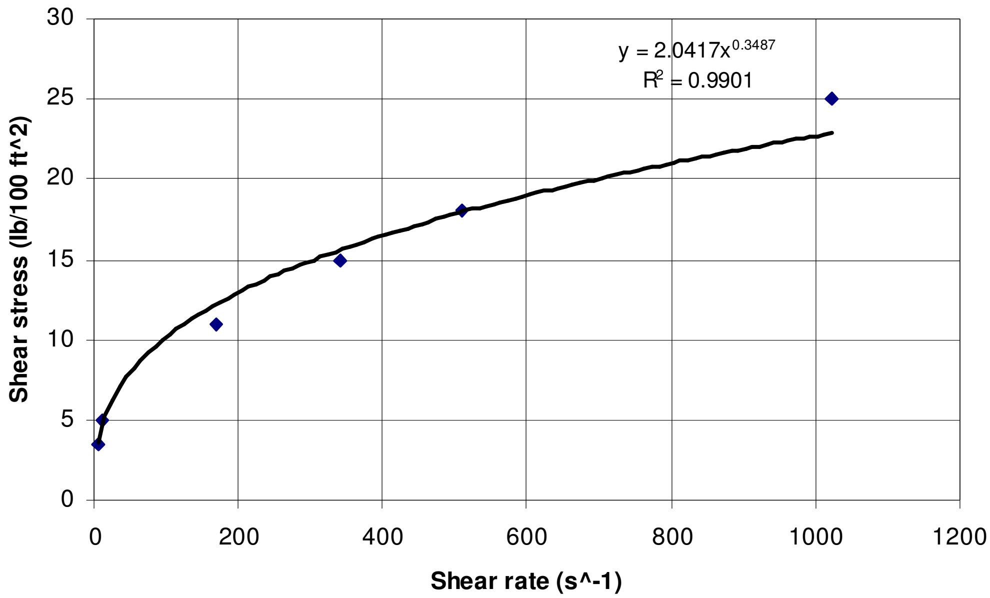

Figure B.2- Flow curves of drilling fluid-2

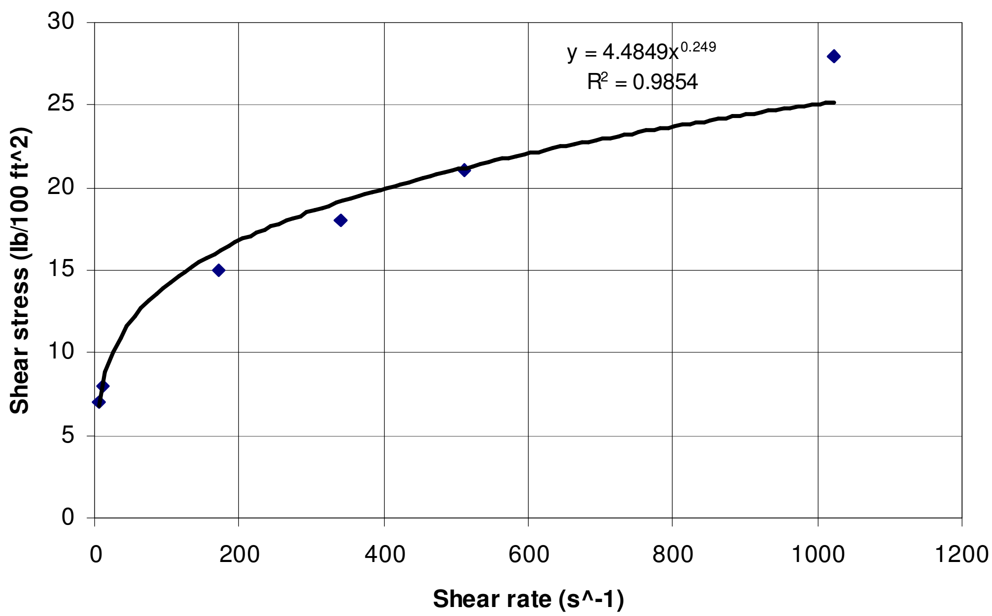

Figure B.3- Flow curves of drilling fluid-3

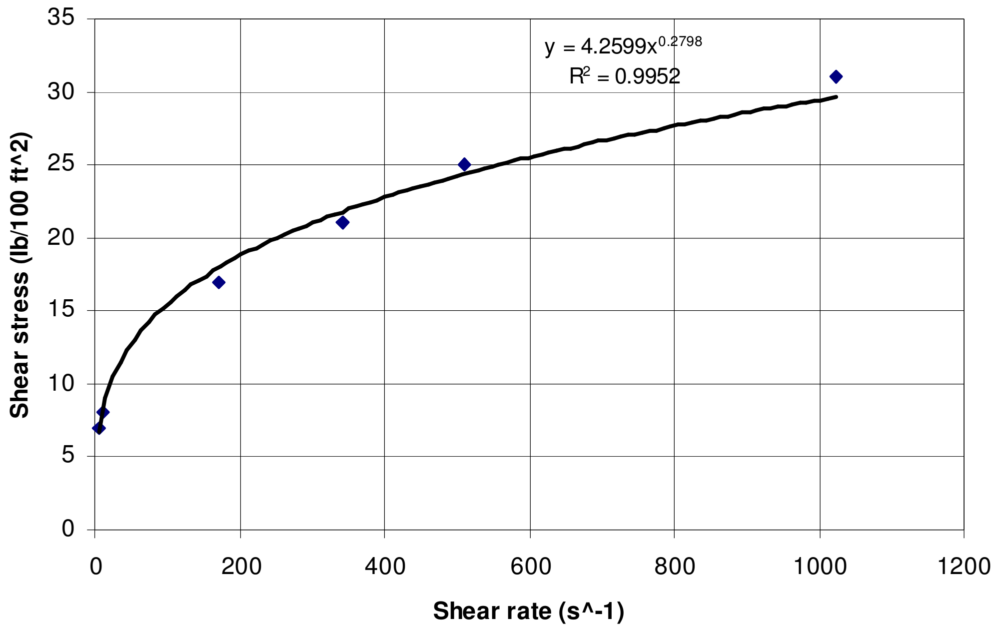

Figure B.4- Flow curves of drilling fluid-4

APPENDIX C

COMPARISON OF MODEL AND CFD PREDICTIONS WITH EXPERIMENTAL DATA

C.1 Single Phase Experiments (Water)

Table C.1 Comparison of the Predicted and Measured Pressure Gradient

			Pressure Gradient (pa/m)			Difference (%)
No	Axial velocity (m/s)	Pipe Rotation (rpm)	Measured	Predicted	ANSYS	Measured-Predicted
1	0.64	0	251	220	222	-14.15
2	0.78	0	340	316	328	-7.44
3	0.95	0	461	448	469	-2.98
4	1.11	0	630	606	626	-4.01
5	1.28	0	837	789	754	-6.06
6	1.42	0	1025	967	960	-5.97
7	1.59	0	1217	1196	1161	-1.76
8	1.78	0	1521	1490	1409	-2.10
9	2.02	0	1992	1910	1744	-4.27
10	2.25	0	2470	2383	2109	-3.63
11	2.49	0	3070	2915	2500	-5.33
12	2.85	0	3849	3835	3140	-0.37
13	3.08	0	4481	4527	3599	1.02
14	3.32	0	5255	5290	4084	0.65

Table C.1 (Continued)

			Pressure Gradient (pa/m)			Difference (%)
No	Axial velocity (m/s)	Pipe Rotation (rpm)	Measured	Predicted	ANSYS	Measured-Predicted
15	3.56	0	5781	5835	4595	0.93
16	0.64	40	311	227	250	-37.13
17	0.78	40	395	330	362	-19.62
18	0.95	40	552	465	508	-18.72
19	1.11	40	677	630	670	-7.38
20	1.28	40	876	820	847	-6.82
21	1.42	40	1106	995	1011	-11.20
22	1.59	40	1321	1220	1215	-8.29
23	1.78	40	1632	1530	1467	-6.66
24	2.02	40	2074	1945	1806	-6.63
25	2.25	40	2564	2400	2174	-6.82
26	2.49	40	3107	2940	2570	-5.69
27	2.85	40	3879	3860	3214	-0.49
28	3.08	40	4547	4548	3676	0.02
29	3.32	40	5316	5306	4165	-0.19
30	3.56	40	5850	6050	4677	3.30
31	0.64	60	321	239	265	-34.23
32	0.78	60	406	336	381	-20.92
33	0.95	60	565	473	530	-19.37
34	1.11	60	688	637	696	-8.02
35	1.28	60	886	825	875	-7.35
36	1.42	60	1130	1000	1040	-13.05
37	1.59	60	1327	1225	1246	-8.33
38	1.78	60	1645	1535	1497	-7.16
39	2.02	60	2109	1960	1840	-7.60
40	2.25	60	2589	2420	2209	-6.96
41	2.49	60	3138	2930	2607	-7.10

Table C.1 (Continued)

No	Axial velocity (m/s)	Pipe Rotation (rpm)	Pressure Gradient (pa/m) Measured	Predicted	ANSYS	Difference (%) Measured-Predicted
42	2.85	60	3917	3870	3253	-1.22
43	3.08	60	4576	4560	3717	-0.34
44	3.32	60	5331	5313	4210	-0.35
45	3.56	60	5900	6090	4722	3.12
46	0.64	80	342	248	282	-38.03
47	0.78	80	423	345	401	-22.47
48	0.95	80	586	483	553	-21.36
49	1.11	80	690	646	719	-6.86
50	1.28	80	900	833	901	-8.02
51	1.42	80	1140	1004	1069	-13.52
52	1.59	80	1337	1230	1278	-8.72
53	1.78	80	1687	1541	1532	-9.49
54	2.02	80	2151	2000	1876	-7.57
55	2.25	80	2628	2450	2246	-7.25
56	2.49	80	3151	2960	2645	-6.46
57	2.85	80	3979	3880	3294	-2.55
58	3.08	80	4641	4570	3760	-1.55
59	3.32	80	5404	5320	4251	-1.58
60	3.56	80	5931	6120	4766	3.09
61	0.64	100	348	270	298	-29.03
62	0.78	100	430	365	420	-17.92
63	0.95	100	589	500	577	-17.82
64	1.11	100	693	660	745	-4.96
65	1.28	100	904	843	927	-7.26
66	1.42	100	1147	1015	1096	-12.96
67	1.59	100	1349	1260	1306	-7.06
68	1.78	100	1691	1565	1566	-8.03

Table C.1 (Continued)

No	Axial velocity (m/s)	Pipe Rotation (rpm)	Pressure Gradient (pa/m) Measured	Predicted	ANSYS	Difference (%) Measured-Predicted
69	2.02	100	2145	2010	1912	-6.72
70	2.25	100	2646	2465	2285	-7.33
71	2.49	100	3169	2980	2684	-6.34
72	2.85	100	3983	3910	3338	-1.87
73	3.08	100	4647	4590	3804	-1.24
74	3.32	100	5416	5340	4295	-1.42
75	3.56	100	5978	6157	4814	2.91
76	0.64	120	353	295	311	-19.67
77	0.78	120	433	390	438	-11.11
78	0.95	120	592	535	598	-10.64
79	1.11	120	694	695	772	0.16
80	1.28	120	907	900	957	-0.76
81	1.42	120	1149	1050	1126	-9.47
82	1.59	120	1355	1280	1338	-5.89
83	1.78	120	1694	1580	1597	-7.22
84	2.02	120	2166	2040	1945	-6.17
85	2.25	120	2655	2490	2324	-6.64
86	2.49	120	3175	3000	2693	-5.85
87	2.85	120	3996	3940	3379	-1.43
88	3.08	120	4658	4630	3848	-0.6
89	3.32	120	5421	5375	4342	-0.86
90	3.56	120	5986	6180	4956	3.14
	Average Difference by taking absolute value of difference (%)					8.1

C.2 Cuttings Transport Experiments (Horizontal Case)

Table C.2 Comparison of the CFD and Experimental Data

			Pressure Gradient (pa/m)			Difference (%)
No	Axial velocity (m/s)	Pipe Rotation (rpm)	ROP (m/s)	Measured	ANSYS	Measured-ANSYS
1	11.41	0	0.0050	1461	1244	-17.42
2	11.24	99	0.0050	1409	1657	14.94
3	7.63	122	0.0050	1164	1448	19.58
4	7.40	80	0.0050	1230	1098	-12.08
5	7.61	0	0.0052	1335	995	-34.13
6	9.16	98	0.0052	1219	1267	3.78
7	9.29	61	0.0052	1463	1810	19.16
8	5.39	122	0.0052	978	1267	22.77
9	5.64	98	0.0052	1057	769	-37.40
10	5.82	80	0.0052	1066	1176	9.36
11	7.49	61	0.0052	1299	1176	-10.45
12	7.68	62	0.0069	1751	1357	-29.00
13	5.94	62	0.0068	1559	1457	-7.05
14	5.90	80	0.0068	1466	1403	-4.49
15	5.88	99	0.0068	1425	1318	-8.06
16	5.76	122	0.0068	1410	1267	-11.30
17	7.57	80	0.0069	1661	1450	-14.62
18	7.67	99	0.0069	1631	1629	-0.16
19	9.41	62	0.0069	1735	1448	-19.83
20	9.40	80	0.0069	1693	2172	22.05
21	9.39	121	0.0069	1721	2081	17.30
22	11.22	0	0.0069	1621	1267	-27.94
23	11.32	61	0.0069	1750	1629	-7.45
24	11.34	80	0.0069	1718	1647	-4.31
25	11.32	99	0.0069	1717	1727	0.61
26	11.33	122	0.0069	1752	1866	6.09
27	13.25	0	0.0083	1713	2172	21.13

Table C.2 (Continued)

			Pressure Gradient (pa/m)			Difference (%)
No	Axial velocity (m/s)	Pipe Rotation (rpm)	ROP (m/s)	Measured	ANSYS	Measured-ANSYS
28	11.45	0	0.0083	1912	1688	-13.22
29	11.47	122	0.0083	1883	1957	3.77
30	11.45	99	0.0083	1855	1733	-7.04
31	11.48	62	0.0083	1853	1611	-14.98
32	11.46	80	0.0083	1844	1629	-13.21
33	9.48	0	0.0083	1705	1551	-9.94
34	9.51	122	0.0083	1825	1497	-21.90
35	9.66	99	0.0083	1809	2081	13.10
36	7.69	0	0.0083	1498	1086	-37.99
37	9.49	62	0.0083	1888	1810	-4.31
38	5.72	61	0.0083	1671	1176	-42.07
39	5.67	80	0.0083	1510	1176	-28.37
40	5.64	98	0.0083	1427	1578	-21.34
41	7.55	122	0.0083	1647	1578	-4.34
42	7.56	98	0.0083	1676	2055	18.43
43	7.61	61	0.0083	1897	1357	-39.79
44	7.57	80	0.0083	1746	1249	-39.82
45	11.41	0	0.0101	1808	1448	-24.88
46	9.50	0	0.0101	1988	1629	-22.09
47	11.39	62	0.0101	1989	2534	21.50
48	11.39	122	0.0101	1964	1811	-8.45
49	11.39	99	0.0101	1961	1753	-11.87
50	9.52	122	0.0101	1936	1448	-33.71
51	9.52	99	0.0101	1923	2443	21.29
52	9.54	80	0.0101	1951	1810	-7.83
53	9.52	61	0.0101	2015	1538	-30.99
54	7.70	122	0.0101	1789	1746	-2.43

Table C.2 (Continued)

No	Axial velocity (m/s)	Pipe Rotation (rpm)	Pressure Gradient (pa/m) ROP (m/s)	Measured	ANSYS	Difference (%) Measured-ANSYS
55	7.71	98	0.0101	1798	2262	20.50
56	7.71	80	0.0101	1877	1538	-22.03
57	7.68	62	0.0101	2024	2353	13.94
58	5.82	122	0.0101	1592	1367	-16.45
59	5.86	99	0.0101	1696	1475	-14.99
60	5.85	62	0.0101	1905	1654	-15.17
61	10.06	80	0.0038	3485	3540	1.55
62	8.23	120	0.0025	2821	3090	8.69
63	10.06	120	0.0025	2932	3200	8.38
64	8.23	120	0.0038	3209	3210	0.04
65	8.23	120	0.0038	3430	3533	2.92
66	8.23	40	0.0025	3319	3650	9.06
67	8.23	40	0.0038	4038	4200	3.85
68	8.23	80	0.0038	4038	4150	2.69
69	8.23	120	0.0038	3872	4100	5.55
	Average Difference by taking absolute value of difference (%)					15.14

APPENDIX D

GRAFICS ABOUT MODEL AND EXPERIMENT RESULTS

This appendix presents model predictions and CFD simulations compared with experimental frictional pressure gradient inside concentric annulus for various pipe rotation speeds and flow rates.

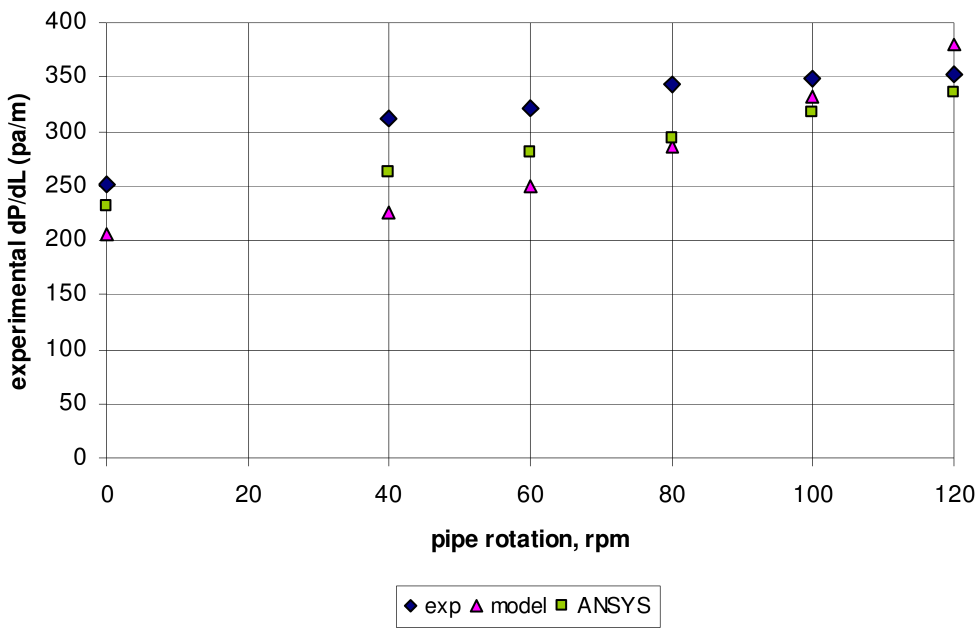

Figure D.1- Comparison of proposed model with experimental data for average fluid velocity=0.64 m/s

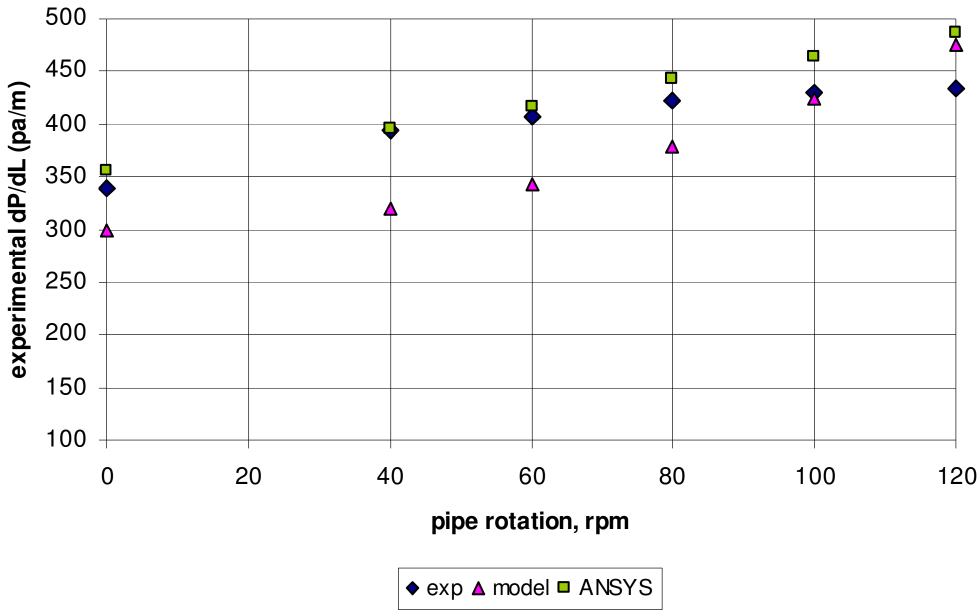

Figure D.2- Comparison of proposed model with experimental data for average fluid velocity=0.78 m/s

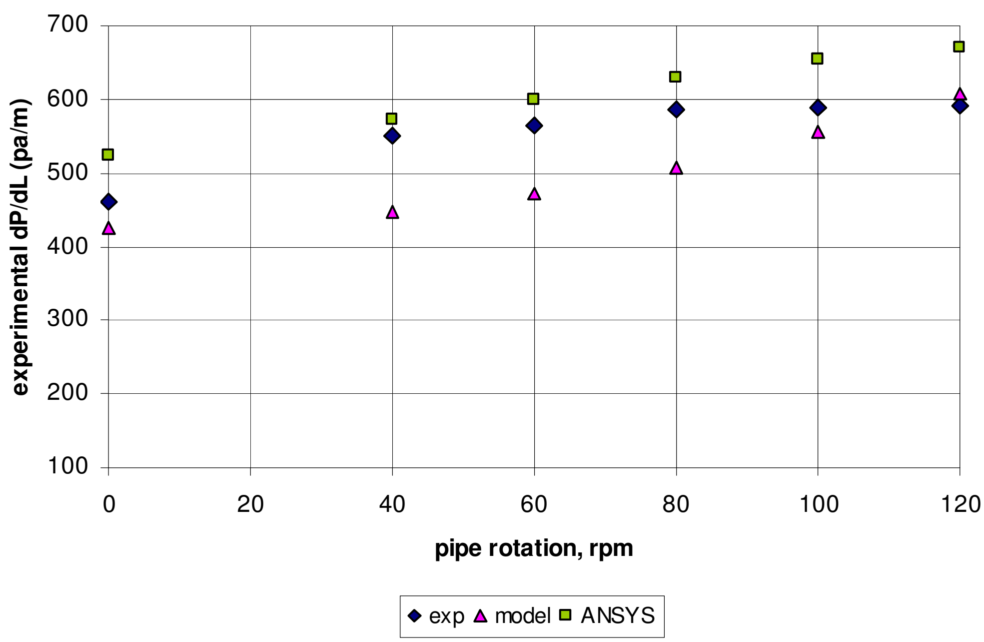

Figure D.3- Comparison of proposed model with experimental data for average fluid velocity=0.95 m/s

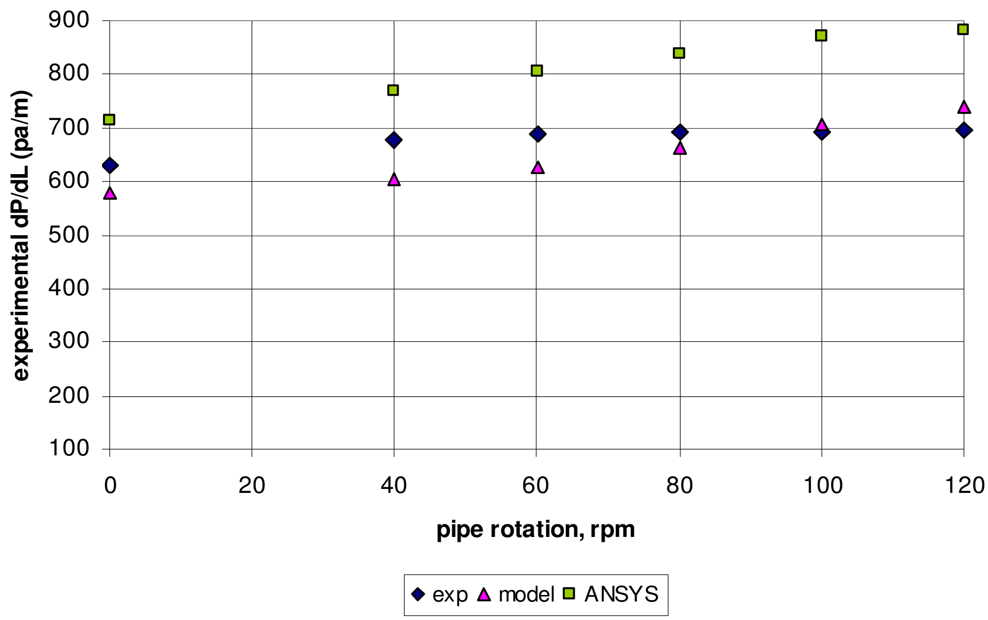

Figure D.4- Comparison of proposed model with experimental data for average fluid velocity=1.11 m/s

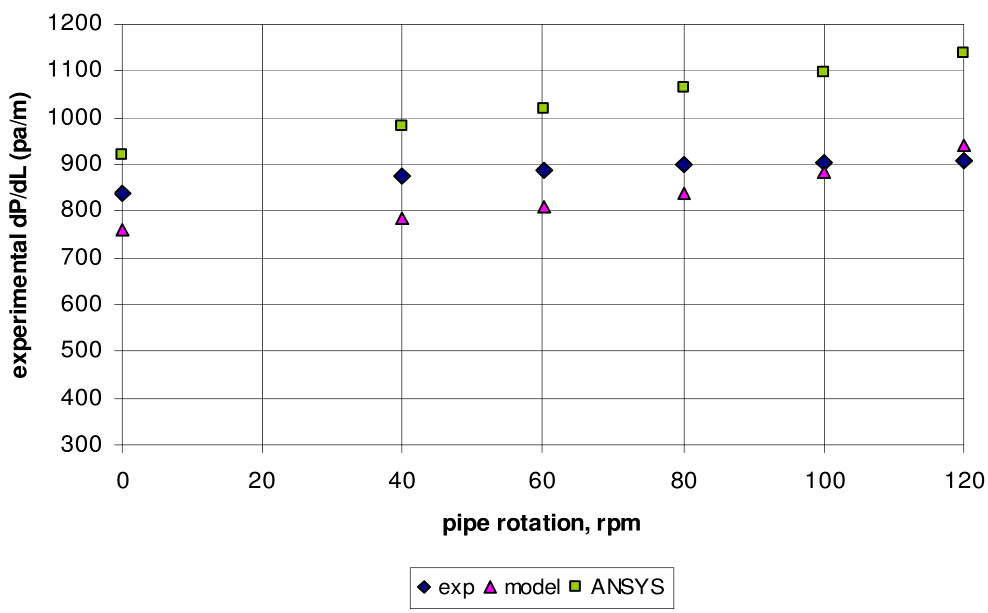

Figure D.5- Comparison of proposed model with experimental data for average fluid velocity=1.28 m/s

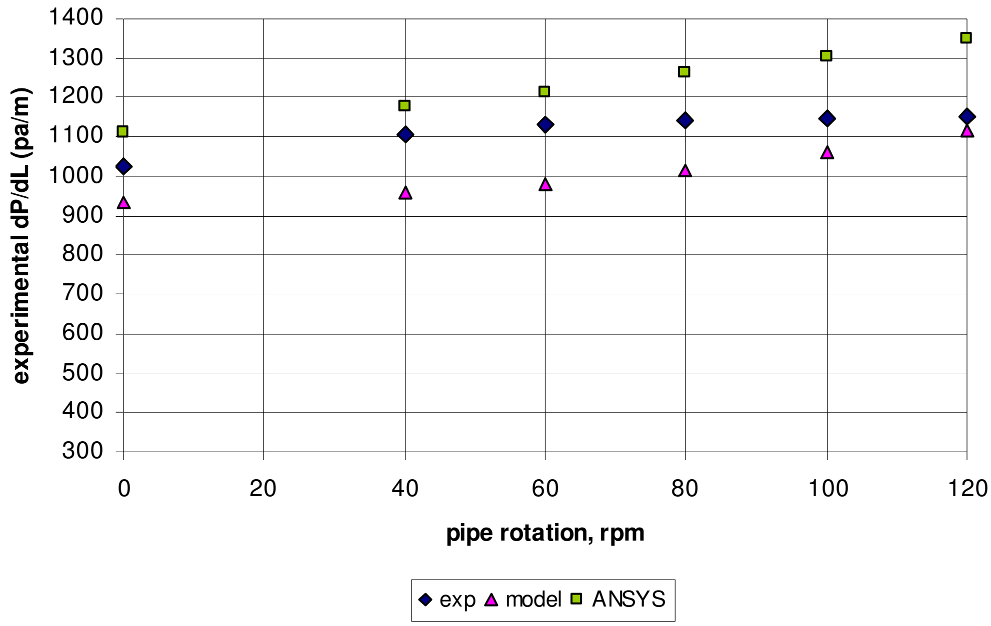

Figure D.6- Comparison of proposed model with experimental data for average fluid velocity=1.59 m/s

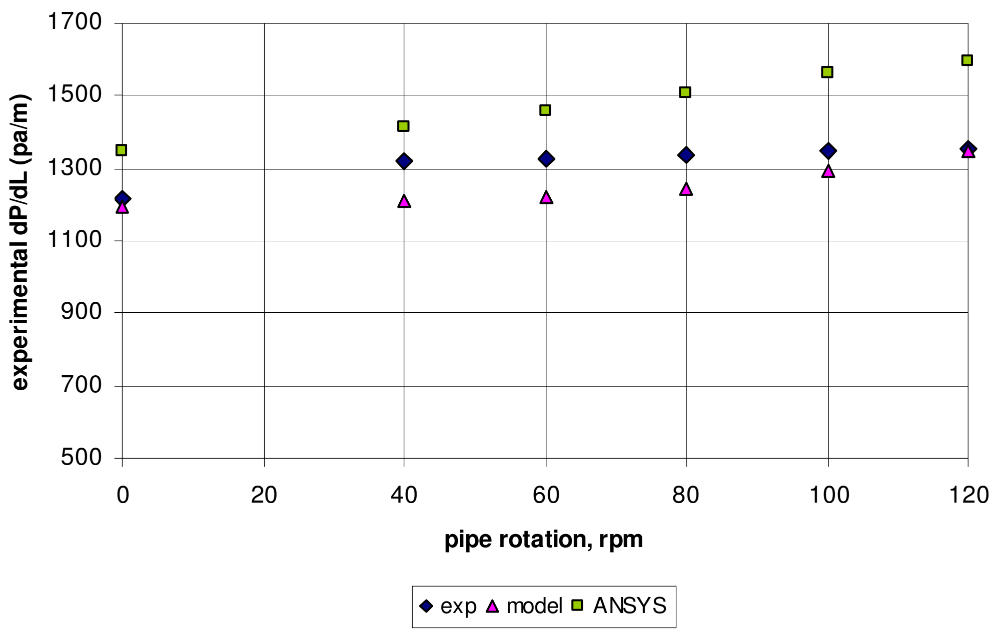

Figure D.7- Comparison of proposed model with experimental data for average fluid velocity=1.59 m/s

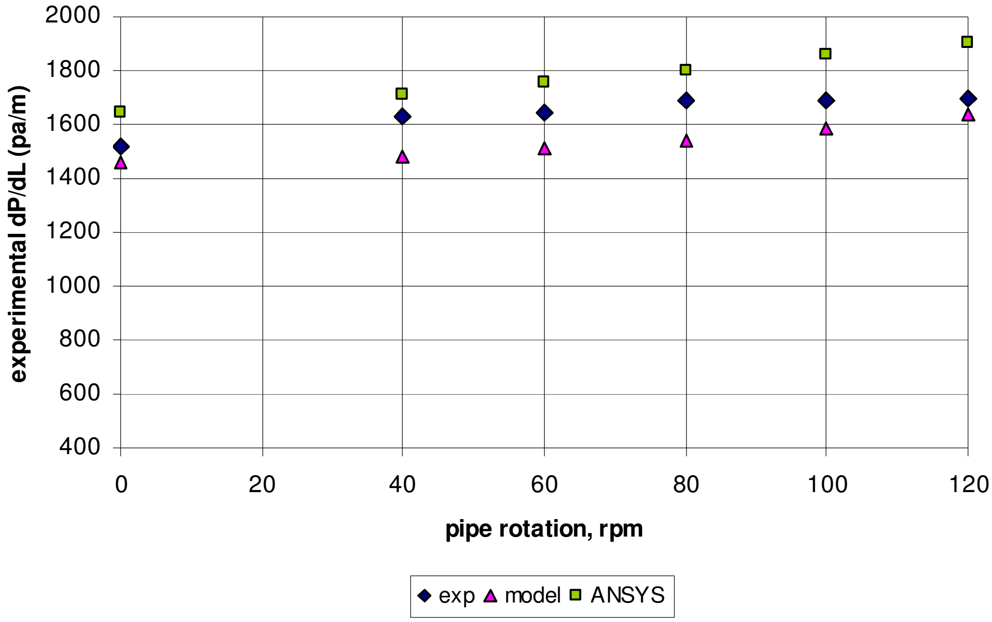

Figure D.8- Comparison of proposed model with experimental data for average fluid velocity=1.78 m/s

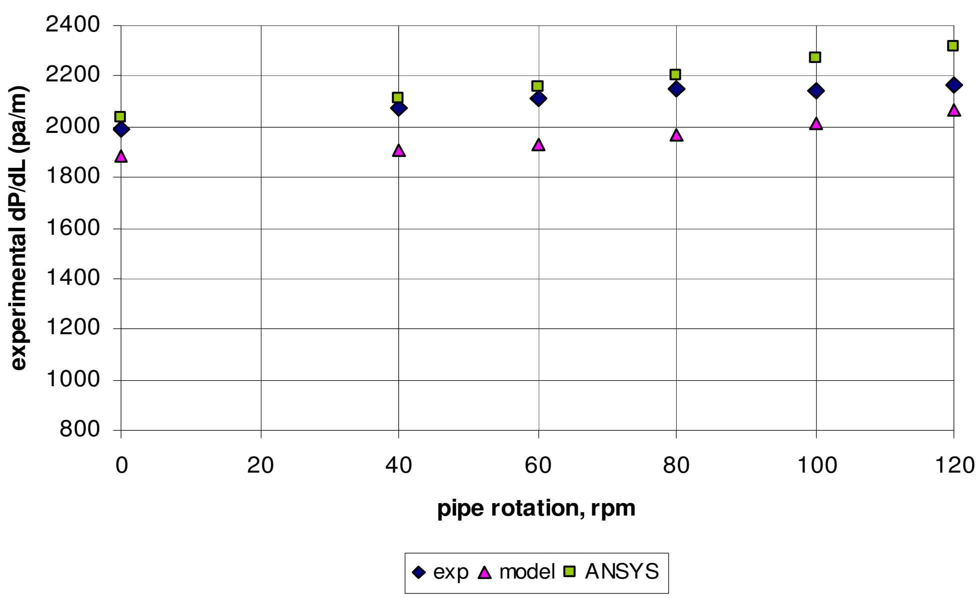

Figure D.9- Comparison of proposed model with experimental data for average fluid velocity=2.02 m/s

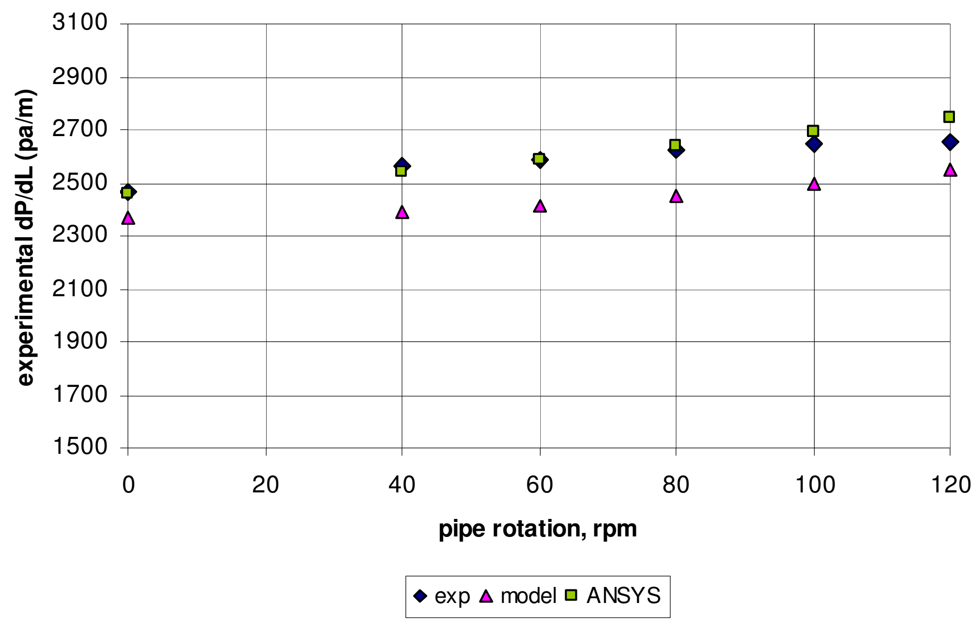

Figure D.10- Comparison of proposed model with experimental data for average fluid velocity=2.25 m/s

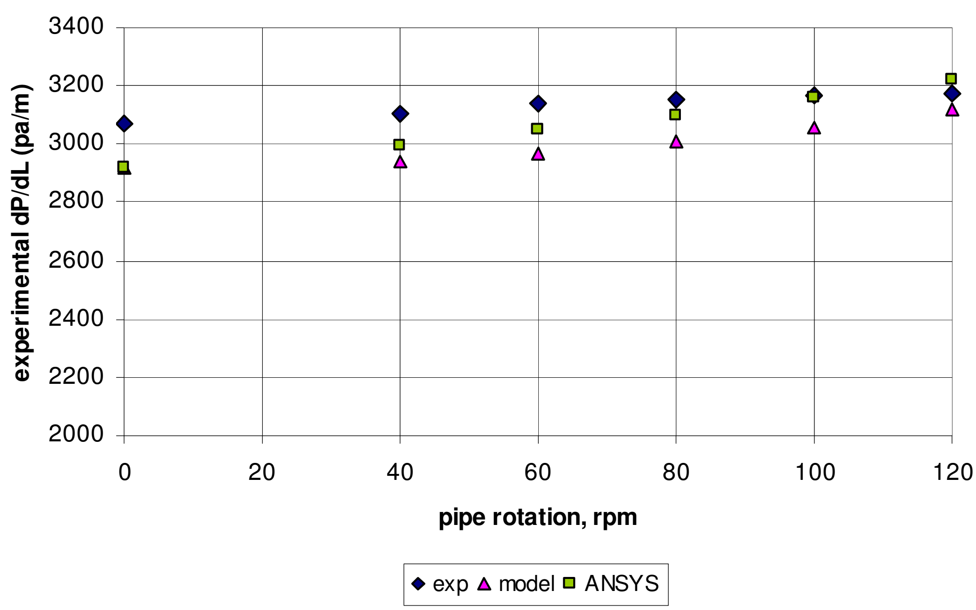

Figure D.11- Comparison of proposed model with experimental data for average fluid velocity=2.49 m/s

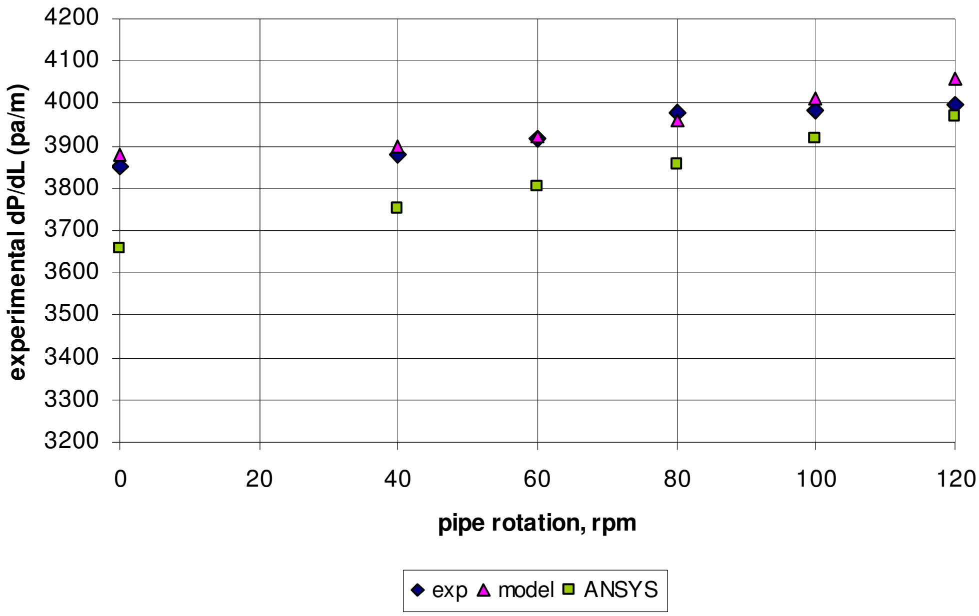

Figure D.12- Comparison of proposed model with experimental data for average fluid velocity=2.85 m/s

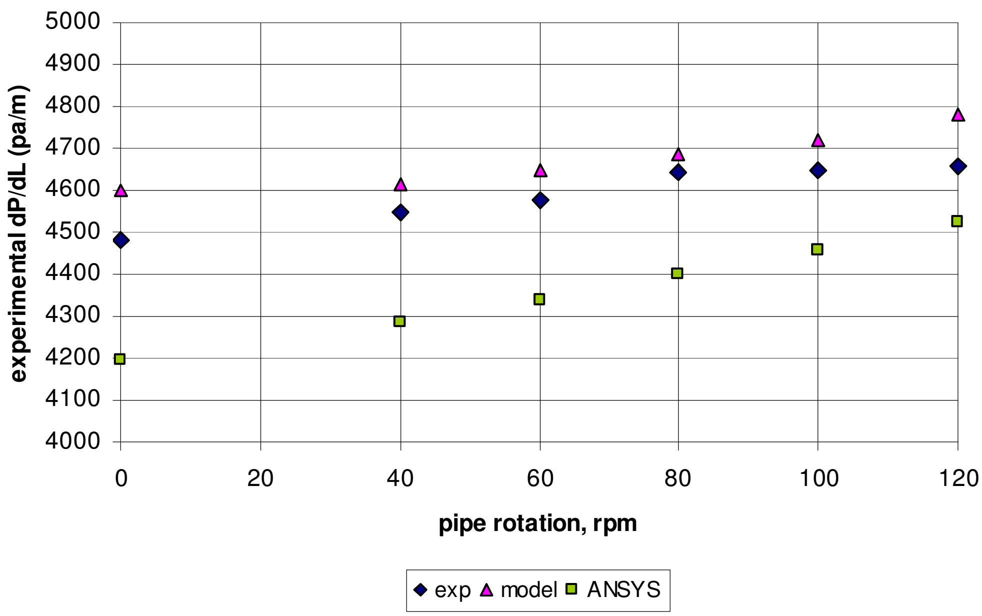

Figure D.13- Comparison of proposed model with experimental Data for average fluid velocity=3.08 m/s

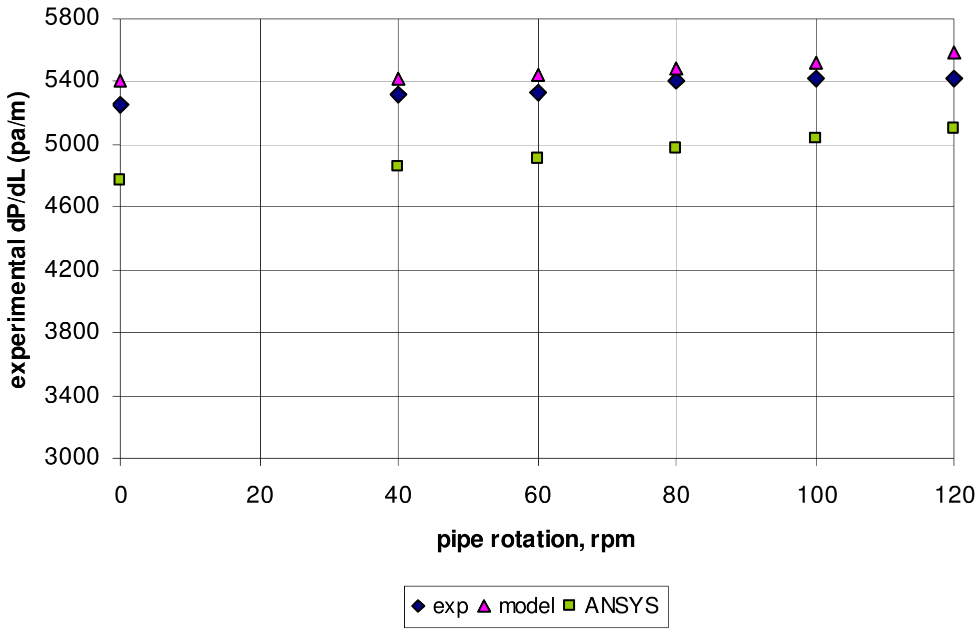

Figure D.14- Comparison of proposed model with experimental data for average fluid velocity=3.32 m/s

APPENDIX E

INPUT DATA FOR COMPUTATIONAL FLUID DYNAMICS SOFTWARE (ANSYS Workbench)

- 1.5 in – 1.25 in concentric annulus with a length of 15 in
- Fluid description : Water
- Turbulence model : k-ε
- The flow was assumed to be steady, incompressible, isothermal
- Total number of Nodes : 324975
- Total number of tetrahedral meshes : 2.3×10^6

Ansys Workbench and Ansys CFX Solution Process consist of as follows steps :

1. Create Geometry
   -Design Modeller (or CAD package): define volume of computational domain
2. Create Mesh
   - CFX Mesh: name boundaries, refine CFD mesh
3. Setup Simulation
   - CFX-Pre: materials, boundary conditions, loading, solution controls
4. Solve
   - CFX-Solver: monitor convergence
5. Post-process Results
   - CFX-Post: extract results

A few images is viewed in Figure E.1 –E.6 related to CFD simulator for the solution parts.

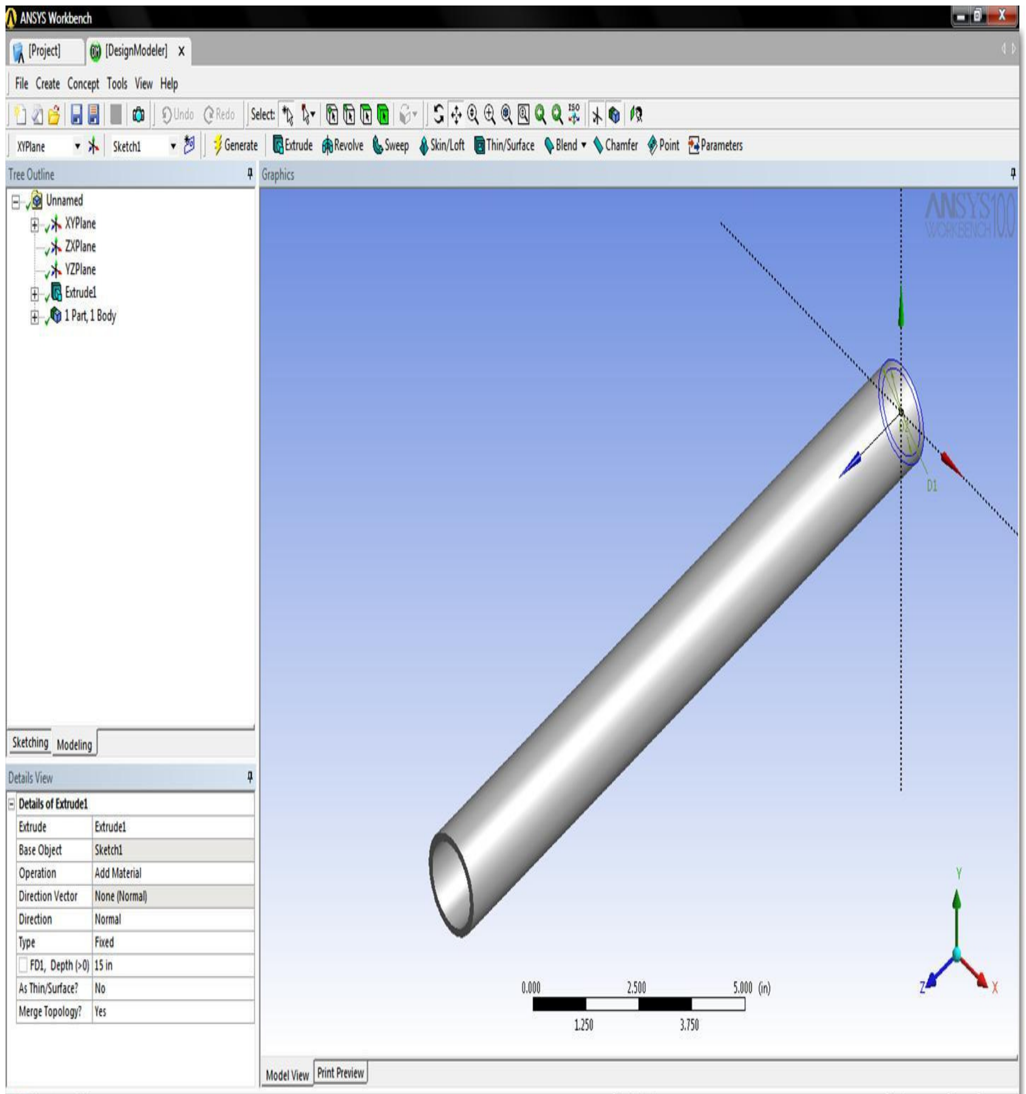

Figure E.1- One of the concentric annulus used CFD simulation

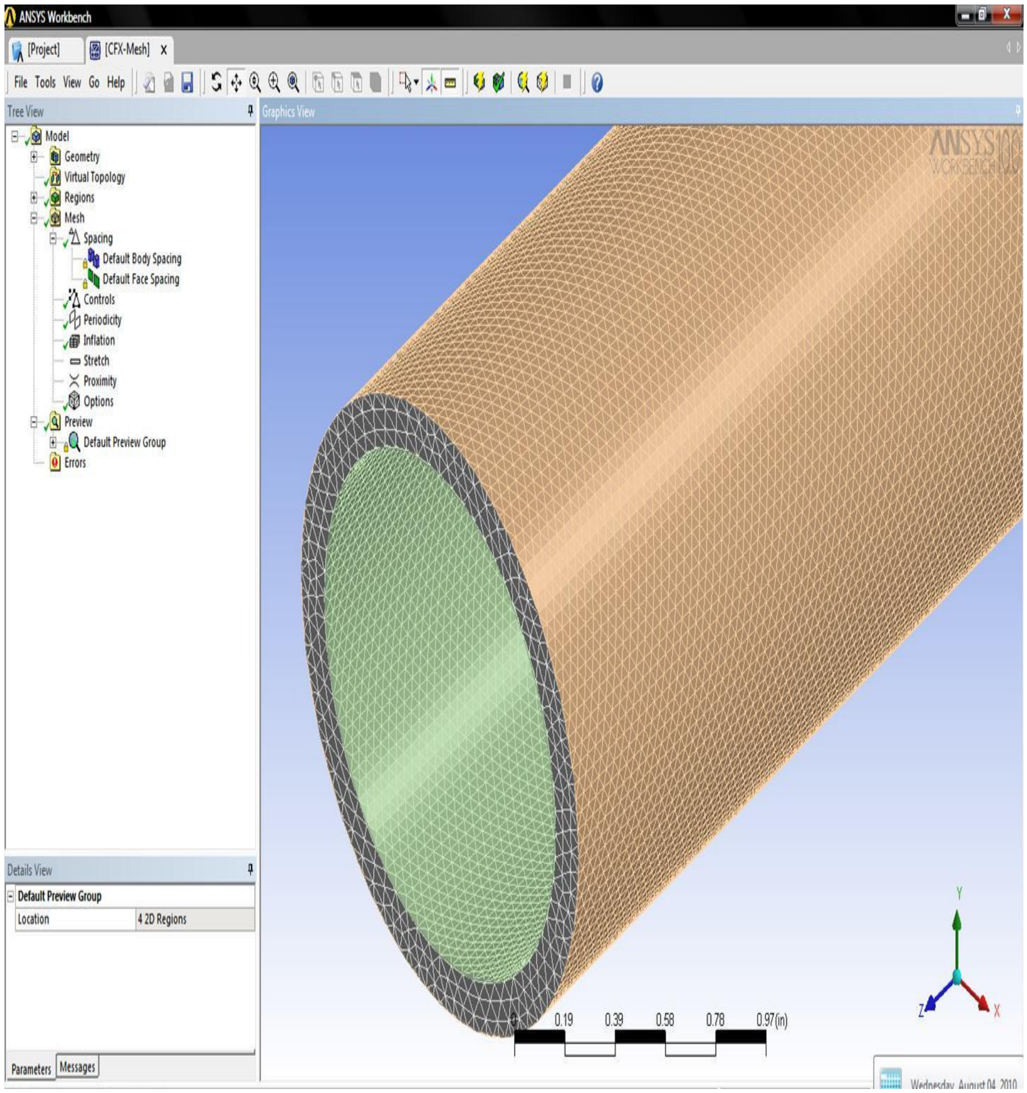

Figure E.2- CFD Model tetrahedral mesh sample for concentric annulus

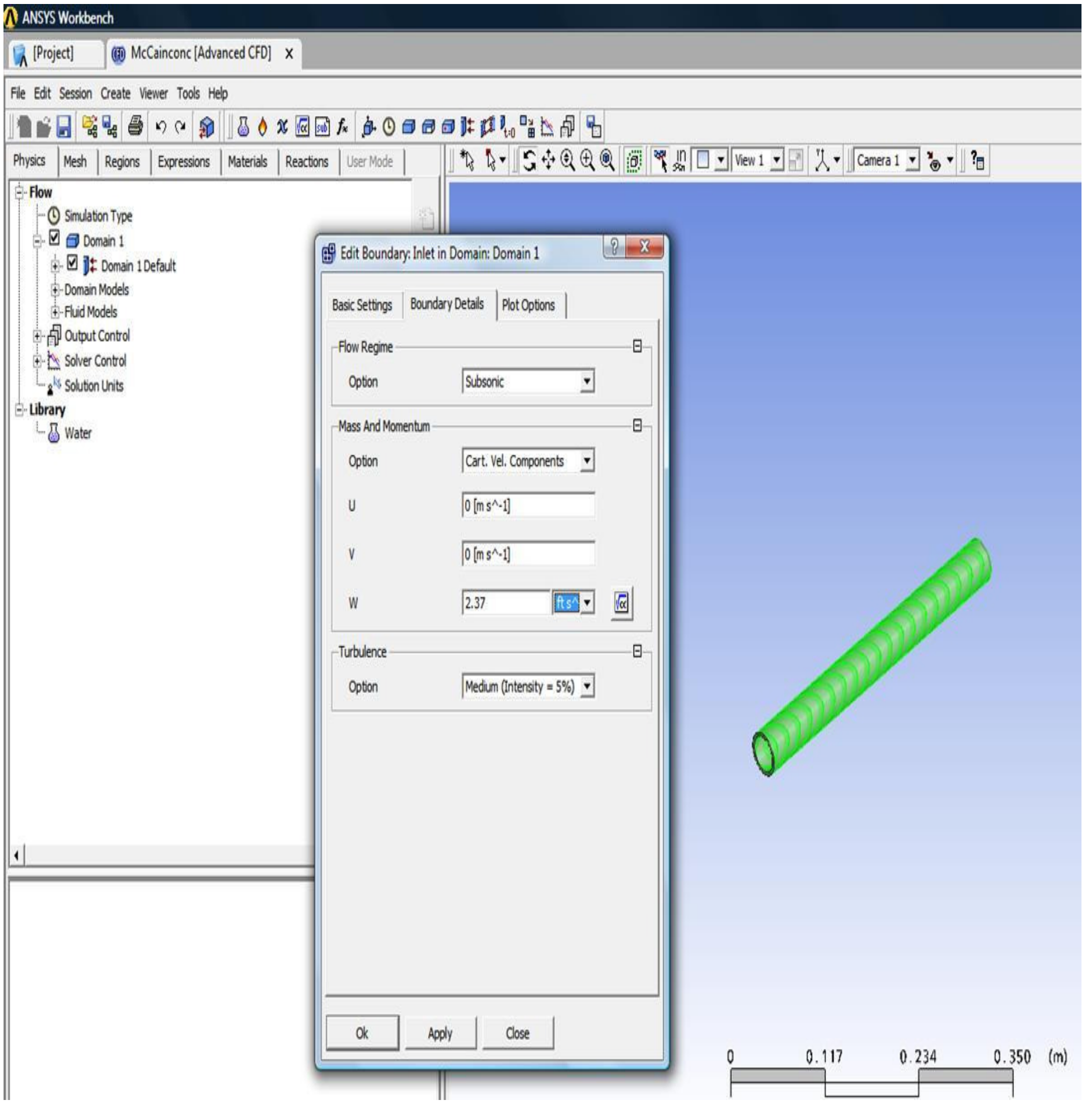

Figure E.3- Input Boundary Conditions to ANSYS CFX

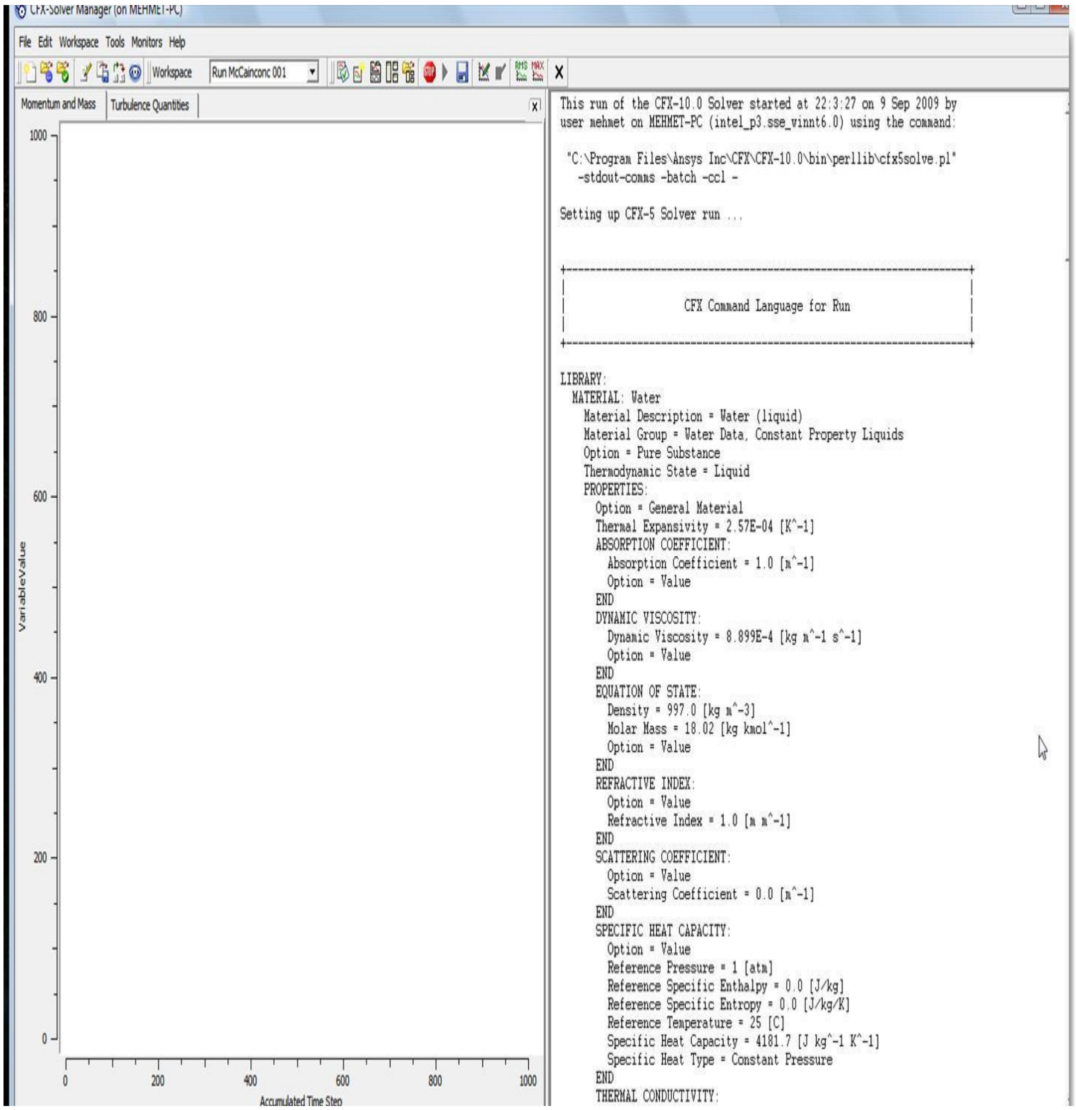

Figure E.4- Start CFX-Solver Manager

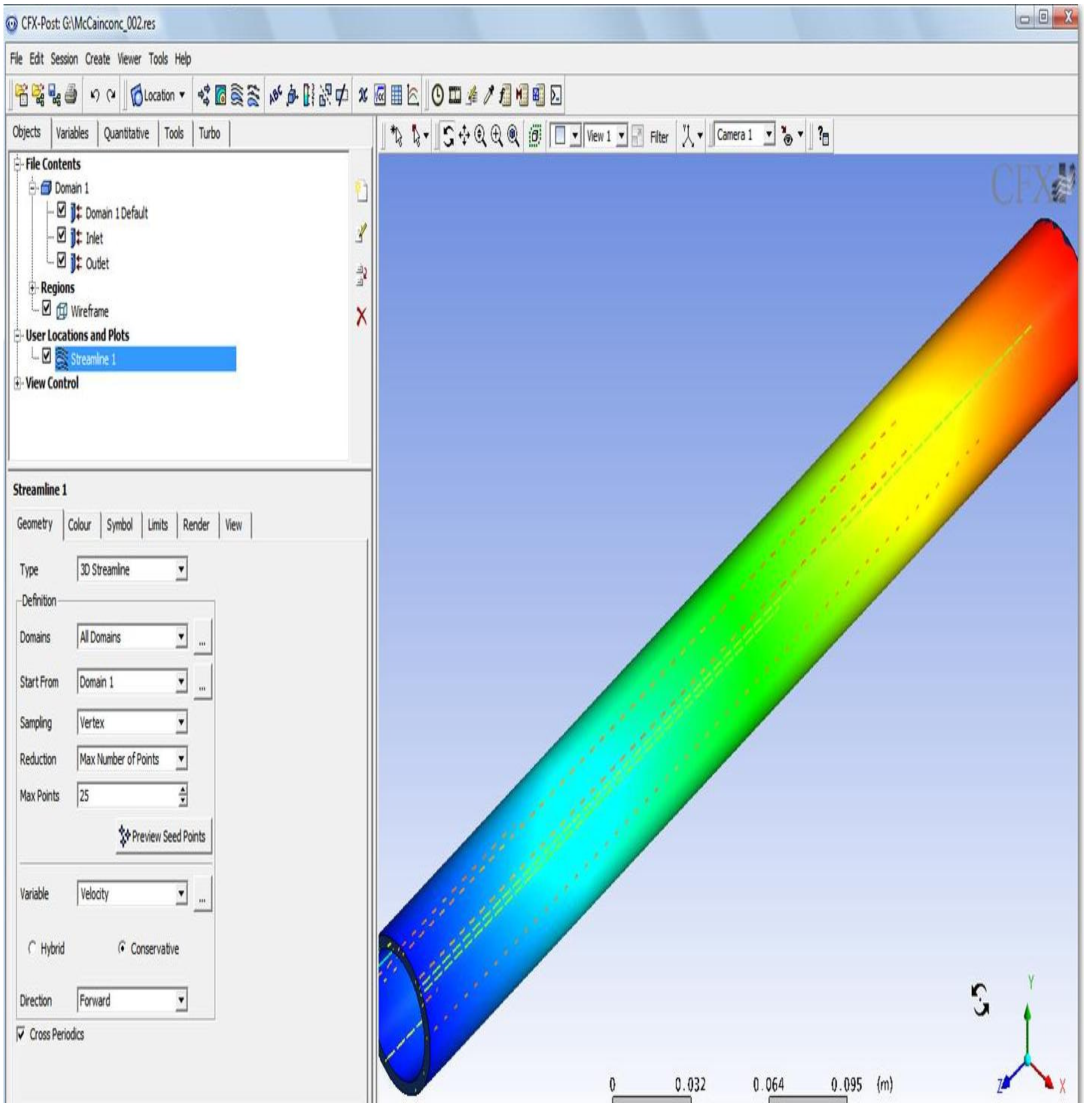

Figure E.5- Streamlines in annulus

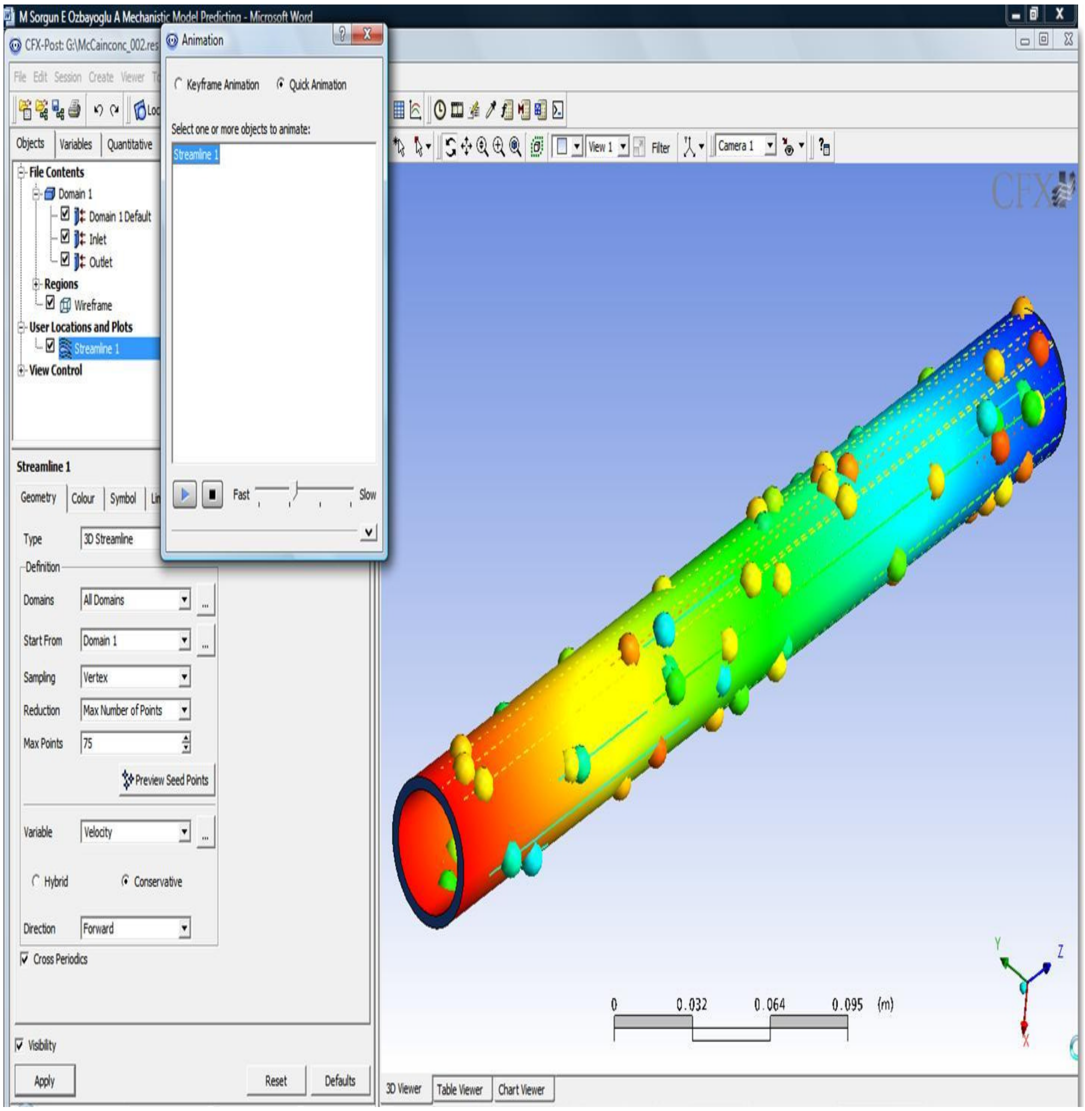

Figure E.6- Fluid particles in concentric annulus

CURRICULUM VITAE

PERSONAL INFORMATION

Surname, Name: Sorgun, Mehmet

Nationality: Turkish (TC)

Date and Place of Birth: 19 September 1977, Afyonkarahisar

Marital Status: Married

Phone: + 90 312 210 48 96

e-mail: mehmetsorgun@gmail.com

EDUCATION

Degree	Institution	Year of Graduation
PhD	METU Petroleum and Natural Gas Engineering	2010
MS	Celal Bayar University Civil Engineering	2004
BS	Dokuz Eylul University Civil Engineering	2001

WORK EXPERIENCE

Year	Place	Enrollment
2004-2010	METU Petroleum and Natural Gas Engineering	Research Asistant
2009-2009 (9 month)	Texas A&M University Petroleum Engineering	Visiting Scholar

AWARDS

Year	Name of Award	Organization
2007	METU Graduate Courses Performance (3.79/4.00)	METU Graduate School of Natural and Applied Science

PUBLICATIONS

SCI and SCI-Expanded Publications

1. Acar, C., **Sorgun M**., "Geothermal Energy: Current Status in Turkey With EU Perspective", Energy Sources Part B, 4:145-154, 2009.
2. Ozbayoglu M.E., Saasen A., **Sorgun M**., Svanes K., " Critical Fluid Velocities for Removing Cuttings Bed Inside Horizontal and Deviated Wells" , Petroleum Science and Technology, 28:594-602, 2010.
3. Ozbayoglu M.E., **Sorgun M**., Saasen A., Svanes K.,"Hole Cleaning Performance of Light-Weight Drilling Fluids During Horizontal Underbalanced Drilling", Journal of Canadian Petroleum Technology,49, No.4, 21-26, 2010.
4. **Sorgun M.**, Ozbayoglu M.E.,'' Predicting Frictional Pressure Loss During Horizontal Drilling for Non-Newtonian Fluids'', Energy Sources Part A (accepted).
5. **Sorgun M.**, Ozbayoglu M.E., Aydin I.,'' Modeling and Experimental Study of Newtonian Fluid Flow in Annulus'', Journal of Energy Resource Technology (accepted).
6. Ettahadi R.O., **Sorgun M**., " A Critical Evaluation for Iranian Natural Gas Resources ", Energy Sources Part B: Economics, Planning , and Policy Esb-08-046 (accepted).
7. Ozbayoglu M.E, **Sorgun M**.," Frictional Pressure Loss Estimation of Non-Newtonian Fluids in Realistic Annulus with Pipe Rotation", Journal of Canadian International Petroleum Technology (accepted).
8. **Sorgun M.**, Aydin I., Ozbayoglu M.E.,''Friction Factors Low and High Viscous Fluids with Cuttings in Horizontal and Deviated Drilling with Pipe Rotation'', Journal of Petroleum Science and Engineering (submitted).
9. **Sorgun M.,** Schubert J.J., Aydin I., Ozbayoglu M.E., ''Modeling of Newtonian Fluids in Annular Geometries with Pipe Rotation", Journal of Fluids Engineering (submitted).

International Journal Papers

10. Ozbayoglu M.E., Saasen A., **Sorgun M.**, Svanes K., " Pipe Rotation Effect on Hole Cleaning for Water-Based Drilling Fluids in Horizontal and Deviated Wells", Journal of Petroleum Technology , Vol :60, No :11, 65-69, November 2008.

Full-Length International Conference Proceedings Papers

11. Ozbayoglu M.E., Saasen A., **Sorgun M.**, Svanes K., " Estimation Of Critical Fluid Velocity Preventing Cuttings Bed Development In Highly Inclined Wells" , Ipetgas 2007, 16th International Petroleum And Natural Gas Congress and Exhibition Of Turkey, May 29-31, 2007, Ankara.

12. Ozbayoglu M.E., Saasen A., **Sorgun M.**, Svanes K., "Hole Cleaning Performance of Light-Weight Drilling Drilling Fluids During Horizontal Underbalanced Drilling", 8th Canadian International Petroleum Conference (58th Annual Technical Meeting), Calgary, Alberta, Canada, 12-14 June, 2007.

13. Ozbayoglu M.E., Saasen A., **Sorgun M.**, Svanes K., "Estimating Critical Velocity to Prevent Bed Development for Horizontal-Inclined Wellbores", SPE/IADC 108005, SPE/IADC Middle East Drilling Technology Conference & Exhibition held in Cairo, Egypt, 22–24 October 2007.

14. Ozbayoglu M.E., Saasen A., **Sorgun M.**, Svanes K., " Effect of Pipe Rotation on Hole Cleaning for Water-Based Drilling Fluids in Horizontal and Deviated Wells", IADC/SPE 114965, IADC/SPE Asia Pacific Drilling Technology Conference & Exhibition held in Jakarta, Indonesia, 25–27 August 2008.

15. **Sorgun M.,** Ozbayoglu M.E," Experimental and Numerical Study of Predicting Frictional Pressure Loss in Concentric Annulus", Ipetgas 2009,

17th International Petroleum And Natural Gas Congress and Exhibition Of Turkey , 13-15 May, 2009, Ankara.

16. Ozbayoglu M.E, **Sorgun M**.," Frictional Pressure Loss Estimation of Non-Newtonian Fluids in Realistic Annulus with Pipe Rotation", Canadian International Petroleum Conference(CIPC) (60th Annual Technical Meeting), Calgary, Alberta , Canada, 16-18 June , 2009.

17. Ozbayoglu M.E, **Sorgun M**.,"Critical Fluid Velocity Estimation of Water-Based Drilling Fluids During Horizontal and Inclined Underbalanced Drilling with Pipe Rotation'', SPE 127300, Oil& Gas India Conference and Exhibition (OGIC) held in Mumbai, India, 20-22 January 2010.

18. **Sorgun M.,** Schubert J.J., Aydin I., Ozbayoglu M.E., ''Modeling of Newtonian Fluids in Annular Geometries with Pipe Rotation", ASME 2010 3RD Joint US-European Fluids Engineering Meeting, Montreal, Canada, 1-5 August 2010.